

Durham E-Theses

Tropical Homotopy Continuation and Laurent Phenomenon Algebras

DAISEY, OLIVER,JAMES

How to cite:

DAISEY, OLIVER,JAMES (2025) *Tropical Homotopy Continuation and Laurent Phenomenon Algebras*, Durham theses, Durham University. Available at Durham E-Theses Online:
<http://etheses.dur.ac.uk/16120/>

Use policy

The full-text may be used and/or reproduced, and given to third parties in any format or medium, without prior permission or charge, for personal research or study, educational, or not-for-profit purposes provided that:

- a full bibliographic reference is made to the original source
- a [link](#) is made to the metadata record in Durham E-Theses
- the full-text is not changed in any way

The full-text must not be sold in any format or medium without the formal permission of the copyright holders.

Please consult the [full Durham E-Theses policy](#) for further details.

Tropical Homotopy Continuation and Laurent Phenomenon Algebras

Oliver Daisey

A Thesis presented for the degree of
Doctor of Philosophy



Department of Mathematical Sciences
Durham University
United Kingdom

June 2025

Tropical Homotopy Continuation and Laurent Phenomenon Algebras

Oliver Daisey

Submitted for the degree of Doctor of Philosophy

June 2025

Abstract: Tropical geometry and the theory of Laurent phenomenon algebras (LPAs) both provide powerful frameworks for understanding algebro geometric objects in both pure and applied contexts. This thesis explores both of these topics. We extend Anders Jensen's technique of tropical homotopy continuation for computing stable intersections to the setting of Bergman fans, with applications to chemical reaction network theory and rigidity theory. On the other hand, we investigate the structure of LPAs arising from the configurations of lines on del Pezzo surfaces and explicitly describe a new finite-type LPA cluster structure on the homogeneous coordinate ring of the Cayley plane.

Declaration

The work in this thesis is based on research carried out in the Department of Mathematical Sciences at Durham University. No part of this thesis has been submitted elsewhere for any degree or qualification.

The work in this thesis is my own, except where otherwise stated.

Copyright © 2025 Oliver Daisey.

“The copyright of this thesis rests with the author. No quotation from it should be published without the author’s prior written consent and information derived from it should be acknowledged.”

Acknowledgements

I would like to begin by expressing my deepest gratitude to my three academic supervisors, Anna Felikson, Tom Ducat, and Yue Ren, for their unwavering support and guidance throughout my research. Their mentorship has profoundly shaped my mathematical interests and left a lasting impression on me. I am especially grateful to Yue Ren for seamlessly taking over Tom Ducat's supervision duties on short notice after Tom's departure from Durham, and for the fresh coffee each morning. It was always appreciated. I also extend my thanks to the wider tropical geometry research group at Durham for the engaging discussions, both mathematical and otherwise.

I am appreciative for the unwavering support offered by my family and friends. To my family, thank you for always providing a warm and welcoming environment to return home to during the holidays. I offer my heartfelt appreciation to my partner for her understanding and kindness from the very beginning of my degree. To my friends, thank you for inspiring me and encouraging me to always aim higher.

Finally, I would like to express my sincere appreciation to the first-class team at Coltraco for their unrelenting support towards my studies. A special thank you to Carl and Adrian for their unfaltering belief in my abilities.

If you're willing to restrict the flexibility of your approach, you can almost always do something better.

— John Carmack

*This thesis is dedicated
to*

Malcom Hoare

Contents

Abstract	3
1 Introduction	17
1.1 Polyhedral geometry	19
1.1.1 Polyhedra and cones	19
1.1.2 Faces and dual cones	20
1.1.3 Regular subdivisions	22
1.2 Tropical geometry	22
1.2.1 Tropical hypersurfaces	23
1.2.2 Tropical varieties	24
1.2.3 Tropical duality	24
1.3 Matroids	25
1.3.1 Definitions	26
1.3.2 Matroids from linear ideals	27
1.3.3 Matroid polytopes & Bergman fans	28
2 Generalised Tropical Homotopy Continuation	31
2.1 Introduction	31
2.2 Background	34

2.2.1	Dual subdivisions and tropical varieties	35
2.2.2	Mixed cells and stable intersections	40
2.2.3	Fine structure on Bergman fans	49
2.3	The Cayley trick & mixed cell cones	51
2.3.1	Cayley trick	52
2.3.2	Mixed cell cones	54
2.4	Starting data	57
2.5	Bergman and Jensen flips	63
2.5.1	Time until Bergman failure	65
2.5.2	Time until Jensen failure	67
2.5.3	Bergman flip	69
2.5.4	Jensen flip	74
2.6	Endgame and Timeouts	78
2.6.1	Endgame	78
2.6.2	Timeouts	80
2.7	The homotopy algorithm	80
2.8	Applications	85
2.8.1	Graph Rigidity	85
2.8.2	Chemical Reaction Networks	87
3	Finite Cluster Structures on E_n Homogeneous Spaces	89
3.1	Overview	89
3.2	Preliminaries	91
3.2.1	Seeds	91
3.2.2	Mutation	92

3.2.3	Laurent phenomenon algebras	95
3.2.4	Finite type	97
3.2.5	Frozen variables	97
3.2.6	Log Calabi-Yau varieties	98
3.2.7	A short interlude on toric geometry	99
3.2.8	Cluster varieties	101
3.2.9	Mirror symmetry	101
3.2.10	Simple algebraic groups	102
3.2.11	Enumerative geometry of del Pezzo surfaces	104
3.3	Giving the coordinate rings an LPA structure	105
3.3.1	Numerical invariants	106
3.3.2	Coxeter projection of Ξ_n	107
3.3.3	A family of log Calabi-Yau varieties	107
3.3.4	Type E_4	108
3.3.5	Type E_5	110
3.3.6	Type E_6	113
3.3.7	Action of a Coxeter rotation	114
3.3.8	Finding an initial seed	115
3.3.9	Summary of the LPA structure	118
3.3.10	Limited progress on type E_7	121

List of Figures	125
------------------------	------------

List of Tables	129
-----------------------	------------

Bibliography	1
---------------------	----------

Chapter 1

Introduction

This thesis explores two distinct but fundamentally related topics in algebraic geometry: tropical homotopy continuation and finite type cluster structures on homogeneous varieties. While these topics originate from different mathematical traditions, they share a common theme in the study of structured geometric objects and their associated algebraic properties.

In the first part of this thesis, we investigate a generalised approach to tropical homotopy continuation, a tropical analogue of numerical homotopy continuation introduced by Jensen [Jen16b]. Tropical geometry provides a combinatorial framework for studying algebraic varieties by replacing classical algebraic structures with piecewise linear counterparts, often described as the “combinatorial shadows” of the algebraic varieties. One is often interested in the intersection of tropical varieties. However, tropical varieties have the structure of polyhedral complexes satisfying a certain balancing condition, which does not always behave nicely with respect to set-theoretic intersections. The stable intersection is a well-defined notion that is much better behaved. It coincides with the set-theoretic intersection in the transverse case, and always produces a balanced polyhedral complex of expected dimension. Many types of problems in algebraic geometry can be reduced to computing a stable intersection of tropical varieties, and thus it is desirable to have an efficient method to compute them. Tropical homotopy continuation reduces the problem of comput-

ing the stable intersection of tropical hypersurfaces to the problem of starting with a known stable intersection, deforming back to the desired intersection, and calculating the way fully mixed cells of the mixed subdivision dual to the overlay of the tropical hypersurfaces change. Originally developed for mixed volume computations in polyhedral homotopies [HS95], the method has been implemented in various computer algebra systems like GFAN [Jen; Jen16a] and HOMOTOPYCONTINUATION.JL [BT18]. We extend Jensen’s framework by incorporating intersections with Bergman fans, which arise naturally in tropical intersection theory and applications such as rigidity theory [Cla+25] and chemical reaction network theory [HHR24].

The second part of this thesis focuses on the study of finite type cluster structures on the homogeneous varieties associated with representations of the exceptional Lie groups of type E_n . A central result concerns the construction of a finite type cluster structure on the complex Cayley plane, which we realise as the cominuscule homogeneous space E_6/P_6 , interpreting E_6 as the root system associated to the configuration of lines on a del Pezzo surface dP_6 . This work utilises the structure of Laurent phenomenon algebras (LPAs), a generalisation of cluster algebras introduced by Lam and Pylyavskyy [LP16]. Cluster algebras were introduced by Fomin and Zelevinsky in [FZ02a] as a tool for studying dual canonical bases and total positivity in semisimple Lie groups. Since then they have exploded in popularity and have found applications in diverse areas of mathematics and physics, such as integrable systems [GI24], quiver representations [Kel08], dilogarithms and conformal field theory [Nak11], and indeed even tropical geometry [SW05]. LPAs retain many structural properties of Fomin and Zelevinsky’s cluster algebras while permitting more general exchange polynomials. We will establish a finite type LPA structure for the Cayley plane, demonstrating that such structures may exist even when finite type cluster algebra structures do not.

The author has developed software packages as an essential component of both parts of this thesis. These include the TROPICALHOMOTOPIES.JL package and LPASEED class for JULIA and SAGEMATH respectively. The former utilises the

open source computer algebra package OSCAR. Both packages are open source and freely available.

1.1 Polyhedral geometry

In this section we review the fundamental notions we need from polyhedral geometry. We make no effort to be comprehensive, and the reader is referred to [Zie12] for a more thorough treatment.

1.1.1 Polyhedra and cones

A *convex set* $S \subseteq \mathbb{R}^n$ is such that if $x, y \in S$, then the line segment $y + (1-t)(x-y)$ is contained in S , where $0 < t < 1$. The *convex hull* $\text{conv}(S)$ of S is the intersection of all convex sets that contain S as a subset. The convex hull of a finite number of points is a *polytope*. A *polyhedron* is defined as any set of the form

$$P = \{x \in \mathbb{R}^n \mid Ax \leq b\}$$

where $b \in \mathbb{R}^r$ and A is a matrix with r rows and n columns. All polytopes are polyhedra, but a polytope is necessarily bounded.

We define a *polyhedral cone* as any set of the form

$$C = \text{pos}(v_1, \dots, v_n) := \{\lambda_1 v_1 + \dots + \lambda_n v_n \mid \lambda_i \geq 0 \text{ for all } i\}$$

where the $v_i \in \mathbb{R}^n$. A polyhedral cone is *simplicial* if it can be generated by linearly independent vectors. Polyhedral cones are special cases of polyhedra that may be written in the form $Ax \leq 0$.

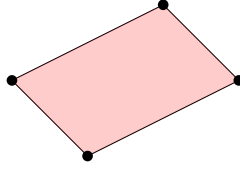


Figure 1.1: A point set and its convex hull.

1.1.2 Faces and dual cones

Given a polyhedron P and a linear functional $w \in (\mathbb{R}^n)^*$, the *face* determined by w is the set

$$\text{face}_w(P) = \{x \in P \mid x \cdot w \leq y \cdot w \text{ for all } y \in P\}.$$

We define the *dimension* of a polyhedron P as the dimension of the smallest affine subspace containing P . A maximal proper face is called a *facet*. Any face of a polyhedron is another polyhedron, and so a face of dimension 0 is called a *vertex*, a face of dimension 1 is called an *edge*. etc. We define the *dual cone* of a cone σ as

$$\sigma^\vee = \{w \in (\mathbb{R}^n)^* \mid \langle x, w \rangle \geq 0 \text{ for all } x \in \sigma\}.$$

Given a face τ of a polyhedron P , we define the *normal cone* $\sigma = \tau^\perp$ as the set

$$\sigma = \{w \in (\mathbb{R}^n)^* \mid \text{face}_w(P) = \tau\}.$$

The (inner) *normal fan* $\mathbf{N}(P)$ of P is the set of all normal cones τ^\perp as τ ranges over the faces of P . Faces and normal cones are in a dimension-reversing correspondence, that is

$$\dim k \text{ faces of } P \longleftrightarrow \text{codim } k \text{ cones in } \mathbf{N}(P)$$

A *polyhedral complex* is a collection of polyhedra where every face of a polyhedron is in the collection, and the intersection of any two polyhedra is either empty or a face of each. A polyhedral complex consisting of cones is called a *polyhedral fan*, or just *fan* for short. We say a polyhedral complex is *pure* if all the maximal polyhedra have the same dimension.

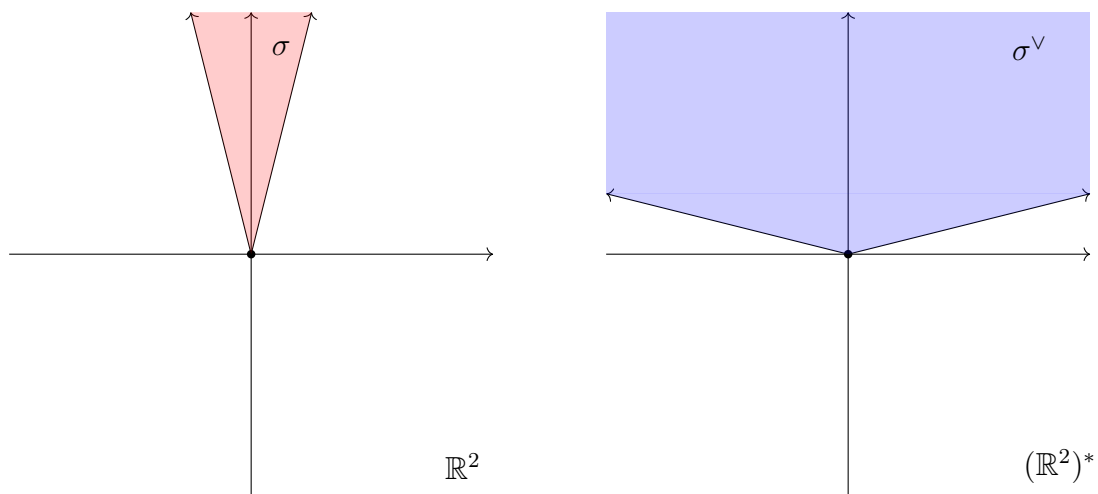


Figure 1.2: A cone σ (in red) and its associated dual cone σ^\vee (in blue).

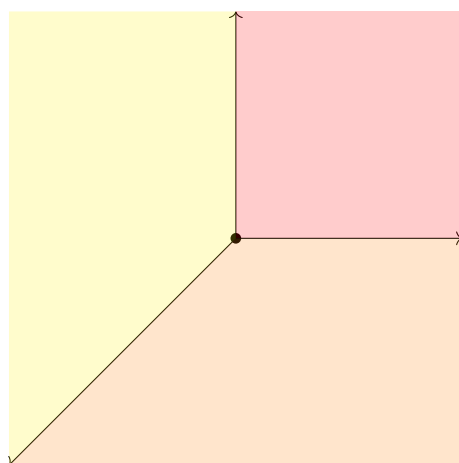


Figure 1.3: A polyhedral fan.

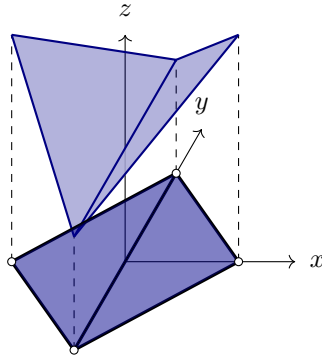


Figure 1.4: A plane polytope P with its lifted polytope, whose lower envelope defines a regular subdivision of P .

1.1.3 Regular subdivisions

A polyhedron P may be partitioned into polyhedra that form a polyhedral complex; such a partition is called a *polyhedral subdivision* of P . Given a collection of points $p_i \in \mathbb{R}^n$ with $i \in \mathcal{I}$, there is a standard way to obtain a subdivision of $P := \text{conv}(p_i)$, which we now describe: We give each point a height w_i for $i \in \mathcal{I}$, and define the *lifted polytope*

$$\hat{P} := \text{conv}((p_i, w_i) \mid i \in \mathcal{I}).$$

Define the projection $\pi : \mathbb{R}^{n+1} \rightarrow \mathbb{R}^n$ by $(x_1, \dots, x_n, w) \mapsto (x_1, \dots, x_n)$ and call a facet of \hat{P} *visible from below* if its inner pointing normal vector u satisfies the condition $u \cdot e_w > 0$, where $e_w \in \mathbb{R}^{n+1}$ is the vector $(0, \dots, 0, 1)$. The polyhedra $\pi(Q)$, where Q ranges over facets of \hat{P} visible from below, define a polyhedral subdivision of P . This construction is referred to as the *regular subdivision* of P induced by the heights $w_i \in \mathcal{I}$.

1.2 Tropical geometry

In this section we survey the elements of tropical geometry that we need for the chapter on tropical homotopy continuation. Recall that tropical geometry aims to study algebraic varieties via their combinatorial analogues; balanced weighted polyhedral complexes connected in codimension one. The canonical reference for

the material in this section is the textbook by Diane Maclagan and Bernd Sturmfels [MS15].

1.2.1 Tropical hypersurfaces

Let $\mathbb{T} := (\mathbb{R} \cup \{\infty\}, \oplus, \odot)$ denote the min-plus tropical semiring and fix a multivariate (Laurent) polynomial ring $\mathbb{T}[x^\pm] := \mathbb{T}[x_0^\pm, x_1^\pm, \dots, x_n^\pm]$. A tropical polynomial $f(x) \in \mathbb{T}[x^\pm]$ is said to *vanish* at $w \in \mathbb{R}^n$ if the minimum in $f(w)$ is achieved at least twice. We define the *tropical hypersurface*

$$\text{Trop}(f) := \{w \in \mathbb{R}^n \mid f \text{ vanishes at } w\}.$$

Tropical polynomials can be realised by Laurent polynomials over valued fields. In the following, let K be an algebraically closed field with a valuation $\text{val} : K \rightarrow \Gamma \cup \{\infty\}$. This means val satisfies the properties

1. $\text{val}(a) = \infty \iff a = 0$,
2. $\text{val}(ab) = \text{val}(a) + \text{val}(b)$,
3. $\text{val}(a + b) \geq \min(\text{val}(a), \text{val}(b))$ with equality if $\text{val}(a) \neq \text{val}(b)$.

A polynomial $f(x_1, \dots, x_n) = \sum_{u \in \text{Supp}(f)} c_u x^u \in K[x_1^\pm, \dots, x_n^\pm]$ tropicalises according to the formula

$$\text{trop} : \sum_{u \in \text{Supp}(f)} c_u x^u \mapsto \bigoplus_{u \in \text{Supp}(f)} \text{val}(c_u) \odot u \cdot x$$

which corresponds to replacing classical addition and multiplication by tropical addition and subtraction, whilst replacing the c_u with their valuations. Since K is algebraically closed, K admits a splitting $\psi : \Gamma \cup \{\infty\} \rightarrow K$ with $\text{val}(\psi(w)) = w$. Hence, provided the image of val is exactly \mathbb{T} , any tropical polynomial arises as the tropicalisation of a polynomial over K .

1.2.2 Tropical varieties

Let $I \subseteq K[x_1^\pm, \dots, x_n^\pm]$ be an ideal with variety $X = V(I)$ in $(K^*)^n$. We define the tropicalisation of X by

$$\text{Trop}(X) := \bigcap_{f \in I} \text{Trop}(f) \subseteq \mathbb{R}^n.$$

Note that in general $\text{Trop}(X)$ does *not* equal the intersection $\bigcap_{i=1}^m \text{Trop}(f_i)$ for Laurent polynomials $f_i \in K[x_1^\pm, \dots, x_n^\pm]$ with $I = (f_1, \dots, f_m)$. In the case that it does, we refer to $\{f_1, \dots, f_m\}$ as a *tropical basis* for I .

We have the following fundamental result:

Theorem 1.2.1 (Kapranov's Theorem) *Let $X = V(I)$ and suppose the valuation $\text{val} : K \rightarrow \Gamma \cup \{\infty\}$ is nontrivial. The tropical variety $\text{Trop}(X)$ coincides with the set*

$$\overline{\{(\text{val}(y_1), \dots, \text{val}(y_n)) \mid (y_1, \dots, y_n) \in X\}}$$

where the closure is taken in the Euclidean topology.

1.2.3 Tropical duality

There is a duality between tropical hypersurfaces and regular subdivisions that we now describe. Write $f = \bigoplus_{u \in \text{Supp}(f)} c_u \odot u \cdot x$, where $\text{Supp}(f) = \{u \mid c_u \neq \infty\}$. We obtain a regular subdivision of the *Newton polytope*

$$\text{Newt}(f) = \text{conv}(\text{Supp}(f))$$

by lifting each $u \in \text{Supp}(f)$ by the height c_u and projecting the lower faces. Denote the inner normal fan of the lifted polytope $\widehat{\text{Newt}}(f) \subseteq \mathbb{R}^{n+1}$ by $\mathbf{N}(\widehat{\text{Newt}}(f))$. Each lower face in $\widehat{\text{Newt}}(f)$ has a dual cone σ in $\mathbf{N}(\widehat{\text{Newt}}(f))$, such that there exists $v \in \sigma$ with $v \cdot e_{n+1} > 0$. As such, σ has a nonempty intersection with the hyperplane H defined by the equality $x_{n+1} = 1$. We set the polyhedron dual to τ as the projection $\pi(\sigma \cap H)$, where π is the projection map sending $\widehat{\text{Newt}}(f)$ to $\text{Newt}(f)$. These dual

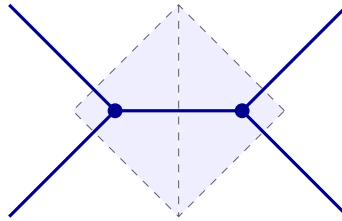


Figure 1.5: An illustration of the duality between regular subdivisions and tropical hypersurfaces. The blue tropical hypersurface is dual to the regular subdivision shown in Figure 1.4.

polyhedra form a polyhedral complex.

Now let $w \in \mathbb{R}^n$ and suppose $w \in \text{Trop}(f)$. Then the minimum in $f(w)$ is achieved at least twice, which means there are at least two monomials $u_i \in \text{Supp}(f)$ with

$$c_i + w \cdot u_i \leq c_j + w \cdot u_j \text{ for all } u_j \in \text{Supp}(f) \text{ with } j \neq i.$$

The point $(w_1, \dots, w_n, 1) \in \mathbf{N}(\widehat{\text{Newt}}(f)) \cap H$ defines a lower face of $\widehat{\text{Newt}}(f)$ containing all $u_\ell \in \text{Supp}(f)$ such that, for all $u_j \in \text{Supp}(f)$ with $j \neq \ell$,

$$\begin{aligned} (w_1, \dots, w_n, 1) \cdot (u_\ell, c_\ell) &\leq (w_1, \dots, w_n, 1) \cdot (u_j, c_j) \\ \iff c_\ell + w \cdot u_\ell &\leq c_j + w \cdot u_j. \end{aligned}$$

We therefore see that the required exponent vectors u_ℓ are exactly the monomials $u_i \in \text{Supp}(f)$ where the minimum in $f(w)$ is achieved. The converse is also true; given a lower face with at least two vertices, the dual polyhedron will be contained in $\text{Trop}(f)$. So $\text{Trop}(f)$ is exactly the $(n-1)$ -skeleton of the described dual polyhedral complex.

1.3 Matroids

Matroids are fundamental objects that describe the properties of linear dependence. We will see that they naturally describe tropicalisations of linear ideals, and correspondingly they play an important role in tropical geometry.

1.3.1 Definitions

In all the following definitions, fix a *ground set* $E = \{1, 2, \dots, n\}$. We can define a matroid M with ground set E in multiple equivalent ways. In each case, we associate a nonempty collection of subsets of E to M with a rule for how to move from one subset to another. The proof that all the following definitions are equivalent can be found in virtually any textbook that treats matroids (see [Oxl06] or [MS15] for instance).

Definition 1.3.1 (Independent sets). A *matroid* $M = (E, \mathcal{I})$ consists of a finite ground set E and a collection \mathcal{I} of subsets of E , called *independent sets*, satisfying the following axioms:

1. **Hereditary property:** If $I \in \mathcal{I}$ and $I' \subseteq I$, then $I' \in \mathcal{I}$.
2. **Non-triviality:** The empty set is independent, i.e., $\emptyset \in \mathcal{I}$.
3. **Exchange property:** If $I_1, I_2 \in \mathcal{I}$ and $|I_1| < |I_2|$, then there exists an element $e \in I_2 \setminus I_1$ such that $I_1 \cup \{e\} \in \mathcal{I}$.

Equivalently, one may define a matroid using minimal dependent sets:

Definition 1.3.2 (Circuits). A *matroid* $M = (E, \mathcal{C})$ consists of a finite ground set E and a collection \mathcal{C} of subsets of E , called *circuits*, satisfying the following axioms:

1. **Non-emptiness:** $\mathcal{C} \neq \emptyset$.
2. **Minimality:** No circuit properly contains another, i.e., if $C_1, C_2 \in \mathcal{C}$ and $C_1 \subseteq C_2$, then $C_1 = C_2$.
3. **Circuit elimination:** If $C_1, C_2 \in \mathcal{C}$ and $e \in C_1 \cap C_2$, then there exists a circuit $C_3 \subseteq (C_1 \cup C_2) \setminus \{e\}$.

The maximal independent sets of a matroid are called *bases*. Indeed, by the same proof as in linear algebra, all bases are the same size. We have the following definition in terms of bases:

Definition 1.3.3 (Bases). A *matroid* $M = (E, \mathcal{B})$ consists of a finite ground set E and a collection \mathcal{B} of subsets of E , called *bases*, satisfying the following axioms:

1. **Non-emptiness:** $\mathcal{B} \neq \emptyset$; that is, there exists at least one basis.
2. **Basis exchange property:** If $B_1, B_2 \in \mathcal{B}$ and $e \in B_1 \setminus B_2$, then there exists an element $f \in B_2 \setminus B_1$ such that $(B_1 \setminus \{e\}) \cup \{f\} \in \mathcal{B}$.

The *rank* of an independent set I is the cardinality of I . Given a subset S of E , we set the rank of S to be the rank of the largest independent subset of S . We say S is *closed* or a *flat* if it is not possible to add an element in $E \setminus S$ to increase the rank of S . The *closure* of S is the intersection of all closed sets containing S .

Definition 1.3.4 (Flats). A *matroid* $M = (E, \mathcal{F})$ consists of a finite ground set E and a collection \mathcal{F} of subsets of E , called *flats*, satisfying the following axioms:

1. **Ground set containment:** $E \in \mathcal{F}$ and $\emptyset \in \mathcal{F}$.
2. **Closure under intersection:** If $F_1, F_2 \in \mathcal{F}$, then $F_1 \cap F_2 \in \mathcal{F}$.
3. **Flatness condition:** If $F \in \mathcal{F}$ and $e \in E \setminus F$, then $F \cup \{e\}$ is not a flat if and only if there exists a basis B of M such that $B \cap F$ is a basis of F .

A matroid is said to be *realisable* if it is equal to the column matroid of a matrix A . This matroid has ground set equal to the columns of A , and the independent subsets are precisely the linearly independent columns.

1.3.2 Matroids from linear ideals

Given a linear ideal I generated by homogeneous linear forms $\ell_1, \dots, \ell_k \in K[x_1, \dots, x_n]$, associate the $k \times n$ matrix A whose i th row is given by the coefficients of ℓ_i . Let \mathcal{B} be a basis for $\ker(A)$, and let B be the matrix whose rows are given by the vectors in \mathcal{B} . We associate to I the matroid on the columns of B . Concretely, this means that

1. The rank function of the matroid is given by the rank of the corresponding submatrix of B ,
2. The bases are maximally independent subsets of columns,
3. The circuits correspond to minimally dependent sets of columns.

The linear forms corresponding to circuits of B form a tropical basis for I . We refer to $\text{Trop}(V(I))$ as a *tropicalised linear space*. It is the realisable version of a tropical linear space as we will shortly discuss.

1.3.3 Matroid polytopes & Bergman fans

Given a matroid $M = (E, \mathcal{B})$ on a ground set E with bases \mathcal{B} , the *matroid polytope* of M is the negative of the convex hull of indicator vectors of its bases:

$$P_M = \text{conv}\{-e_B \mid B \in \mathcal{B}\}$$

where $e_B = \sum_{i \in B} e_i$ is the indicator vector of the basis B in $\mathbb{R}^{|E|}$, with e_i denoting the standard basis vectors.

Example 1.3.5. Let M be the uniform matroid $U_{2,4}$ whose bases are all 2-element subsets of $1, 2, 3, 4$. The matroid polytope $P_M \subseteq \mathbb{R}^4$ has vertices of the form $-(e_i + e_j)$ where $i, j \in \{1, 2, 3, 4\}$ and $i \neq j$.

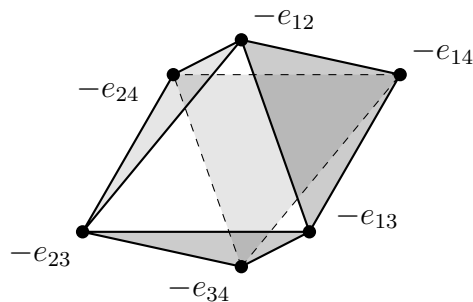


Figure 1.6: The matroid polytope associated to the uniform matroid $U_{2,4}$. The picture is drawn on the hyperplane $x_4 = 0$.

The matroid polytope is contained within the hyperplane $\sum_{i \in E} x_i = -r(M)$, where $r(M)$ is the rank of the matroid. The edges of P_M correspond to basis exchanges. The faces of P_M have an interpretation as contractions and restrictions of M [Oxl06]. We call a face F of P_M *loopless* if every element of E appears in at least one basis defining a vertex of F . The loopless faces have dimension at least $r(M)$. Loopless faces are dual to tropical cones by the formula

$$\sigma_{P_M}(F) = \{w \in \mathbb{R}^{|E|} \mid \text{face}_w(P_M) = F\}.$$

We refer to the polyhedral fan $\{\sigma_{P_M}(F) \mid F \text{ a loopless face of } P_M\}$ as the *Bergman fan* of M . It should be viewed as the special case of a tropical linear space that arises from a tropical Plücker vector with identical tropically nonzero entries. We will not touch upon this subject in this thesis and leave the details to [MS15].

Remark 1.3.1 Note that we define the matroid polytope to have vertices equal to the negatives of indicator vectors. This is in contrast to [MS15], where $\sigma_{P_M}(F)$ is defined to be all $w \in \mathbb{R}^{|E|}$ whose corresponding linear functional is maximised exactly at F (instead of minimised).

Chapter 2

Generalised Tropical Homotopy Continuation

The work in this chapter was joint with Yue Ren.

2.1 Introduction

In [Jen16b], Anders Jensen introduced a tropical analogue of homotopy continuation in numerical algebraic geometry. Instead of computing the intersection of n algebraic hypersurfaces in \mathbb{C}^n , tropical homotopy continuation computes the (stable) intersection of n tropical hypersurfaces in \mathbb{R}^n . Jensen's main motivation was the computation of mixed volumes and mixed cells, which are an important ingredient for polyhedral homotopies [HS95]. The algorithm was initially implemented in GFAN [Jen; Jen16a], where it is still powering the mixed volume computation to date. Since then, polynomial system solvers like HOMOTOPYCONTINUATION.JL [BT18] have picked up the algorithms and are using them for polyhedral homotopies.

In this chapter, we generalise Jensen's approach to allow for intersections with Bergman fans. This is made possible because the duality between tropical hypersurfaces and Newton subdivisions is the same as the duality between tropical linear spaces

and matroid subdivisions. Unlike Newton polytopes however, matroid polytopes can be very complicated even for unassuming examples. We therefore focus on Bergman fans, which can be described by chains of flats. Whilst the sheer amount of chains is equally complicated, tracking individual chains is not difficult.

Our work is motivated by tropical intersections that arise in several applications, such as in generic root counts [HR24], generalisation of polyhedral homotopies [HHR24], or tropical critical points of affine matroids [AEP24], as well as the recent proliferation of intersection theory on matroids following the seminal work by Adiprasito, Huh, and Katz [AHK18]. Concretely, we explore an application in rigidity theory [Cla+25], in which we explain how to deal with cases where intersects include inverted Bergman fans and all intersects share a common lineality space, and an application that arises in chemical reaction network theory [HHR24].

All algorithms in this chapter are implemented using the computer algebra system OSCAR. The corresponding code is open source and can be found at

<https://github.com/oliverdaisey/TropicalHomotopyContinuation.jl>

Overview of the homotopy algorithm and the paper

In Section 2.2 we fix our notation by giving a quick rundown of the required background in tropical geometry. This builds upon the introduction in Section 1.2, but we place special emphasis on the notions of dual supports, dual heights, and dual cells, as well as their mixed counterparts. These dual structures are introduced to remove the need to distinguish between certain concepts on matroid and Newton polytopes that play a similar role in our framework. For example, loopless faces of matroid polytopes are dual to cones of Bergman fans and positive dimensional cells of Newton subdivisions are dual to polyhedra of tropical hypersurfaces. We refer to both as dual cells.

In Section 2.3, we introduce mixed cells cones similar to those in [Jen16b, Section 4].

As in [Jen16b] we will emphasise describing its facets and how it can be computed using the Cayley Trick.

In Section 2.4, we discuss how to construct starting data for a desired target mixed supports and mixed heights. This starting data consists of starting supports and heights, as well as all initial mixed cells. Our approach is the same as Jensen’s regeneration technique [Jen16b, Section 7.2]. We avoid Jensen’s total degree construction [Jen16b, Section 7.1], as our starting data involves user-given Bergman fans, which makes it impossible to predict the initial mixed cells without a small computation. We also comment on possible homotopy paths connecting starting heights to target heights.

In Section 2.5, we explain the fundamental building blocks of tropical homotopy continuation, namely how to determine when a mixed subdivision changes, and how to compute said change. To avoid the need to work with matroid polytopes and their loopless faces in entirety, we work with chains of flats of the underlying matroid instead. This requires us to track chains of flats separately from changes in the hypersurface dual supports: The *time until Bergman failure* measures when the chain of flats changes under the assumption that the supporting hypersurface dual cells remain unchanged, and the *time until Jensen failure* measures when the hypersurface dual cells change under the assumption that the supporting chain of flats remains unchanged. The resulting operations we apply to the mixed cells are called *Bergman flips* and *Jensen flips* respectively.

In Section 2.6, we explain how to handle the path in two boundary cases that we refer to as *timeouts* and *endgames*. Timeouts are necessary when dual heights are formally sent to ∞ and lead to a smaller dual support. For a tropical polynomial for example, this means a coefficient becomes tropically zero and thus the polynomial loses a monomial. Endgame deals with the task of computing the tropical intersection point for a target mixed height, even if the intersection is potentially non-transverse.

In Section 2.7, we assemble the overall algorithm, combining all algorithms from all previous sections, and in Section 2.8, we discuss the applications in rigidity theory

and chemical reaction network theory.

2.2 Background

We begin by reviewing the relevant concepts from tropical geometry. The main focus are the dualities between

1. tropical hypersurfaces and Newton subdivisions [MS15, §3.1] [Jos21, §1],
2. tropical linear spaces and matroid subdivisions [MS15, §4.4] [Jos21, §10],
3. stable intersections and mixed cells [MS15, §3.6+4.6].

For the sake of simplicity, we will deviate from [MS15; Jos21] and define tropical hypersurfaces and linear spaces as balanced polyhedral complexes dual to appropriate subdivisions of Newton and matroid polytopes respectively.

Convention 2.2.1 For the entirety of this chapter, let $\mathbb{T} := (\mathbb{R} \cup \{\infty\}, \oplus, \odot)$ denote the min-plus tropical semiring and let $\mathbb{T}[x^\pm] := \mathbb{T}[x_1^\pm, \dots, x_n^\pm]$ be multivariate (Laurent) polynomial ring. We will use $[n]$ to denote the set $\{1, \dots, n\}$. Moreover, fix

1. $S_{\text{lin}} := \{-e_B \mid B \in M\} \subseteq \mathbb{Z}^n$ the vertices of a matroid polytope P_M , where M is a matroid on $[n]$ of rank k and $e_B := \sum_{i \in B} e_i \in \mathbb{Z}^n$ is the indicator vector of basis B . For the sake of algorithmic efficiency, we will assume M to be linearly realisable, though we will remark on alternatives for non-realisable matroids where applicable.
2. $S_{k+1}, \dots, S_n \subseteq \mathbb{Z}^n$ finite sets of cardinality at least two.

We will refer to S_{lin} and S_{k+1}, \dots, S_n as *dual supports* of a Bergman fan and tropical hypersurfaces, respectively.

Before we begin, we make some clarifying remarks on Convention 2.2.1.

Remark 2.2.2

1. We previously remarked about this in Remark 1.3.1, but to reiterate: Readers familiar with [MS15, Section 4.2] and [Jos21, Section 10] may be surprised by the minus signs in the definition of S_{lin} . Their purpose is to make the dualities between tropical hypersurfaces and Newton subdivisions consistent with the dualities between tropical linear spaces and matroid subdivisions, allowing us to define both hypersurfaces and linear spaces in Definition 2.2.3.
2. We introduce S_{lin} mainly for notational reasons. Our algorithms will generally use a realisation matrix or individual chains of flats rather than the bases or circuits of M , see Section 2.4 and Section 2.5.
3. The sets S_{k+1}, \dots, S_n are not to be confused with the monomial supports of the target system. From Section 2.5 onwards, they are the monomial supports of the starting system.

2.2.1 Dual subdivisions and tropical varieties

Definition 2.2.1. A *dual height* is either

1. the zero vector $0 \in \mathbb{T}^{S_{\text{lin}}}$, or
2. a vector $c_i \in \mathbb{T}^{S_i}$ that is tropically non-zero in at least two coordinates, i.e., $c_i = (c_{i,\alpha})_{\alpha \in S_i}$ with $c_{\alpha_1} \neq \infty \neq c_{\alpha_2}$ for at some $\alpha_1 \neq \alpha_2$.

A *dual space* is a space of such dual heights, i.e., either $\mathbb{H}^{S_{\text{lin}}} := \{0\} \subseteq \mathbb{T}^{S_{\text{lin}}}$ or $\mathbb{H}^{S_i} := \mathbb{T}^{S_i}$.

In the following definition, a regular subdivision of a set $S \subseteq \mathbb{Z}^n$ with respect to a height $c = (c_\alpha)_{\alpha \in S} \in \mathbb{T}^S$ is the regular subdivision of $\{\alpha \in S \mid c_\alpha \neq \infty\}$ with respect to $(c_\alpha)_{\alpha \in S, c_\alpha \neq \infty}$ as per [MS15, Definition 2.3.8] and [Jos21, Section 1.2].

Definition 2.2.2. A *dual cell candidate* is one of the following dual support subsets:

1. $s_{\text{lin}} \subseteq S_{\text{lin}}$ loopless, i.e., $\bigcup_{-e_B \in s_{\text{lin}}} B = [n]$,
2. $s_i \subseteq S_i$ of cardinality at least 2.

A dual cell candidate $s \subseteq S$ is a *dual cell* induced by a dual height $c \in \mathbb{H}^S$ if it arises as the vertex set of a cell in the regular subdivision on S induced by c . As $\mathbb{H}^{S_{\text{lin}}} = \{0\}$, this means that dual cells $s_{\text{lin}} \subseteq S_{\text{lin}}$ are vertices of faces of the matroid polytope P_M .

A *dual subdivision* of S induced by a dual height $c \in \mathbb{H}^S$ is the set of all dual cells induced by c :

$$D_S(c) := \{s \subseteq S \mid s \text{ dual cell induced by } c\}.$$

While different dual heights may induce the same dual subdivision, we assume that a dual subdivision comes with the data of the heights that give rise to it.

Definition 2.2.3. Any dual cell $s \in D_S(c)$ defines a *tropical polyhedron* (here, tropical refers to the polyhedron being part of a tropical variety in \mathbb{R}^n , and not to it being tropically convex) by

$$\sigma(c, s) := \{w \in \mathbb{R}^n \mid \text{the minimum in } f_S(c)(w) \text{ is attained at } s\},$$

where $f_S(c) := \bigoplus_{\alpha \in S} c_\alpha \odot x^{\odot \alpha}$. Note that $s \subseteq s'$ implies $\sigma_S(c, s) \supseteq \sigma_S(c, s')$ and vice versa, hence maximal $\sigma_S(c, s)$ arise from minimal s .

The set of all such polyhedra form a polyhedral complex, which we refer to as the *tropical variety* with dual support S induced by c :

$$\Sigma_S(c) := \{\sigma_S(c, s) \mid s \in D_S(c)\}.$$

Equipping the maximal polyhedra with weights

$$\text{mult}_{\Sigma_S(c)}(\sigma_S(c, s)) = \text{lattice length of } \text{conv}(s)$$

in the hypersurface case and

$$\text{mult}_{\Sigma_S(c)}(\sigma_S(c, s)) := 1$$

in the linear case provides $\Sigma_S(c)$ with the structure of a balanced polyhedral complex. For $S = S_{\text{lin}}$ and $c = 0$, $\Sigma_{S_{\text{lin}}}(0)$ is commonly known as a *Bergman fan*. It is a special case of a tropical linear space. For $S = S_i$, $\Sigma_{S_i}(c_i)$ is commonly known as a *tropical hypersurface*.

Remark 2.2.3 Note that the definition of the hypersurface multiplicities in the form of lattice length or volume does not work for Bergman fans of non-uniform matroids, hence the two separate definitions in Definition 2.2.3. As an example, one can take the non-Fano matroid [Oxl92, Section 1.5], which has a realisation as the column matroid of the following matrix over \mathbb{Q} :

$$\begin{pmatrix} 1 & 0 & 1 & 0 & 1 & 0 & 1 \\ 0 & 1 & 1 & 0 & 0 & 1 & 1 \\ 0 & 0 & 0 & 1 & 1 & 1 & 1 \end{pmatrix},$$

One can check that its matroid polytope has the following two minimal loopless faces, which have lattice volume 4 and 1 respectively:

$$\text{conv}(e_{137}, e_{127}, e_{136}, e_{126}, e_{135}, e_{125}, e_{134}, e_{124}) \text{ and } \text{conv}(e_{567}, e_{156}, e_{256}, e_{356}, e_{456}).$$

Example 2.2.4. Let M be the uniform matroid on the ground set $[4]$ of rank 2. Its bases are 2-elements subsets of $[4]$, yielding the dual support

$$S_{\text{lin}} = \{-e_{12}, -e_{13}, -e_{14}, -e_{23}, -e_{24}, -e_{34}\} \quad \text{where } e_{ij} = e_i + e_j.$$

Its matroid polytope P_M in \mathbb{R}^4 is a bipyramid with 4 minimal loopless faces, see Figure 2.1 left:

$$\begin{aligned} &\text{conv}(-e_{12}, -e_{13}, -e_{14}), \quad \text{conv}(-e_{12}, -e_{23}, -e_{24}), \\ &\text{conv}(-e_{13}, -e_{23}, -e_{34}), \quad \text{conv}(-e_{14}, -e_{24}, -e_{34}) \subseteq \text{conv}(S_{\text{lin}}). \end{aligned}$$

Its Bergman fan $\Sigma_{S_{\text{lin}}}(0)$ in \mathbb{R}^4 is invariant under translation by $\mathbb{R} \cdot (1, 1, 1, 1)$ and is made up of 4 maximal cones, see Figure 2.1 right:

$$\mathbb{R}_{\geq 0} \cdot e_1 + \mathbb{R} \cdot (1, 1, 1, 1), \quad \mathbb{R}_{\geq 0} \cdot e_2 + \mathbb{R} \cdot (1, 1, 1, 1),$$

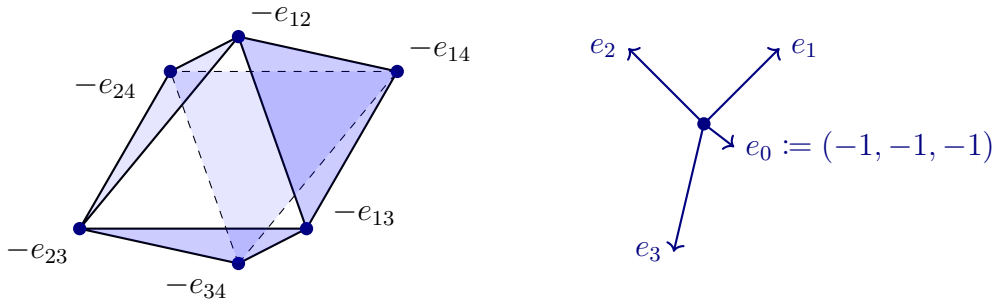


Figure 2.1: The matroid polytope P_M for the uniform matroid $U_{4,2}$ (left) with minimal loopless faces shaded in blue, and its Bergman fan (right). The pictures show the projection of the matroid polytope onto the hyperplane $x_4 = 0$, and the intersection of the Bergman fan with the hyperplane $x_4 = 0$.

$$\mathbb{R}_{\geq 0} \cdot e_3 + \mathbb{R} \cdot (1, 1, 1, 1), \quad \mathbb{R}_{\geq 0} \cdot e_4 + \mathbb{R} \cdot (1, 1, 1, 1).$$

We note the following fact that will be important in Section 2.4. We have $\Sigma_{S_{\text{lin}}}(0) = \text{Trop}(\langle l_1, l_2 \rangle)$, where $l_1 = c_{1,1}x_1 + \cdots + c_{1,4}x_4$, $l_2 = c_{2,1}x_1 + \cdots + c_{2,4}x_4 \in \mathbb{Q}[x_1, \dots, x_4]$ and the $c_{i,j} \in \mathbb{Q}$ are generic.

Example 2.2.5.

1. Let $S_3 := \{(0, 0, 0, 1), (0, 0, 0, 0)\} \subseteq \mathbb{Z}^4$ and $c_3 := (0, 0) \in \mathbb{T}^{S_3}$. Then S_4 has a single dual cell candidate $s_3 := S_3$, which is why tropical hypersurface $\Sigma_{S_3}(c_3)$ consists solely of the tropical polyhedron $\sigma_{S_3}(s_3, c_3) = (e_4)^\perp$, the hyperplane used in the illustration of Figure 2.1.
2. Let $S_4 := \{(1, 1, 1, 0), (0, 0, 0, 0)\} \subseteq \mathbb{Z}^4$ and $c_{4,t} := (0, t) \in \mathbb{T}^{S_4}$ for $t \in \mathbb{R}$. Then S_4 has a single dual cell candidate $s_4 := S_4$, which is why the tropical hypersurface $\Sigma_{S_4}(c_{4,t})$ consists solely of the tropical polyhedron $\sigma_{S_4}(s_4, c_{4,t}) = (e_1 + e_2 + e_3)^\perp + \frac{1}{3}(t, t, t, 0)$. In particular, $\sigma_{S_4}(s_4, c_{4,t})$ goes through the points $\frac{1}{3}(t, t, t, 0)$, $(t, 0, 0, 0)$, $(0, t, 0, 0)$, and $(0, 0, t, 0)$.
3. Let $S_4 := \{(1, 1, 0, 0), (0, 0, 0, 0)\} \subseteq \mathbb{Z}^4$ and $c_{4,t} := (0, t) \in \mathbb{T}^{S_4}$ for $t \in \mathbb{R}$. Then S_4 has a single dual cell candidate $s_4 := S_4$, which is why tropical hypersurface $\Sigma_{S_4}(c_{4,t})$ consists solely of the tropical polyhedron $\sigma_{S_4}(s_4, c_{4,t}) =$

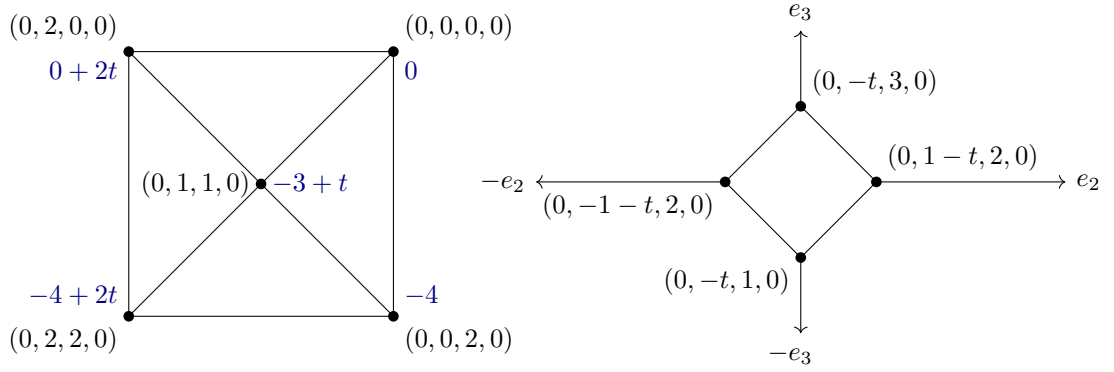


Figure 2.2: The dual subdivision $D_{S_4}(c_{4,t})$ and tropical hypersurface $\Sigma_{S_4}(c_{4,t})$ of Example 2.2.5 (4). Not illustrated is the invariance of $\Sigma_{S_4}(c_{4,t})$ under translation by $\text{Span}(e_1, e_4)$ as $D_{S_4}(c_{4,t})$ is contained in $\text{Span}(e_1, e_4)^\perp$. The illustrated rays of $\Sigma_{S_4}(c_{4,t})$ have multiplicity 2.

$(e_1 + e_2)^\perp + \frac{1}{2}(t, t, 0, 0)$. In particular, $\sigma_{S_4}(s_4, c_{4,t})$ goes through the points $\frac{1}{2}(t, t, t, 0)$, $(t, 0, 0, 0)$ and $(0, t, 0, 0)$.

4. Let

$$S_4 := \{(0, 0, 0, 0), (0, 1, 1, 0), (0, 2, 0, 0), (0, 0, 2, 0), (0, 2, 2, 0)\} \subseteq \mathbb{Z}^4,$$

$$c_{4,t} := (0, -3, 0, -4, -4) + (0, t, 2t, 0, 2t) \in \mathbb{T}^{S_4} \quad \text{for } t \in \mathbb{R}.$$

Then the dual subdivision $D_{S_4}(c_{4,t})$ is independent of t , consisting of 8 edges that form the edge graph of a square pyramid, see Figure 2.2. The combinatorics of the tropical hypersurface $\Sigma_{S_4}(c_{4,t})$ is therefore equally independent of t . As $D_{S_4}(c_{4,t})$ is contained in $\text{Span}(e_1, e_4)^\perp$, $\Sigma_{S_4}(c_{4,t})$ is invariant under translation by $\text{Span}(e_1, e_4)$. As t varies, $\Sigma_{S_4}(c_{4,t})$ moves in direction $\pm e_2$. This is easiest seen from the fact that

$$\Sigma_{S_4}(c_{4,t}) = \text{Trop}(f(x_1, t \odot x_2, x_3, x_4))$$

$$\text{for } f := 0 \oplus (-3) \odot x_2 x_3 \oplus x_2^2 \oplus (-4) \odot x_3^2 \oplus (-4) \odot x_2^2 x_3^2,$$

where $\text{Trop}(\cdot)$ denotes the tropical hypersurface of a tropical polynomial.

2.2.2 Mixed cells and stable intersections

In this section, we fix the notation regarding mixed cells and stable intersections. For the sake of simplicity, we introduce stable intersections as in [MS15, Definition 3.6.11 and Proposition 3.6.12].

Definition 2.2.6. Let $\sigma_1, \dots, \sigma_\ell$ be polyhedra in \mathbb{R}^n . We say $\sigma_1, \dots, \sigma_\ell$ intersect *transversally*, if $\sigma_1 \cap \dots \cap \sigma_\ell \neq \emptyset$ and for all faces $\tau_i \subseteq \sigma_i$ we have

$$\tau_1 \cap \dots \cap \tau_\ell \neq \emptyset \implies \text{codim}(\tau_1 \cap \dots \cap \tau_\ell) = \text{codim}(\tau_1) + \dots + \text{codim}(\tau_\ell).$$

Let $\Sigma_1, \dots, \Sigma_\ell$ be pure polyhedral complexes in \mathbb{R}^n . We say $\Sigma_1, \dots, \Sigma_\ell$ intersect *transversally*, if for all polyhedra $\sigma_i \in \Sigma_i$ either $\sigma_1, \dots, \sigma_\ell$ are disjoint or $\sigma_1, \dots, \sigma_\ell$ intersect transversally.

Definition 2.2.7. The *stable intersection* of two transversally intersecting balanced polyhedral complexes Σ_1, Σ_2 in \mathbb{R}^n is the polyhedral complex

$$\Sigma_1 \wedge \Sigma_2 := \{\sigma_1 \cap \sigma_2 \mid \sigma_1 \in \Sigma_1 \text{ and } \sigma_2 \in \Sigma_2\}$$

equipped with the multiplicities given for each $\tau = \sigma_1 \cap \sigma_2$ by

$$\text{mult}_{\Sigma_1 \wedge \Sigma_2}(\tau) := \text{mult}_{\Sigma_1}(\sigma_1) \cdot \text{mult}_{\Sigma_2}(\sigma_2) \cdot [N_\tau : N_{\sigma_1} + N_{\sigma_2}],$$

where $N := \mathbb{Z}^n$ and $[\cdot : \cdot]$ denotes the index of sublattices, where for any polyhedron $\sigma \subset \mathbb{R}^n$, the associated lattice is defined by

$$N_\sigma := \text{Span}_{\mathbb{Z}} \{v_1 - v_2 \mid v_1, v_2 \in \sigma \cap N\}.$$

The *stable intersection* of any two balanced polyhedral complexes Σ_1, Σ_2 in \mathbb{R}^n is

$$\Sigma_1 \wedge \Sigma_2 := \lim_{\varepsilon \rightarrow 0} \Sigma_1 \wedge (\varepsilon \cdot v + \Sigma_2),$$

where $v \in \mathbb{R}^n$ is chosen such that Σ_1 and $\varepsilon \cdot v + \Sigma_2$ intersect transversally.

Note that Definition 2.2.7 is independent of the choice of v by [MS15, Proposition 3.6.12]. Moreover, $\Sigma_1 \wedge \Sigma_2$ is either empty or a balanced polyhedral complex

of codimension $\text{codim}(\Sigma_1 \wedge \Sigma_2) = \text{codim}(\Sigma_1) + \text{codim}(\Sigma_2)$ [MS15, Theorem 3.6.10] and $\Sigma_1 \wedge (\Sigma_2 \wedge \Sigma_3) = (\Sigma_1 \wedge \Sigma_2) \wedge \Sigma_3$ for balanced polyhedral complexes $\Sigma_1, \Sigma_2, \Sigma_3$ [MS15, Remark 3.6.4]. The latter allows us to write $\Sigma_1 \wedge \Sigma_2 \wedge \Sigma_3$ without specifying the order of operations.

Definition 2.2.8. We refer to the disjoint union $\mathbf{S} := S_{\text{lin}} \sqcup \bigsqcup_{i=k+1}^n S_i$ as the *mixed support*, a product of dual heights $\mathbf{c} := (0, c_{k+1}, \dots, c_n) \in \{0\} \times \prod_{i=k+1}^n \mathbb{T}^{S_i}$ as a *mixed height*, and the space of dual heights $\mathbb{H}^{\mathbf{S}} := \{0\} \times \prod_{i=k+1}^n \mathbb{T}^{S_i}$ as the *mixed height space*. We also abbreviate $\mathbb{H}_{\mathbb{R}}^{\mathbf{S}} := \{0\} \times \prod_{i=k+1}^n \mathbb{R}^{S_i}$.

Definition 2.2.9. A *mixed cell candidate* is a subset $\mathbf{s} = s_{\text{lin}} \sqcup \bigsqcup_{i=k+1}^n s_i \subseteq \mathbf{S}$, where $s_{\text{lin}}, s_{k+1}, \dots, s_n$ are dual cell candidates. A mixed cell candidate $\mathbf{s} \subseteq \mathbf{S}$ is a *mixed cell* induced by a mixed height $\mathbf{c} \in \mathbb{H}^{\mathbf{S}}$, if $\text{conv}(s_{\text{lin}} + s_{k+1} + \dots + s_n)$ is a cell in the regular subdivision of $S_{\text{lin}} + S_{k+1} + \dots + S_n$ induced by the coefficients of $f_{\mathbf{s}}(\mathbf{c}) := f_{S_{\text{lin}}}(c_{\text{lin}}) \odot (\odot_{i=k+1}^n f_{S_i}(c_i))$. We denote the set of all mixed cells induced by \mathbf{c} by

$$D_{\mathbf{S}}(\mathbf{c}) := \{\mathbf{s} \subseteq \mathbf{S} \mid \mathbf{s} \text{ mixed cell induced by } \mathbf{c}\}.$$

A mixed cell $\mathbf{s} \in D_{\mathbf{S}}(\mathbf{c})$ is *transverse*, if $s_{\text{lin}} \in D_{S_{\text{lin}}}(0)$ and all $s_i \in D_{S_i}(c_i)$ are minimal. We say $D_{\mathbf{S}}(\mathbf{c})$ is *transverse*, if all $\mathbf{s} \in D_{\mathbf{S}}(\mathbf{c})$ are transverse under \mathbf{c} .

Definition 2.2.10. Fix a mixed height $\mathbf{c} \in \mathbb{H}^{\mathbf{S}}$. Then any mixed cell $\mathbf{s} = s_{\text{lin}} \sqcup \bigsqcup_{i=1}^k s_i \in D_{\mathbf{S}}(\mathbf{c})$ defines a tropical polyhedron $\sigma_{\mathbf{S}}(\mathbf{c}, \mathbf{s}) \subseteq \mathbb{R}^n$ by

$$\sigma_{\mathbf{S}}(\mathbf{c}, \mathbf{s}) := \{w \in \mathbb{R}^n \mid \text{the minimum in } f_{\mathbf{S}(\mathbf{c})}(w) \text{ is attained at } s_{\text{lin}} + s_{k+1} + \dots + s_n\}.$$

The polyhedral complex $\Sigma_{\mathbf{S}}(\mathbf{c})$ is the set of all such polyhedra:

$$\Sigma_{\mathbf{S}}(\mathbf{c}) := \{\sigma_{\mathbf{S}}(\mathbf{c}, \mathbf{s}) \mid \mathbf{s} \in D_{\mathbf{S}}(\mathbf{c})\}.$$

Example 2.2.11. Consider

- $S_{\text{lin}} := \{-e_{ij} \mid 1 \leq i < j \leq 4\}$, $c_{\text{lin}} = 0$ from Example 2.2.4,
- $S_3 := \{(0, 0, 0, 1), (0, 0, 0, 0)\}$, $c_3 := (0, 0)$ from Example 2.2.5 (1),

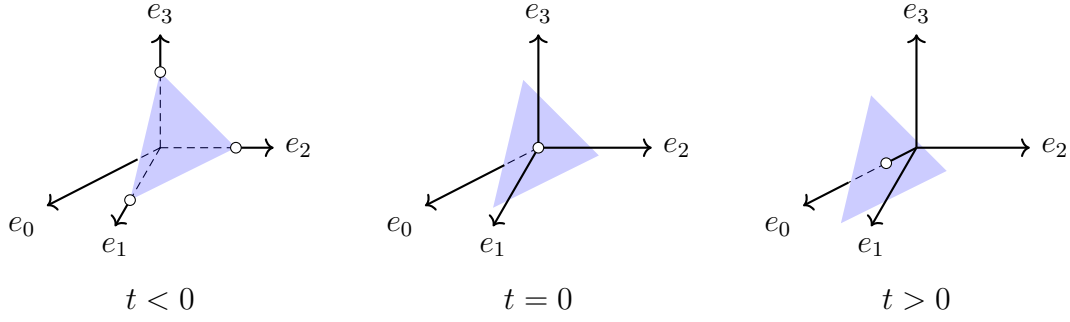


Figure 2.3: $\Sigma_{S_{\text{lin}}}(0) \cap \Sigma_{S_3}(c_3) \cap \Sigma_{S_4}(c_{4,t})$ from Example 2.2.11. The rays represent $\Sigma_{S_{\text{lin}}}(0) \cap \Sigma_{S_3}(c_3)$ while the shaded area represents $\Sigma_{S_4}(c_{4,t})$ for various t . The white points are stable intersection points.

- $S_4 := \{(1, 1, 1, 0), (0, 0, 0, 0)\}$, $c_{4,t} := (0, t)$ from Example 2.2.5 (2).

Then $\Sigma_{S_{\text{lin}}}(0)$ and $\Sigma_{S_3}(c_3)$ intersect transversally and their intersection consists of four rays generated by e_1 , e_2 , e_3 , and $e_0 = -e_1 - e_2 - e_3$ as illustrated in Figure 2.1.

Hence, we have

$$\Sigma_{S_{\text{lin}}}(0) \cap \Sigma_{S_3}(c_3) \cap \Sigma_{S_4}(c_{4,t}) = \begin{cases} \{\frac{1}{3}(t, t, t, 0)\} & \text{if } t \leq 0, \\ \{(t, 0, 0, 0), (0, t, 0, 0), (0, 0, t, 0)\} & \text{if } t \geq 0, \end{cases}$$

and the intersection is transverse for $t \neq 0$, see Figure 2.3. For the mixed cells, one can verify that

$$D_{\mathbf{S}}(\mathbf{c}_t) = \begin{cases} \{\{-e_{14}, -e_{24}, -e_{34}\} \sqcup S_3 \sqcup S_4\} & \text{if } t \leq 0, \\ \{S_{\text{lin}} \sqcup S_3 \sqcup S_4\} & \text{if } t = 0, \\ \{\{-e_{12}, -e_{13}, -e_{14}\} \sqcup S_3 \sqcup S_4, \{-e_{12}, -e_{23}, -e_{24}\} \sqcup S_3 \sqcup S_4, \\ \{-e_{13}, -e_{23}, -e_{34}\} \sqcup S_3 \sqcup S_4\} & \text{if } t \geq 0, \end{cases}$$

where $\mathbf{S} := S_{\text{lin}} \sqcup S_3 \sqcup S_4$ and $\mathbf{c} := (0, c_3, c_{4,t})$.

Example 2.2.12. Consider

- $S_{\text{lin}} := \{-e_{ij} \mid 1 \leq i < j \leq 4\}$, $c_{\text{lin}} = 0$ from Example 2.2.4,
- $S_3 := \{(0, 0, 0, 1), (0, 0, 0, 0)\}$, $c_3 := (0, 0)$ from Example 2.2.5 (1),

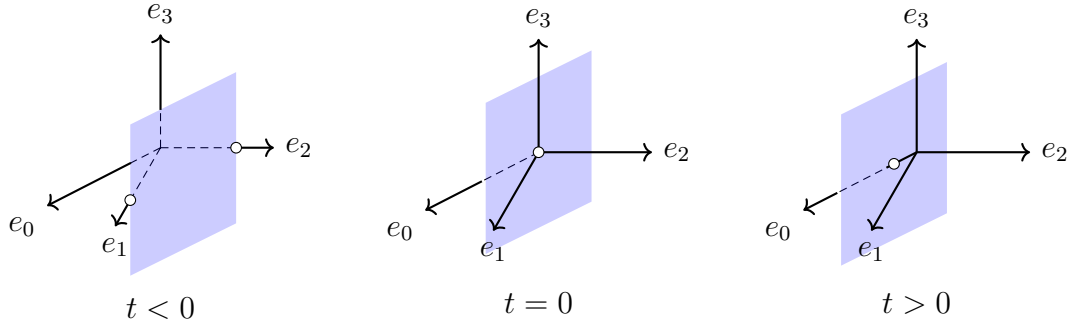


Figure 2.4: $\Sigma_{S_{\text{lin}}}(0) \cap \Sigma_{S_3}(c_3) \cap \Sigma_{S_4}(c_{4,t})$ from Example 2.2.12. The rays represent $\Sigma_{S_{\text{lin}}}(0) \cap \Sigma_{S_3}(c_3)$ while the shaded area represents $\Sigma_{S_4}(c_{4,t})$ for various t . The white points are stable intersection points. At $t = 0$ the ray $\mathbb{R}_{\geq 0} \cdot e_3$ lies on $\Sigma_{S_4}(c_{4,t})$.

- $S_4 := \{(1, 1, 0, 0), (0, 0, 0, 0)\}$, $c_{4,t} := (0, t)$ from Example 2.2.5 (3).

Then $\Sigma_{S_{\text{lin}}}(0)$ and $\Sigma_{S_3}(c_3)$ intersect transversally and their intersection consists of four rays generated by e_1 , e_2 , e_3 , and $e_0 = -e_1 - e_2 - e_3$ as illustrated in Figure 2.1.

Hence, we have:

$$\Sigma_{S_{\text{lin}}}(0) \cap \Sigma_{S_3}(c_3) \cap \Sigma_{S_4}(c_{4,t}) = \begin{cases} \{\frac{1}{3}(t, t, t, 0)\} & \text{if } t \leq 0, \\ \{(t, 0, 0, 0), (0, t, 0, 0)\} & \text{if } t \geq 0, \end{cases}$$

and the intersection is transverse for $t \neq 0$, see Figure 2.4. For the mixed cells, one can verify that

$$D_{\mathbf{S}}(\mathbf{c}_t) = \begin{cases} \{\{-e_{14}, -e_{24}, -e_{34}\} \sqcup S_3 \sqcup S_4\} & \text{if } t \leq 0, \\ \{S_{\text{lin}} \sqcup S_3 \sqcup S_4\} & \text{if } t = 0, \\ \{\{-e_{12}, -e_{13}, -e_{14}\} \sqcup S_3 \sqcup S_4, \{-e_{12}, -e_{23}, -e_{24}\} \sqcup S_3 \sqcup S_4\} & \text{if } t \geq 0, \end{cases}$$

where $\mathbf{S} := S_{\text{lin}} \sqcup S_3 \sqcup S_4$ and $\mathbf{c} := (0, c_3, c_{4,t})$.

Example 2.2.13. Consider

- $S_{\text{lin}} := \{-e_{ij} \mid 1 \leq i < j \leq 4\}$, $c_{\text{lin}} = 0$ from Example 2.2.4,
- $S_3 := \{(0, 0, 0, 1), (0, 0, 0, 0)\}$, $c_3 := (0, 0)$ from Example 2.2.5 (1),

- and the following from Example 2.2.5 (4).

$$S_4 := \{(0, 0, 0, 0), (0, 1, 1, 0), (0, 2, 0, 0), (0, 0, 2, 0), (0, 2, 2, 0)\} \subseteq \mathbb{Z}^4,$$

$$c_{4,t} := (0, -3, 0, -4, -4) + (0, t, 2t, 0, 2t) \in \mathbb{T}^{S_4} \quad \text{for } t \in \mathbb{R}.$$

Then $\Sigma_{S_{\text{lin}}}(0)$ and $\Sigma_{S_3}(c_3)$ intersect transversally and their intersection consists of four rays generated by e_1, e_2, e_3 , and $e_0 = -e_1 - e_2 - e_3$ as illustrated in Figure 2.1.

Lemma 2.2.4 *Let $\mathbf{c} := (0, c_{k+1}, \dots, c_n) \in \mathbb{H}^{\mathbf{S}}$ be a mixed height. For any mixed cell $\mathbf{s} := s_{\text{lin}} \sqcup \bigsqcup_{i=k+1}^n s_i \in D_{\mathbf{S}}(\mathbf{c})$ we have the equality of polyhedra*

$$\sigma_{\mathbf{S}}(\mathbf{c}, \mathbf{s}) = \sigma_{S_{\text{lin}}}(0, s_{\text{lin}}) \cap \sigma_{S_{k+1}}(c_{k+1}, s_{k+1}) \cap \dots \cap \sigma_{S_n}(c_n, s_n).$$

Moreover, $\sigma_{S_{\text{lin}}}(0, s_{\text{lin}}), \sigma_{S_{k+1}}(c_{k+1}, s_{k+1}), \dots, \sigma_{S_n}(c_n, s_n)$ intersect transversally if and only if $\mathbf{s} \in D_{\mathbf{S}}(\mathbf{c})$ is transverse.

Proof. For the “ \subseteq ” inclusion, consider $w \in \sigma_{\mathbf{S}}(\mathbf{c}, \mathbf{s})$, i.e., $w \in \mathbb{R}^n$ such that the minimum in $f_{\mathbf{S}(\mathbf{c})}(w)$ is attained at $s_{\text{lin}} + s_{k+1} + \dots + s_n$.

Assume that the minimum in $f_{S_i}(c_i)$ is not attained at s_i for some $i = k+1, \dots, n$, say $i = n$, which means that there are $\alpha, \beta \in s_n$ such that $c_{n,\alpha} + w \cdot \alpha < c_{n,\beta} + w \cdot \beta$. Consequently, for all $\gamma_{\text{lin}} \in S_{\text{lin}}$ and $\gamma_i \in S_i$ we have

$$\begin{aligned} & (c_{\text{lin},\gamma_{\text{lin}}} + c_{k+1,\gamma_{k+1}} + \dots + c_{n-1,\gamma_{n-1}} + c_{n,\alpha}) + w \cdot (\gamma_{\text{lin}} + \gamma_{k+1} + \dots + \gamma_{n-1} + \alpha) \\ & < (c_{\text{lin},\gamma_{\text{lin}}} + c_{k+1,\gamma_{k+1}} + \dots + c_{n-1,\gamma_{n-1}} + c_{n,\beta}) + w \cdot (\gamma_{\text{lin}} + \gamma_{k+1} + \dots + \gamma_{n-1} + \beta) \end{aligned} \quad (2.2.1)$$

contradicting that the minimum in $f_{\mathbf{S}(\mathbf{c})}(w)$ is attained at $s_{\text{lin}} + s_{k+1} + \dots + s_n$. Hence the minimum in $f_{S_i}(c_i)$ has to be attained at s_i , and one can similarly show that the minimum in $f_{S_{\text{lin}}}(c_{\text{lin}})$ is attained in s_{lin} . Thus $w \in \sigma_{S_{\text{lin}}}(0, s_{\text{lin}}) \cap \sigma_{S_{k+1}}(c_{k+1}, s_{k+1}) \cap \dots \cap \sigma_{S_n}(c_n, s_n)$.

For the “ \supseteq ” inclusion, consider $w \in \sigma_{S_{\text{lin}}}(0, s_{\text{lin}}) \cap \sigma_{S_{k+1}}(c_{k+1}, s_{k+1}) \cap \dots \cap \sigma_{S_n}(c_n, s_n)$, i.e., $w \in \mathbb{R}^n$ such that the minimum in $f_{S_{\text{lin}}}(c_{\text{lin}})$ and $f_{S_i}(c_i)$ are attained at s_{lin} and s_i , respectively.

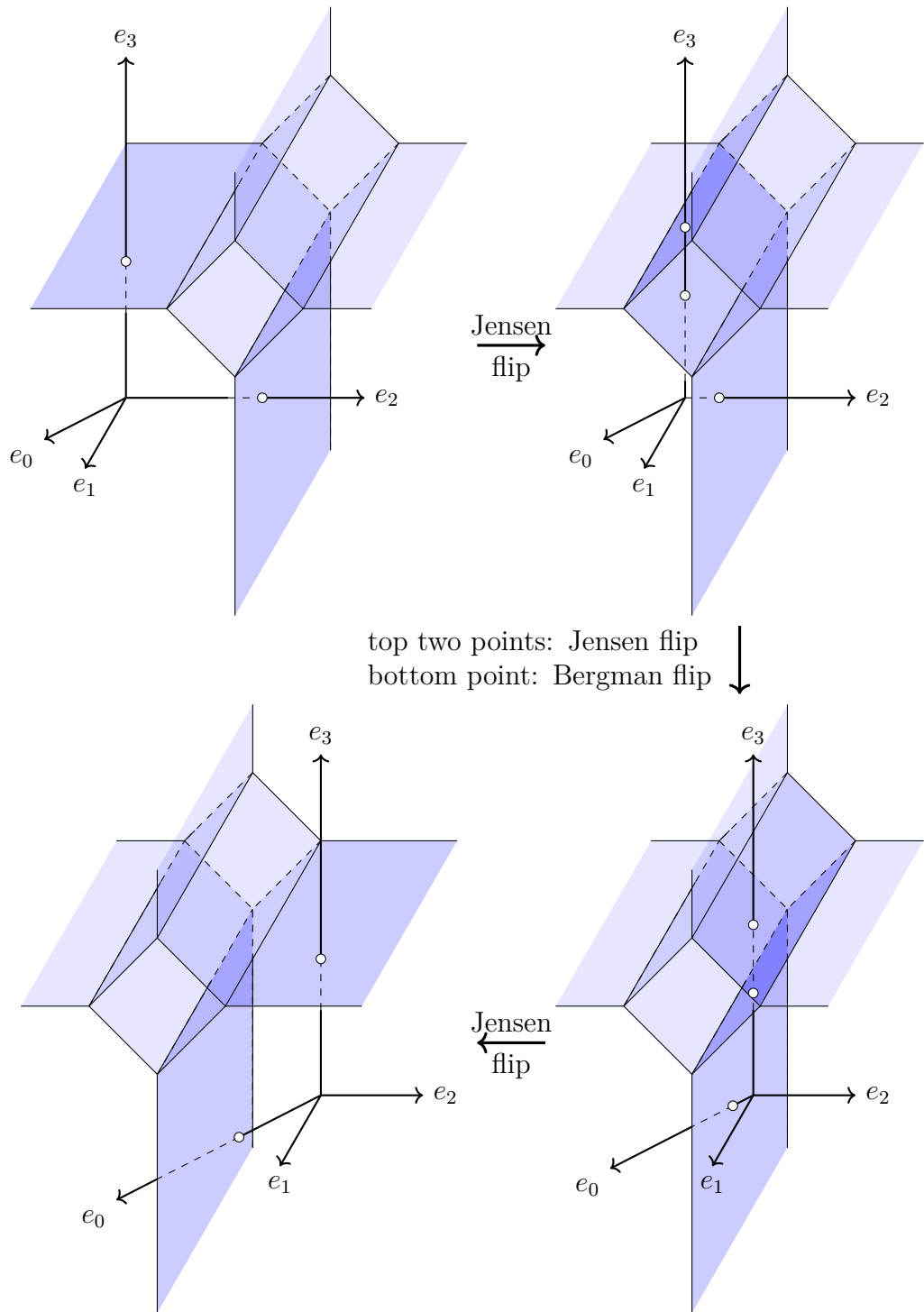


Figure 2.5: $\Sigma_{S_{\text{lin}}}(0) \cap \Sigma_{S_3}(c_3) \cap \Sigma_{S_4}(c_{4,t})$ from Example 2.2.13. The rays represent $\Sigma_{S_{\text{lin}}}(0) \cap \Sigma_{S_3}(c_3)$ while the shaded area represents $\Sigma_{S_4}(c_{4,t})$ for various t . The white points are stable intersection points.

Assume that the minimum in $f_{\mathbf{s}(\mathbf{c})}(w)$ is not attained at $s_{\text{lin}} + s_{k+1} + \cdots + s_n$, which means there are $\alpha, \beta \in s_{\text{lin}}$ or $\alpha, \beta \in s_i$ such that Equation (2.2.1) holds for all valid γ . Using the same argument, it follows that the minimum in $f_{S_{\text{lin}}}(w)$ is not attained at s_{lin} or the minimum in some $f_{S_i}(w)$ is not attained at s_i , contradicting our initial assumptions. This completes the proof for the desired equality.

Now suppose $\sigma_{S_{\text{lin}}}(0, s_{\text{lin}}), \sigma_{S_{k+1}}(c_{k+1}, s_{k+1}), \dots, \sigma_{S_n}(c_n, s_n)$ intersect transversally. As $\text{codim}(\sigma_{S_{\text{lin}}}) \geq k$ and $\text{codim}(\sigma_{S_i}(c_i, s_i)) \geq 1$, this necessarily implies $\text{codim}(\sigma_{S_{\text{lin}}}) = k$ and $\text{codim}(\sigma_{S_i}(c_i, s_i)) = 1$, which in turn implies that $s_{\text{lin}} \in D_{S_{\text{lin}}}(0)$ and $s_i \in D_{S_i}(c_i)$ are minimal. Moreover, no proper faces of the σ may intersect, which implies that $\mathbf{s} \in D_{\mathbf{S}}(\mathbf{c})$ is minimal. Hence $\mathbf{s} \in D_{\mathbf{S}}(\mathbf{c})$ is transverse. The converse follows similarly. \square

Corollary 2.2.5 *Let $\mathbf{c} = (0, c_{k+1}, \dots, c_n) \in \mathbb{H}^{\mathbf{S}}$ be a mixed height. We have the equality of subsets of \mathbb{R}^n*

$$|\Sigma_{\mathbf{S}}(\mathbf{c})| = |\Sigma_{S_{\text{lin}}}(0) \wedge \Sigma_{S_{k+1}}(c_{k+1}) \wedge \cdots \wedge \Sigma_{S_n}(c_n)|,$$

and $\Sigma_{S_{\text{lin}}}(0), \Sigma_{S_{k+1}}(c_{k+1}), \dots, \Sigma_{S_n}(c_n)$ intersect transversally if and only if $D_{\mathbf{S}}(\mathbf{c})$ is transverse.

Example 2.2.14. The intersection of a Bergman fan and a binomial hypersurface is shown in Figure 2.6.

Next, we state an important lemma that shows how $\sigma_{\mathbf{S}}(\mathbf{s}, \mathbf{c})$ can be computed from \mathbf{s} and \mathbf{c} only.

Lemma 2.2.6 *Let $\mathbf{s} = (s_{\text{lin}}, s_{k+1}, \dots, s_n) \in D_{\mathbf{S}}(\mathbf{c})$ be a transverse mixed cell induced by $\mathbf{c} = (0, c_{k+1}, \dots, c_n)$. In particular, this means $s_i = \{\alpha_i, \beta_i\}$ for $\alpha_i \neq \beta_i$. Let $A_{\mathbf{s}}$ be the matrix with rows*

1. $\alpha_{\text{lin}} - \beta_{\text{lin}} \in \mathbb{R}^n$ for some fixed $\alpha_{\text{lin}} \in s_{\text{lin}}$ and $\beta_{\text{lin}} \in s_{\text{lin}} \setminus \{\alpha_{\text{lin}}\}$,
2. $\alpha_i - \beta_i \in \mathbb{R}^n$ for $i = k+1, \dots, n$,

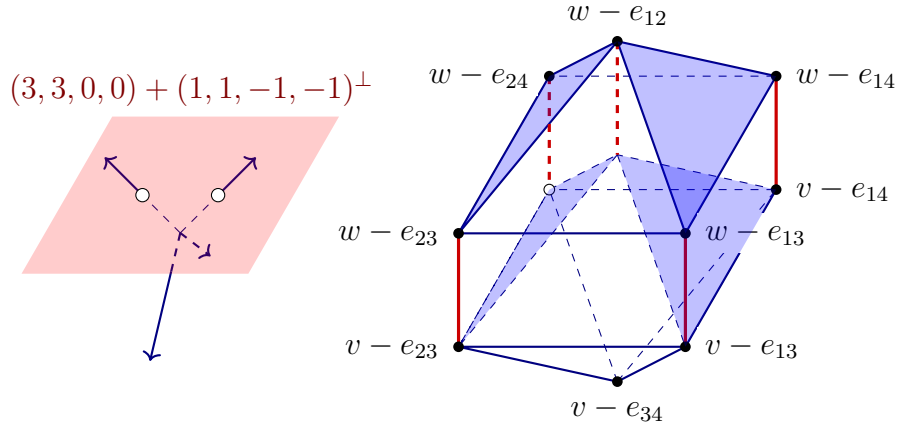


Figure 2.6: Bergman fan and hypersurface with two intersection points and mixed cells.

and let $b_{\mathbf{c}}$ be the vector with entries

1. $0 \in \mathbb{R}$ for each $\beta_{\text{lin}} \in s_{\text{lin}} \setminus \{\alpha_{\text{lin}}\}$,
2. $c_{i,\alpha_i} - c_{i,\beta_i} \in \mathbb{R}$ for $i = k + 1, \dots, n$.

Then $A_{\mathbf{s}}$ has a left-inverse $A_{\mathbf{s}}^{-1}$, i.e., $A_{\mathbf{s}}^{-1} \cdot A_{\mathbf{s}} = \text{Id}_n$, and $\{A_{\mathbf{s}}^{-1} \cdot b_{\mathbf{c}}\} = \sigma_{\mathbf{S}}(\mathbf{s}, \mathbf{c})$.

Proof. As $\mathbf{s} \in D_{\mathbf{S}}(\mathbf{c})$ is transverse, $A_{\mathbf{s}}$ is of full-rank and $\sigma_{\mathbf{S}}(\mathbf{s}, \mathbf{c})$ is a point in the relative interior of $\sigma_{S_{\text{lin}}}(s_{\text{lin}}, 0)$ and all $\sigma_{S_i}(s_i, c_i)$, say $\sigma_{\mathbf{S}}(\mathbf{s}, \mathbf{c}) = \{w\}$. From the fact $A_{\mathbf{s}}$ is of full rank, we see that $A_{\mathbf{s}}$ must have a left-inverse $A_{\mathbf{s}}^{-1}$. From the fact $\sigma_{\mathbf{S}}(\mathbf{s}, \mathbf{c})$ is a point, we have that

$$\sigma_{S_{\text{lin}}}(s_{\text{lin}}, 0) \cap \bigcap_{i=k+1}^n \sigma_{S_i}(s_i, c_i) = \text{AffineSpan}(\sigma_{S_{\text{lin}}}(s_{\text{lin}}, 0)) \cap \bigcap_{i=k+1}^n \text{AffineSpan}(\sigma_{S_i}(s_i, c_i)),$$

and consequently $A_{\mathbf{s}} \cdot w = b_{\mathbf{c}}$. Combining both yields the statement of the lemma. \square

Corollary 2.2.7 *Let $\mathbf{s} = (s_{\text{lin}}, s_{k+1}, \dots, s_n) \in D_{\mathbf{S}}(\mathbf{c} + \varepsilon \cdot \mathbf{u})$ be a mixed cell induced by $\mathbf{c} + \varepsilon \cdot \mathbf{u}$ for $\mathbf{c} = (0, c_{k+1}, \dots, c_n)$ and $\varepsilon > 0$ sufficiently small. Assume further that \mathbf{s} is transverse, so that $s_i = \{\alpha_i, \beta_i\}$ with $\alpha_i \neq \beta_i$. Let $A_{\mathbf{s}}$ be the matrix with rows*

1. $\alpha_{\text{lin}} - \beta_{\text{lin}} \in \mathbb{R}^n$ for some fixed $\alpha_{\text{lin}} \in s_{\text{lin}}$ and $\beta_{\text{lin}} \in s_{\text{lin}} \setminus \{\alpha_{\text{lin}}\}$,
2. $\alpha_i - \beta_i \in \mathbb{R}^n$ for $i = k + 1, \dots, n$,

and let $b_{\mathbf{c}}$ be the vector with entries

1. $0 \in \mathbb{R}$ for each $\beta_{\text{lin}} \in s_{\text{lin}} \setminus \{\alpha_{\text{lin}}\}$,
2. $c_{i,\alpha_i} - c_{i,\beta_i} \in \mathbb{R}$ for $i = k + 1, \dots, n$.

Then $A_{\mathbf{s}}$ has a left-inverse $A_{\mathbf{s}}^{-1}$, i.e., $A_{\mathbf{s}}^{-1} \cdot A_{\mathbf{s}} = \text{Id}_n$, and

$$A_{\mathbf{s}}^{-1} \cdot b_{\mathbf{c}} \in \sigma_{\mathbf{S}}(\mathbf{s}, \mathbf{c}) \cap \left(\Sigma_{S_{\text{lin}}}(0) \wedge \bigwedge_{i=k+1}^n \Sigma_{S_i}(c_i) \right).$$

Proof. Follows from Lemma 2.2.6 and the description of stable intersections given in Proposition 2.2.8. \square

We conclude this section with an alternate description of stable intersections via dual height perturbations.

Proposition 2.2.8 *Let Σ_1, Σ_2 be two balanced polyhedral complexes, and suppose $\Sigma_2 = \Sigma_S(c)$ arises from dual support $S \subseteq \mathbb{Z}^n$ and dual height $c \in \mathbb{T}^S$. Then there is an open dense subset $U \subseteq \mathbb{R}^S$ such that Σ_1 and $\Sigma(c + \varepsilon \cdot u)$ are transverse for $\varepsilon > 0$ sufficiently small and $u \in U$. Moreover, we have*

$$\Sigma_1 \wedge \Sigma_2 = \lim_{\varepsilon \rightarrow 0} \Sigma_1 \wedge \Sigma_S(c + \varepsilon \cdot u). \quad (2.2.2)$$

Proof. Without loss of generality, we may assume $c \in \mathbb{R}^S$. To show the existence of an open dense subset $U \subseteq \mathbb{R}^S$, consider any subset $s \subseteq S$ that is maximal-dimensional in the sense that $\dim(\text{conv}(s)) = \dim(\text{conv}(S))$. Any $c' \in \mathbb{R}^S$ defines a hyperplane $H(s, c) = \{w \in \mathbb{R}^n \mid c'_\alpha + \alpha \cdot w = c'_\beta + \beta \cdot w \text{ for all } \alpha, \beta \in s\}$, which contains the cell $\sigma_S(s, c')$ if $s \in D_S(c')$. There is a Euclidean dense open subset of $U'_s \subseteq \mathbb{R}^S$ such that $H(s, c)$ is transverse to Σ_1 for all $c' \in U'_s$. Let $U' := \bigcap_{s \subseteq S \text{ maximal}} U'_s$. Then a valid choice for U is given by

$$U := \{u \in \mathbb{R}^S \mid c + \varepsilon \cdot u \in U' \text{ for } \varepsilon > 0 \text{ sufficiently small}\},$$

which is an open dense subset of \mathbb{R}^S because U' is open and dense.

We now show Equation (2.2.2) in two steps: First, that both sides coincide set-theoretically, and secondly that the multiplicities are the same. The set-theoretic equality follows from the fact that for any $s \subseteq S$ the map

$$\{c' \in \mathbb{R}^S \mid s \in D_S(c')\} \rightarrow \{\text{sets in } \mathbb{R}^n\}, \quad c' \mapsto \sigma_S(s, c')$$

is continuous with respect to the Hausdorff metric, see e.g. [MS15, Section 3.6]. The equality of multiplicities follows from [AHR16, Theorem 5.7] combined with the fact that around every converging sequence of intersecting polyhedra the recession fans of $\Sigma_2 = \Sigma_S(c)$ and $\Sigma_S(c + \varepsilon \cdot u)$ coincide. \square

2.2.3 Fine structure on Bergman fans

The Bergman fan $\Sigma_{S_{\text{lin}}}(0)$ defined in Definition 2.2.3 is a subfan of the normal fan $\mathbf{N}(P_M)$ of the matroid polytope $P_M = \text{conv}(S_{\text{lin}})$. It is the coarsest possible polyhedral fan structure on its support $|\Sigma_{S_{\text{lin}}}(0)|$ and consistent with the definitions in [MS15, Section 4.2] and [Jos21, Section 10.8].

Working with $\Sigma_{S_{\text{lin}}}(0)$ however requires working with S_{lin} , which is something we want to avoid. We therefore introduce a second polyhedral structure known as the fine structure [AK06].

Definition 2.2.15. Any chain of flats of the matroid M

$$\emptyset \subsetneq F_1 \subsetneq \cdots \subsetneq F_r \subsetneq F_{r+1} = [n]$$

gives rise to a simplicial cone $\text{cone}(e_{F_1}, \dots, e_{F_{r+1}})$ where $e_{F_j} := \sum_{i \in F_j} e_i$. These cones form a simplicial fan with support $|\Sigma_{S_{\text{lin}}}(0)|$ [MS15, Theorem 4.2.6]. We call it the *fine (polyhedral) structure* on $|\Sigma_{S_{\text{lin}}}(0)|$ and denote it by $\Sigma_{S_{\text{lin}}}^{\text{fine}}(0)$.

Definition 2.2.16. We call a mixed height $\mathbf{c} \in C_{\mathbf{S}}(\mathbf{s})$ *finely generic* if the tropical intersection point $\sigma_{\mathbf{S}}(\mathbf{s}, \mathbf{c})$ lies in the interior of a maximal cone of the fine structure $\Sigma_{S_{\text{lin}}}(0)$.

Lemma 2.2.9 *Let $\mathbf{s} \subseteq \mathbf{S}$ be a mixed cell candidate. Then there is a open dense set $U \subseteq C_{\mathbf{S}}(\mathbf{s})$ such that \mathbf{c} is finely generic for all $\mathbf{c} \in U$.*

Proof. If $\mathbf{c} \in C_{\mathbf{S}}(\mathbf{s})$ is not finely generic, then $\sigma_{\mathbf{S}}(\mathbf{s}, \mathbf{c})$ lies on a 1-codimensional cone of the fine structure $\Sigma_{S_{\text{in}}}^{\text{fine}}(0)$. Let $\omega_1, \dots, \omega_\ell \in \mathbb{R}^n$ such that all 1-codimensional cones of $\Sigma_{S_{\text{in}}}^{\text{fine}}(0)$ lie in $\bigcup_{i=1}^{\ell} \omega_i^\perp$. Let $A_{\mathbf{s}, \mathbf{c}}^{-1}$ and $b_{\mathbf{c}}$ be the matrix and vector from Lemma 2.2.6 so that $\sigma_{\mathbf{S}}(\mathbf{s}, \mathbf{c}) = A_{\mathbf{s}, \mathbf{c}}^{-1} \cdot b_{\mathbf{c}}$. Recall that $A_{\mathbf{s}, \mathbf{c}}^{-1}$ only depends on which entries of \mathbf{c} are tropically non-zero, which means that $A_{\mathbf{s}, \mathbf{c}}^{-1} = A_{\mathbf{s}, \mathbf{c}'}^{-1} =: A_{\mathbf{s}}^{-1}$ for all $\mathbf{c}, \mathbf{c}' \in C_{\mathbf{S}}(\mathbf{s})$. Setting $U := C_{\mathbf{S}}(\mathbf{s}) \cap (A_{\mathbf{s}}^{-1})^{-1}(\bigcup_{i=1}^{\ell} \omega_i^\perp)$, U is an open dense subset of $C_{\mathbf{S}}(\mathbf{s})$, as $A_{\mathbf{s}, \mathbf{c}}^{-1}$ is the left inverse of $A_{\mathbf{s}, \mathbf{c}}$ and thus surjective. \square

Remark 2.2.10 Throughout this chapter, our intersection data includes a linear dual cell s_{in} which is dual to a maximal cone of the Bergman fan in which the tropical intersection point lies. In practice, however, we only keep track of the chain of flats that the tropical intersection point gives rise to.

Remark 2.2.11 Note that the mixed height space has a natural stratification

$$\mathbb{H}^{\mathbf{S}} = \bigsqcup_{\mathbf{S}' \subseteq \mathbf{S}} \mathbb{H}_{\mathbb{R}}^{\mathbf{S}'},$$

where $\mathbb{H}^{\mathbf{S}}$ is a natural space of mixed heights and each $\mathbb{H}_{\mathbb{R}}^{\mathbf{S}'}$ is a Euclidean space. This is important for the concept of mixed cell cones in Section 2.3, and we will discuss how to switch between the strata in Section 2.6.

We now restate Lemma 2.2.6 for chains of flats.

Lemma 2.2.12 *Let (\mathbf{s}, \mathbf{c}) be a transverse mixed cell whose tropical intersection point gives rise to the maximal chain of flats $\emptyset \subsetneq F_1 \subsetneq \dots \subsetneq F_k = [n]$. Let s_1, \dots, s_k where each $s_i =: \{\alpha_{i,1}, \alpha_{i,2}\} \subseteq \mathbb{Z}^n$ with*

$$\bigcap_{i=1}^k s_i^\perp = \text{Span}(e_{F_1}, \dots, e_{F_k}).$$

Let $A_{\mathbf{s}, \mathbf{c}}$ be the matrix with rows $\alpha_{i,1} - \alpha_{i,j} \in \mathbb{R}^n$ and let $b_{\mathbf{c}}$ be the vector with entries $c_{i,j} - c_{i,1} \in \mathbb{R}$, where $i \in \{0, k+1, \dots, n\}$ and $j \in \{2, \dots, r_i\}$ with $c_{i,j} \neq \infty$. Then

$A_{\mathbf{s},\mathbf{c}}$ has a left-inverse $A_{\mathbf{s},\mathbf{c}}^{-1}$, i.e., $A_{\mathbf{s},\mathbf{c}}^{-1} \cdot A_{\mathbf{s},\mathbf{c}} = \text{Id}_n$, and $\sigma_{\mathbf{S}}(\mathbf{s}, \mathbf{c}) = A_{\mathbf{s},\mathbf{c}}^{-1} \cdot b_{\mathbf{c}}$.

Proof. With reference to the proof of Lemma 2.2.6, the equations in $A_{\mathbf{s},\mathbf{c}}w = b_{\mathbf{c}}$ arising from the rows corresponding to s_{lin} correspond to requiring that w lies inside $\text{Span}(\sigma_{s_{\text{lin}}}(0))$. Since $\text{Span}(\sigma_{s_{\text{lin}}}(0)) = \text{Span}(e_{F_1}, \dots, e_{F_k})$, an equivalent condition is to ask that $w \in s_i^\perp$ for each i . Hence $\alpha_{i,1} \cdot w = \alpha_{i,2} \cdot w = 0$ which means $(\alpha_{i,1} - \alpha_{i,2}) \cdot w = 0$, exactly the equations induced by the rows we added. By dimensional considerations these new rows are linearly independent, so the new $A_{\mathbf{s},\mathbf{c}}$ must determine the same tropical point w . \square

2.3 The Cayley trick & mixed cell cones

Since our homotopy method boils down to detecting when mixed cells change, we would like a way to write down the conditions the mixed heights must satisfy to realise a mixed cell candidate \mathbf{s} as a mixed cell.

Definition 2.3.1. Let \mathbf{s} be a mixed cell candidate. We define the *mixed cell cone* to be the closure of all real mixed heights under which \mathbf{s} is a mixed cell:

$$C_{\mathbf{S}}(\mathbf{s}) := \text{cl}\left(\{\mathbf{c} \in \mathbb{H}_{\mathbb{R}}^{\mathbf{S}} \mid \mathbf{s} \in D_{\mathbf{S}}(\mathbf{c})\}\right),$$

where $\text{cl}(\cdot)$ denotes closure in the Euclidean topology.

Lemma 2.3.1 *The mixed cell cone $C_{\mathbf{S}}(\mathbf{s})$ is closed polyhedral cone for any mixed cell candidate \mathbf{s} . Moreover, $C_{\mathbf{S}}(\mathbf{s})$ is maximal-dimensional if and only if \mathbf{s} is minimal, in which case we also have for all $c \in \mathbb{H}_{\mathbb{R}}^{\mathbf{S}}$*

$$\mathbf{s} \in D_{\mathbf{S}}(\mathbf{c}) \quad \iff \quad \mathbf{c} \in \text{relint}(C_{\mathbf{S}}(\mathbf{s})).$$

Proof. Given a lift $\mathbf{c} \in \mathbb{H}_{\mathbb{R}}^{\mathbf{S}}$ inducing \mathbf{s} , it is clear that any positive scalar multiple $\lambda\mathbf{c}$ induces the same mixed cell \mathbf{s} . Thus $\text{relint}(C_{\mathbf{S}}(\mathbf{s}))$ is a cone. Taking the closure, we obtain a closed polyhedral cone.

If $\mathbf{c} \in \text{relint}(C_{\mathbf{S}}(\mathbf{s}))$, then by definition $\mathbf{s} \in D_{\mathbf{S}}(\mathbf{c})$. Conversely, if $\mathbf{s} \in D_{\mathbf{S}}(\mathbf{c})$, then since \mathbf{s} is minimal, \mathbf{c} induces a transverse intersection locally around \mathbf{s} . This property is generic (i.e. any perturbation of \mathbf{c} will also induce a transverse intersection) which shows that $\mathbf{c} \in \text{relint}(C_{\mathbf{S}}(\mathbf{s}))$. \square

Since \mathbf{s} is a cell in a mixed subdivision of $S_1 + \cdots + S_k$, we cannot directly write down the inequalities for $C_{\mathbf{S}}$. However, it turns out the geometry of the mixed subdivisions of $S_1 + \cdots + S_k$ is neatly captured in the *Cayley embedding* of S_1, \dots, S_k . We will associate \mathbf{s} to a maximal cell candidate in the convex hull of the Cayley embedding. Thereafter we will see that the heights that realise \mathbf{s} in the mixed subdivision are exactly the heights that realise the maximal cell candidate in the Cayley polytope.

2.3.1 Cayley trick

We define for each $1 \leq i \leq k$ an embedding

$$\begin{aligned} \pi_i : S_i &\rightarrow \mathbb{R}^{n+k} \\ s &\mapsto (s, e_{n+i}) \end{aligned}$$

where the e_j are standard basis vectors in \mathbb{R}^{n+k} . In other words the first n coordinates of $\pi_i(s)$ are given by s , and the $n+i$ th coordinate is 1, with all others set to 0.

The *Cayley embedding* is the inclusion of each S_i into \mathbb{R}^{n+k} by these maps; the *Cayley polytope* is the convex hull

$$\text{Cayley}_{\mathbf{S}} := \text{conv}(\pi_i(S_i) \mid 1 \leq i \leq k).$$

By intersecting $\text{Cayley}_{\mathbf{S}}$ with the linear subspace defined by setting the last k coordinates to $\frac{1}{k}$, we obtain (up to appropriate scalings) the Minkowski sum $S_1 + \cdots + S_k$. Indeed, a cell inside a regular subdivision of $\text{Cayley}_{\mathbf{S}}$ projects down to H to give a Minkowski cell. By choosing a dual cell candidate from each polytope defining $\text{Cayley}_{\mathbf{S}}$, the projection to H gives a mixed cell.

Theorem 2.3.2 ([Jos21, Theorem 4.3] Cayley trick) *The regular subdivisions of $\text{Cayley}_{\mathbf{S}}$ are in an order preserving bijective correspondence with the mixed subdivisions of $S_1 + \dots + S_k$. In particular, we have*

$$\text{mixed cells} \leftrightarrow \text{Cayley cells with a dual cell candidate taken from each polytope.}$$

It is easy to see that $\text{Cayley}_{\mathbf{S}}$ lives in the plane $\sum_{j=n+1}^{n+k} x_j = 1$, so we can draw the picture of the Cayley embedding of two polytopes.

Example 2.3.2. Let $S_1 = \{(0, 0), (1, 0), (0, 1), (1, 1)\}$ and $S_2 = \{(0, 0), (2, 0), (2, 1)\}$ define the monomial support of our tropical hypersurfaces. Set all heights in S_1 to be tropically zero and set the heights in S_2 to $(2, 1, 0)$. Written as a matrix of column vectors, the Cayley embedding is given by

$$\text{Cayley}_{(S_1, S_2)} = \begin{pmatrix} 0 & 1 & 0 & 1 & 0 & 2 & 2 \\ 0 & 0 & 1 & 1 & 0 & 0 & 1 \\ 1 & 1 & 1 & 1 & 0 & 0 & 0 \\ 0 & 0 & 0 & 0 & 1 & 1 & 1 \end{pmatrix}$$

and the corresponding mixed subdivision of $S_1 + S_2$ is drawn inside a horizontal slice of the Cayley polytope, see Figure 2.7.

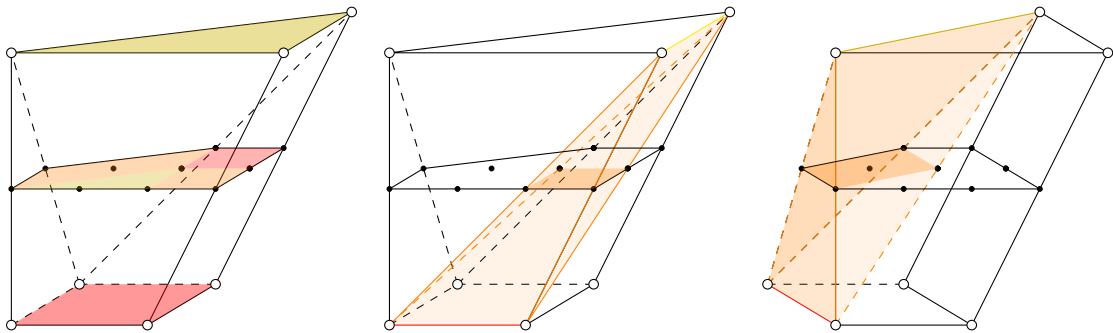


Figure 2.7: The Cayley trick. The mixed subdivision of P and Q arises by taking a horizontal slice of the Cayley polytope (left). The mixed cells are in correspondence with maximal Cayley cells (middle and right).

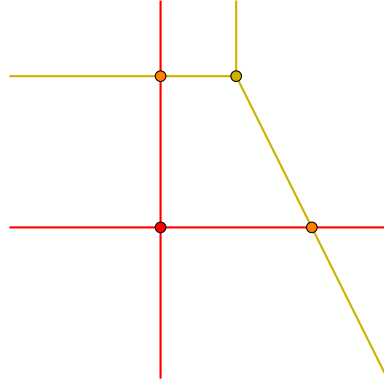


Figure 2.8: The arrangement of the tropical hypersurfaces dual to P and Q .

2.3.2 Mixed cell cones

We now describe how to compute the inequalities that describe the mixed cell cone when \mathbf{s} is transverse.

Lemma 2.3.3 *Let $\mathbf{s} = (s_{\text{lin}}, s_{k+1}, \dots, s_n)$ be a transverse mixed cell candidate. Set $\ell = |S_{\text{lin}} \setminus s_{\text{lin}}| - \dim(s_{\text{lin}}^\perp)$ where $s_{\text{lin}}^\perp := \{u \in \mathbb{R}^n \mid u \cdot (\alpha - \beta) = 0 \text{ for all } \alpha, \beta \in s_{\text{lin}}\}$ and $m = \sum_{i=k+1}^n |s_i|$. We have that $C_{\mathbf{S}}(\mathbf{s})$ is equal to the intersection of $\ell + m - 2(n - k)$ irredundant halfspaces. Each of their normals are given by a circuit of the Cayley matrix A of \mathbf{S} .*

Proof. By the Cayley trick, for the heights \mathbf{c} to give rise to \mathbf{s} as a mixed cell, it is equivalent to check that the Cayley cell indexed by \mathbf{s} in the Cayley embedding arises as a maximal cell in the regular subdivision of $\text{Cayley}_{\mathbf{S}}$ induced by \mathbf{c} .

We therefore proceed by writing down the inequalities that must hold for each point p not in the active support \mathbf{s} , namely that p is lifted higher than everything in \mathbf{s} . Since \mathbf{s} is transverse, each dual cell candidate $s_{\text{lin}}, s_{k+1}, \dots, s_n$ comprising \mathbf{s} is minimal. It is easy to see then that the submatrix of the Cayley matrix A indexed by the points of the hypersurface dual supports s_{k+1}, \dots, s_n has nullity 0. The submatrix indexed by all of \mathbf{s} therefore has nullity equal to the nullity of s_{lin} . We can obtain an augmented dual support s'_{lin} by removing affine linearly dependent vectors from s_{lin} until the nullity is 0. Then, since a linear functional will minimise at s_{lin} if and

only if it minimises at s'_{lin} , we finally have that the submatrix of $\text{Cayley}_{\mathbf{s}}$ indexed by $\mathbf{s}' := \mathbf{s} \setminus s_{\text{lin}} \cup s'_{\text{lin}}$ has nullity 0, and a complete set of irredundant inequalities for $C_{\mathbf{s}}(\mathbf{s})$ may be found by considering circuits involving \mathbf{s} and a point not in \mathbf{s} . We now describe this procedure.

Let A_p be the submatrix of A indexed by \mathbf{s}' and by $p \notin \mathbf{s}$. By assumption this matrix has exactly one more column than it has rows. Appending the heights \mathbf{c} as a row to A_p to obtain the square matrix $A_{p,\mathbf{c}}$, we have that $\det(A_{p,\mathbf{c}}) = 0$ if $\kappa_p \cdot \mathbf{c} = 0$ for some nontrivial $\kappa_p \in \ker(A_p)$. We know from linear algebra that this means all the points lie on the same hyperplane, i.e. they are all lifted to the same height. We know a necessary condition for \mathbf{s} to arise as a mixed cell is that p is lifted higher than \mathbf{s} . This means that increasing the p -th component of \mathbf{c} arbitrarily should be feasible, i.e. $\kappa_p[p] < 0$ and $\kappa_p \cdot \mathbf{c} < 0$ for \mathbf{s} to arise as a mixed cell. The points of \mathbf{s} with p must index a circuit of A_p , since their nullity is 1. In conclusion each inequality may be written as $\kappa_p \cdot \mathbf{c} < 0$ for each p not in \mathbf{s} . \square

Remark 2.3.4 We note two remarks about this computation.

1. If we were to allow the heights of the linear dual support to change, then we would pick up extra equalities that are required to hold to ensure all of s_{lin} remains active in \mathbf{s} . Since our heights are trivial, this is automatic.
2. We pick up an inequality for every point in $S_{\text{lin}} \setminus s_{\text{lin}}$. Even for relatively tame matroids, it does not take long for $|S_{\text{lin}}|$ to range in the order of millions.

We also note that if $M = (E, \{E\})$, then the matroid polytope is simply given by $\{e_E\}$ and the corresponding tropical linear space is equal to \mathbb{R}^n , which recovers the usual case of Jensen [Jen16b].

Later we will see an effective method to determine whether a hypersurface facet of the mixed cell cone is broken before a linear facet. In that setting, we do not have to deal with all the vertices of the matroid polytope.

Example 2.3.3. (Computing the mixed cell cone). We revisit Example 2.3.2. Consider the mixed cell candidate \mathbf{s} indexed by $(0, 0), (1, 0)$ in S_1 and $(2, 0), (2, 1)$ in S_2 (this corresponds to the middle picture in Figure 2.7). Dually, this mixed cell corresponds to the top left point in Figure 2.8. There are three points not involved in \mathbf{s} , which implies that the mixed cell cone $C_{\mathbf{S}}(\mathbf{s})$ will be comprised of three irredundant inequalities. We will compute one of them.

Choose $p = (0, 1) \in S_1$. The relevant submatrix of $\text{Cayley}_{(S_1, S_2)}$ is given by

$$A_p = \begin{pmatrix} 0 & 1 & 0 & 2 & 2 \\ 0 & 0 & 1 & 0 & 1 \\ 1 & 1 & 1 & 0 & 0 \\ 0 & 0 & 0 & 1 & 1 \end{pmatrix}.$$

The nullity of A_p is 1, and a generator for $\ker A_p$ is given by $(1, 0, -1, -1, 1)$ (note that we choose one with the component corresponding to p negative).

We conclude this section with a summary of the algorithm for computing transverse mixed cell cones in the case of a tuple of hypersurfaces, as outlined at the end of Remark 2.3.4.

Algorithm 2.3.5 (`mixed_cell_cone`)

Input: $\mathbf{s} = (s_{\text{lin}}, s_{k+1}, \dots, s_n)$ a transverse mixed cell candidate.

Output: $C_{\mathbf{S}}(\mathbf{s})$, the mixed cell cone associated to \mathbf{s} , i.e.

$$C_{\mathbf{S}}(\mathbf{s}) = \overline{\{\mathbf{c} \in \mathbb{R}^n \mid \mathbf{s} \text{ is a mixed cell induced by the lift } \mathbf{c}\}}.$$

- 1: Choose a tuple (s_1, \dots, s_k) of hypersurface dual supports such that $\bigcap \sigma(s_i) = \text{Span}(\sigma(s_{\text{lin}}))$.
- 2: Set $\mathbf{S} = \mathbf{S} \setminus \{s_{\text{lin}}\} \cup \{s_1, \dots, s_k\}$.
- 3: **for all** ambient points $p \in \mathbf{S}$ not appearing in \mathbf{s} **do**
- 4: Let A_p be the submatrix of $\text{Cayley}_{\mathbf{S}}$ indexed by (s_1, \dots, s_n, p) .
- 5: Choose $\kappa_p \in \ker A_p$ such that $\kappa_p[p] < 0$.

6: **end for**

7: **return** $\{\mathbf{c} \in \mathbb{T}^{\mathbf{S}} \mid \mathbf{c} \cdot \kappa_p \leq 0 \text{ for all } p \notin \{s_1, \dots, s_n\}\}$.

2.4 Starting data

Given a target tropical intersection $\Sigma_{\text{lin}} \wedge \Sigma_{k+1}^{\circ} \wedge \dots \wedge \Sigma_n^{\circ}$ to compute, this section discusses one way to construct the starting data and possible homotopy paths. For the starting data, we use a regeneration approach as used by Jensen [Jen16b, Section 7.2]. The starting hypersurfaces have support equal to the support of tropicalised affine hyperplanes, allowing for easy computation of intersections. Unlike in [Jen16b], the presence of the Bergman fan Σ_{lin} makes it infeasible to give an explicit description of the tropical intersection points, which is why we cannot employ the total degree approach [Jen16b, Section 7.1]. Our homotopy path will be piecewise linear.

Convention 2.4.1 In this section, fix

1. $\Sigma_{\text{lin}} := \Sigma_{S_{\text{lin}}}(0)$ a Bergman fan of a matroid on $[n]$ with dual support $S_{\text{lin}} \subseteq \mathbb{Z}^n$.
As mentioned in Convention 2.2.1, we assume M to be realisable, which means that $\Sigma_{\text{lin}} = \text{Trop}(I_{\text{lin}})$ for some linear ideal $I_{\text{lin}} \subseteq K[x^{\pm}]$ over an algebraically closed field K with valuation $\text{val}: K^* \rightarrow \mathbb{R}$. Note by [MS15, Lemma 2.1.15], there is a homomorphism $\psi: \text{val}(K^*) \rightarrow K^*$ such that $\text{val}(\psi(w)) = w$. We write $p^w := \psi(w)$ and, without loss of generality, we assume that $1 \in \text{val}(K^*)$, which implies that $\mathbb{Q} \subseteq \text{val}(K^*)$.
2. $\Sigma_i^{\circ} := \Sigma_{S_i^{\circ}}(c_i^{\circ})$ tropical hypersurfaces in \mathbb{R}^n with dual support $S_i^{\circ} \subseteq \mathbb{Z}^n$ and dual height $c_i^{\circ} \in \mathbb{T}^{S_i^{\circ}}$.

We write $\mathbf{S}^{\circ} := S_{\text{lin}} \sqcup \bigsqcup_{i=k+1}^n S_i^{\circ}$ and $\mathbf{c}^{\circ} := (c_{\text{lin}}, c_{k+1}^{\circ}, \dots, c_n^{\circ}) \in \mathbb{H}^{\mathbf{S}^{\circ}}$.

Definition 2.4.1. We define

$$V_i^{\downarrow} = \begin{cases} \{e_j \mid \alpha_j \neq 0 \text{ for some } \alpha \in S_i^{\circ}\} & \text{if } |\alpha| = |\beta| \text{ for all } \alpha, \beta \in S_i^{\circ}, \\ \{e_j \mid \alpha_j \neq 0 \text{ for some } \alpha \in S_i^{\circ}\} \cup \{0\} & \text{otherwise,} \end{cases}$$

and $V_i^\uparrow := d_i \cdot V_i^\downarrow$ for $d_i := \max\{|\alpha| \mid \alpha \in S_i^\circ\}$. In other words, $\text{conv}(V_i^\uparrow)$ is the smallest scaled simplex containing S_i . Set $S_i := V_i^\uparrow \cup S_i^\circ$. We refer to $\mathbf{S} := (S_{\text{lin}}, S_{k+1}, \dots, S_n)$ as the *starting mixed support* for \mathbf{S}° , and write $\mathbf{V}^\uparrow := \sqcup_{i=k+1}^n V_i^\uparrow$ and $\mathbf{V}^\downarrow := \sqcup_{i=k+1}^n V_i^\downarrow$.

The next lemma provides the recipe for how to compute the tropical intersection $\Sigma_{\mathbf{S}}(\mathbf{c})$ and the starting mixed cells $D_{\mathbf{S}}(\mathbf{c})$ for a suitable starting mixed height \mathbf{c} .

Lemma 2.4.2 *Let $\mathbf{S} = (S_{\text{lin}}, S_{k+1}, \dots, S_n)$ be the starting mixed support for \mathbf{S}° as defined in Definition 2.4.1. Consider the open subset*

$$\mathcal{C} := \left\{ (0, (c_{k+1,\alpha})_{\alpha \in S_{k+1}}, \dots, (c_{n,\alpha})_{\alpha \in S_n}) \in \mathbb{H}_{\mathbb{R}}^{\mathbf{S}} \mid \right. \\ \left. (\alpha, c_{i,\alpha}) \in \text{AffineSpan}\left(\{(\alpha, c_{i,\alpha'}) \in \mathbb{R}^{n+1} \mid \alpha' \in V_i^\uparrow\}\right) + \mathbb{R}_{>0} \cdot (0, \dots, 0, 1) \right. \\ \left. \text{for } \alpha \notin V_i^\uparrow \right\}.$$

In other words, \mathcal{C} consists of all mixed heights $\mathbf{c} = (c_{k+1}, \dots, c_n)$ for which $(\alpha, c_{i,\alpha})$, $\alpha \notin V_i^\uparrow$, does not lie on a lower face of the lower convex hull.

Then there is an open dense subset $U \subseteq \mathcal{C}$ such that for all $\mathbf{c} = (c_{k+1}, \dots, c_n) \in U$ and $\mathbf{c}^\downarrow := (c_{k+1}^\downarrow, \dots, c_n^\downarrow) \in \mathbb{H}^{\mathbf{V}^\downarrow}$ with $c_i^\downarrow := (d_i^{-1} \cdot c_{i,d_i \cdot \alpha})_{\alpha \in V_i^\downarrow}$:

1. *The following stable intersections are transverse, their supports coincide and consist of a single point:*

$$\left| \Sigma_{S_{\text{lin}}}(0) \wedge \Sigma_{S_{k+1}}(c_{k+1}) \wedge \dots \wedge \Sigma_{S_n}(c_n) \right| \\ = \left| \Sigma_{S_{\text{lin}}}(0) \wedge S_{V_{k+1}^\downarrow}(c_{k+1}^\downarrow) \wedge \dots \wedge \Sigma_{V_n^\downarrow}(c_n^\downarrow) \right| =: \{w\}.$$

Moreover, $\mathbf{s} = (s_{\text{lin}}, s_{k+1}, \dots, s_n) \subseteq \mathbf{S}$ is the unique mixed cell in $D_{\mathbf{S}}(\mathbf{c})$ if and only if $\mathbf{s}^\downarrow := (s_{\text{lin}}, s_{k+1}^\downarrow, \dots, s_n^\downarrow) \subseteq \mathbf{V}^\downarrow$, $s_i^\downarrow := \{\alpha \in V_i^\downarrow \mid d_i \cdot \alpha \in s_i\}$, is the unique mixed cell in $D_{\mathbf{V}^\downarrow}(\mathbf{c}^\downarrow)$.

2. *The intersection point w can be computed as the tropicalisation of the following affine linear ideal*

$$\{w\} = \text{Trop} \left(I_{\text{lin}} + \left\langle \sum_{\alpha \in V_i^\downarrow} \hat{c}_{i,\alpha}^\downarrow \cdot x^\alpha \mid i = k+1, \dots, n \right\rangle \right)$$

for any $\hat{c}_{i,\alpha}^\downarrow \in K^*$ with $\text{val}(\hat{c}_{i,\alpha}^\downarrow) = c_{i,\alpha}^\downarrow$.

Proof. First note that $|\Sigma_{S_i}(c_i)| = |\Sigma_{V_i^\uparrow}((c_{i,\alpha})_{\alpha \in V_i^\uparrow})| = |\Sigma_{V_i^\downarrow}(c_i^\downarrow)|$, and that there is an open subset $U \subseteq \mathcal{C}$ such that $\Sigma_{S_{\text{lin}}}(0)$ and all $\Sigma_{S_i}(c_i)$ intersect transversally. Combining both yields the first statement.

Observe further that $\Sigma_{V_i^\downarrow}(c_i^\downarrow) = \text{Trop}(\sum_{\alpha \in V_i^\downarrow} \hat{c}_{i,\alpha}^\downarrow x^\alpha)$. By the Transverse Intersection Theorem [MS15, Theorem 3.4.12], this gives

$$\begin{aligned} & \text{Trop}\left(I_{\text{lin}} + \left\langle \sum_{\alpha \in V_i^\downarrow} \hat{c}_{i,\alpha}^\downarrow x^\alpha \mid i = k+1, \dots, n \right\rangle\right) \\ &= \text{Trop}(I_{\text{lin}}) \wedge \left(\bigwedge_{i=k+1}^n \text{Trop}(\sum_{\alpha \in V_i^\downarrow} \hat{c}_{i,\alpha}^\downarrow x^\alpha) \right) \end{aligned}$$

which implies the second statement. \square

Example 2.4.2. Consider the target dual support

$$S_i^\circ = \{(4, 0), (2, 2), (2, 1), (1, 2), (1, 1), (0, 0)\} \subseteq \mathbb{Z}^2$$

and the target dual height $c_i^\circ = (5, 5, 5, 5, 5, 5) \subseteq \mathbb{T}^{S_i^\circ}$. Then $V_i^\downarrow = \{(1, 0), (0, 1), (0, 0)\}$, $V_i^\uparrow = \{(4, 0), (0, 4), (0, 0)\}$, and $d_i = 4$. Hence, we obtain the following starting dual support as defined in Definition 2.4.1 and possible starting dual height by Lemma 2.4.2:

$$\begin{aligned} S_i &= \{ (4, 0), (0, 4), (2, 2), (2, 1), (1, 2), (1, 1), (0, 0) \} \subseteq \mathbb{Z}^n, \\ c_i &= (3.03 \quad 3.01 \quad 5.04 \quad 5.01 \quad 5.05 \quad 5.09 \quad 3.02) \in \mathcal{C}. \end{aligned}$$

Note that c_i is indeed a valid starting dual height, as for $\alpha \notin V_i^\uparrow$ the raised points $(\alpha, c_{i,\alpha})$ do not lie on a lower face of the lower convex hull as required by the definition of \mathcal{C} , see Figure 2.9.

As $\text{conv}(S_i)$ is a scaled simplex and its subdivision is trivial, it is evident that $\Sigma_{S_i}(c_i)$ is set-theoretically the tropicalisation of an affine hyperplane, consisting of three rays intersecting in a single apex. The fact that $|\Sigma_{S_i}(c_i)|$ and $\Sigma_{V_i^\downarrow}(c_i^\downarrow)$ coincide for $c_i^\downarrow = 4^{-1} \cdot (3.03, 3.01, 3.02)$ can be checked straightforwardly by verifying that the

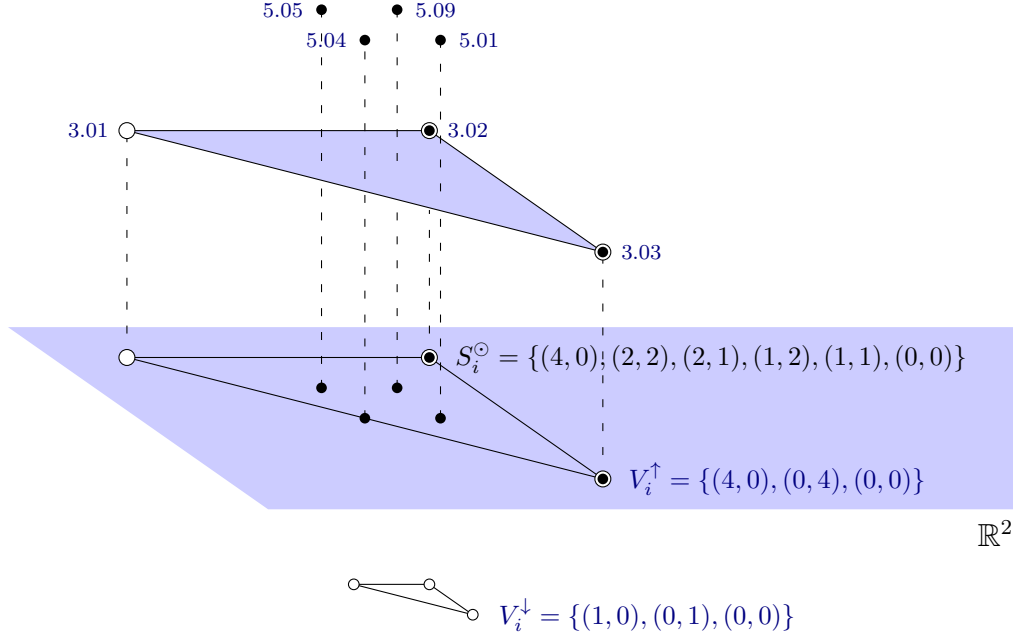


Figure 2.9: Starting dual supports and dual heights from Example 2.4.2

two apexes coincide, i.e., for $w = (w_1, w_2) \in \mathbb{R}^2$

$$3.03 + 4w_1 = 3.01 + 4w_2 = 3.02 \iff 4^{-1} \cdot 3.03 + w_1 = 4^{-1} \cdot 3.01 + w_2 = 4^{-1} \cdot 3.02.$$

Lemma 2.4.2 gives rise to the following algorithm:

Algorithm 2.4.3 (starting_data)

Input: \mathbf{S}° , a target mixed support.

Output: $D_{\mathbf{S}}(\mathbf{c})$, a starting mixed subdivision with $\mathbf{S}^\circ \subseteq \mathbf{S}$.

- 1: Let $I_{\text{lin}} \subseteq K[x^\pm]$ such that $\text{Trop}(I_{\text{lin}}) = \Sigma_{\mathbf{S}_{\text{lin}}}(0)$.
- 2: Let $V_{k+1}^\uparrow, \dots, V_n^\uparrow, V_{k+1}^\downarrow, \dots, V_n^\downarrow \subseteq \mathbb{Z}^n$ be as in Definition 2.4.1.
- 3: Let $\mathcal{C} \subseteq \mathbb{H}_{\mathbb{R}}^{\mathbf{S}}$ be as in Lemma 2.4.2.
- 4: **repeat**
- 5: Pick $\mathbf{c} = (0, c_{k+1}, \dots, c_n) \in \mathcal{C} \cap \mathbb{Q}^{\mathbf{S}}$ random, say $c_i = (c_{i,\alpha})_{\alpha \in S_i}$.
- 6: Set $\mathbf{c}^\downarrow := (c_{k+1}^\downarrow, \dots, c_n^\downarrow) \in \mathbb{H}^{\mathbf{V}^\downarrow}$ with $c_i^\downarrow := (d_i^{-1} \cdot c_{i,d_i \cdot \alpha})_{\alpha \in V_i^\downarrow}$.
- 7: Set $\hat{c}_{i,\alpha}^\downarrow := p^{c_{i,\alpha}^\downarrow} \in K^*$.

8: Compute

$$W := \left| \text{Trop} \left(I_{\text{lin}} + \underbrace{\left\langle \sum_{\alpha \in V_i^\downarrow} \hat{c}_{i,\alpha}^\downarrow \cdot x^\alpha \mid i = k+1, \dots, n \right\rangle}_{=: l_i} \right) \right|.$$

9: **until**

1. W consists of a single point w ,
2. w induces a maximal chain of flats of the matroid of M ,
3. w lies in the relative interior of a maximal cell in each $\text{Trop}(l_i)$.

10: Let $\mathbf{s}^\downarrow := (s_{\text{lin}}, s_{k+1}^\downarrow, \dots, s_n^\downarrow) \in D_{\mathbf{V}^\downarrow}(\mathbf{c}^\downarrow)$ be the unique mixed cell induced by \mathbf{c}^\downarrow .

11: Set $\mathbf{s} := (s_{\text{lin}}, s_{k+1}, \dots, s_n) \subseteq \mathbf{S}$ where $s_i := \{d_i \cdot \alpha \mid \alpha \in s_i^\downarrow\}$.

12: **return** $D_{\mathbf{S}}(\mathbf{c}) = \{\mathbf{s}\}$.

Remark 2.4.4 We note that Algorithm 2.4.3 may not always return a starting mixed cell, for example when the Bergman fan is complete and the mixed volume of the target hypersurface dual supports is zero. In this case, a possible fix is to add extra vertices of a higher-dimensional simplex to construct the supports of step 2 of the algorithm, until the criteria of step 9 can be satisfied.

There are many paths connecting a starting mixed height \mathbf{c} to the target mixed height \mathbf{c}° in the mixed height space $\mathbb{T}^{\mathbf{S}}$. For the sake of simplicity, we only consider paths of the following type:

Definition 2.4.3. A *piecewise linear path* in $\mathbb{H}^{\mathbf{S}}$ is a finite sequence of linear paths in the stratification of Remark 2.2.11, i.e., $\boldsymbol{\gamma}^\bullet = (\boldsymbol{\gamma}^{(1)}, \dots, \boldsymbol{\gamma}^{(\ell)})$ where

$$\boldsymbol{\gamma}^{(i)} : [0, t_{\text{target}}^{(i)}] \longrightarrow \mathbb{T}^{\mathbf{S}}, \quad t \longmapsto \mathbf{c}^{(i)} + t \cdot \mathbf{u}^{(i)}$$

for some $\mathbf{c}^{(i)} \in \mathbb{H}^{\mathbf{S}}$ and $\mathbf{u}^{(i)} \in \mathbb{H}_{\mathbb{R}}^{\mathbf{S}}$ with $\boldsymbol{\gamma}^{(i)}(t_{\text{target}}^{(i)}) = \boldsymbol{\gamma}^{(i+1)}(0)$. Note that we explicitly allow $t_{\text{target}}^{(i)} = \infty$ in which case $\boldsymbol{\gamma}^{(i)}|_{[0, t_{\text{target}}^{(i)})}$ and $\boldsymbol{\gamma}^{(i+1)}|_{[0, t_{\text{target}}^{(i+1)})}$ are on different strata of $\mathbb{H}^{\mathbf{S}}$.

The piecewise linearity allows for the easy computation of when the mixed subdivision changes in Section 2.5.

Definition 2.4.4. Let \mathbf{S} be a support containing the target support \mathbf{S}° , and let $\mathbf{c} \in \mathbb{H}_{\mathbb{R}}^{\mathbf{S}}$ be a mixed height.

1. The *straight line homotopy* is the piecewise linear path $\gamma^\bullet = (\gamma^{(1)}, \gamma^{(2)})$ where

$$\gamma^{(1)}: [0, \infty] \longrightarrow \mathbb{T}^{\mathbf{S}}, \quad t \longmapsto \mathbf{c} + t \cdot \mathbf{u}^{(1)} \quad \text{for } \mathbf{u}_{i,\alpha}^{(1)} := \begin{cases} 0 & \text{if } \alpha \in S_i^\circ \\ 1 & \text{if } \alpha \notin S_i^\circ \end{cases}$$

is the line along which all coordinates indexed by (i, α) with $\alpha \notin S_i^\circ$ are sent to ∞ , and

$$\gamma^{(2)}: [0, 1] \longrightarrow \mathbb{T}^{\mathbf{S}}, \quad t \longmapsto \mathbf{c}^{(2)} + t \cdot (\mathbf{c}^\circ - \mathbf{c}^{(2)}) \quad \text{for } \mathbf{c}^{(2)} := \gamma^{(1)}(\infty)$$

is the line connecting $\mathbf{c}^{(2)}$ to \mathbf{c}° in the euclidean space $\mathbb{H}_{\mathbb{R}}^{\mathbf{S}^\circ} \subseteq \mathbb{H}^{\mathbf{S}}$.

2. The *coordinatewise homotopy* is the piecewise linear path $\gamma^\bullet = (\gamma^{(1)}, \dots, \gamma^{(\ell)})$, where for some fixed enumeration $\mathbf{S} = \{(j_1, \alpha_1), \dots, (j_\ell, \alpha_\ell)\}$ either

$$\gamma^{(i)}: [0, t_{\text{target}}^{(i)}] \longrightarrow \mathbb{T}^{\mathbf{S}}, \quad t \longmapsto \mathbf{c}^{(i)} + t \cdot e_{j_i, \alpha_i} \quad \text{if } t_{\text{target}}^{(i)} := c_{j_i, \alpha_i}^\circ - c_{j_i, \alpha_i} \geq 0$$

or

$$\gamma^{(i)}: [0, t_{\text{target}}^{(i)}] \longrightarrow \mathbb{T}^{\mathbf{S}}, \quad t \longmapsto \mathbf{c}^{(i)} - t \cdot e_{j_i, \alpha_i} \quad \text{if } t_{\text{target}}^{(i)} := c_{j_i, \alpha_i} - c_{j_i, \alpha_i}^\circ \geq 0.$$

Here, $e_{j_i, \alpha_i} \in \mathbb{H}_{\mathbb{R}}^{\mathbf{S}}$ denotes the unit vector of the ordinate indexed by (j_i, α_i) , and $\gamma^{(i)}$ is the line along which this coordinate is sent from c_{j_i, α_i} to c_{j_i, α_i}° .

Essentially, the straight line homotopy aims to minimise the number of linear paths while the coordinatewise homotopy aims to minimise the changes within a linear path.

Example 2.4.5. Suppose the following dual hypersurface support and dual height are part of a target mixed support and a target mixed height:

$$S_i^\circ := \{(4, 0), (2, 2), (0, 4), (2, 0), (0, 2), (0, 0)\} \quad \text{and} \quad c_i^\circ := (2, 0, 2, 0, 0, 0).$$

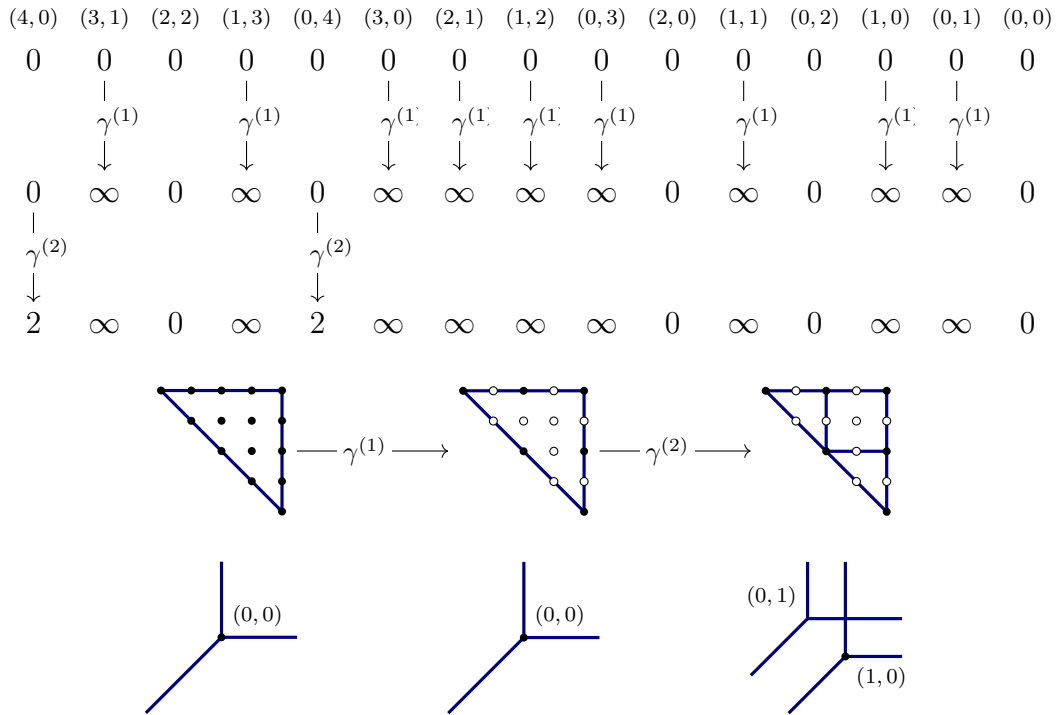


Figure 2.10: Straight line homotopy from Example 2.4.5 and the corresponding change in dual subdivision (axes inverted) and tropical hypersurface (multiplicities omitted).

Algorithm 2.4.3 then constructs $S_i := 4 \cdot V_i^\downarrow \cap \mathbb{Z}^2$, $V_i^\downarrow = \text{conv}(e_1, e_2, 0)$, as part of the starting mixed support. Assume for the sake of simplicity that $c_i := 0 \in \mathbb{H}_{\mathbb{R}}^{S_i}$ is part of the starting mixed height. The straight line homotopy moves all $c_{i,\alpha}$ for $\alpha \notin S_i^\circ$ to ∞ at once, then both $c_{i,(4,0)}$ and $c_{i,(0,4)}$ to 2 at the same time, see Figure 2.10. A possible coordinatewise homotopy first sends all $c_{i,\alpha}$ for $\alpha \notin S_i^\circ$ to ∞ one after the other, then $c_{i,(4,0)}$ to 2, then $c_{i,(0,4)}$ to 2, see Figure 2.11.

2.5 Bergman and Jensen flips

We now describe the main building blocks for our path tracking algorithm. We will work around the need to consult the linear support S_{lin} by exploiting the fine structure on the Bergman fan described in Definition 2.2.15.

Convention 2.5.1 Recall the fixed dual supports S_{lin} and S_{k+1}, \dots, S_n in Convention 2.2.1. In this section, we further fix a linear path in the mixed height space of

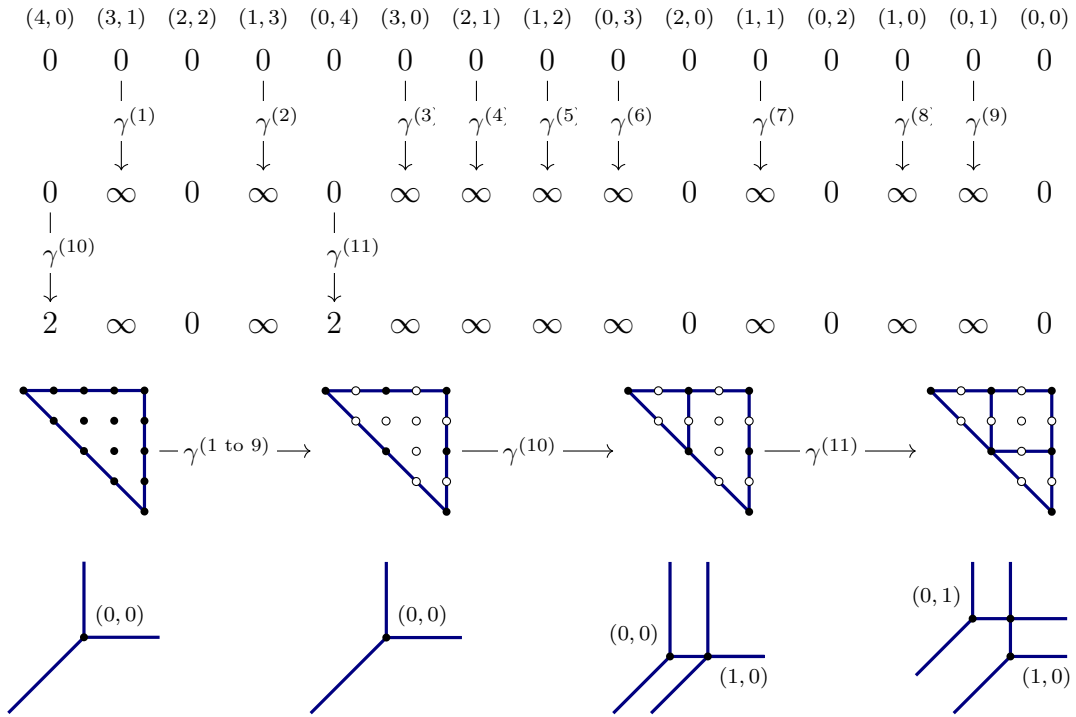


Figure 2.11: Coordinatewise homotopy from Example 2.4.5 and the corresponding change in dual subdivision (axes inverted) and tropical hypersurface (multiplicities omitted).

the form

$$\gamma: [0, t_{\text{target}}] \longrightarrow \mathbb{H}^{\mathbf{S}}, \quad t \longmapsto \mathbf{c} + t \cdot \mathbf{u},$$

for

1. $t_{\text{target}} \in \mathbb{T}$, a not necessarily finite target time.
2. $\mathbf{c} \in \mathbb{H}^{\mathbf{S}}$, a not necessarily finite starting height.
3. $\mathbf{u} \in \mathbb{H}_{\mathbb{R}}^{\mathbf{S}} := \{0\} \times \mathbb{R}^{S_{k+1}} \times \dots \times \mathbb{R}^{S_n}$, a finite direction.

We assume that $D_{\mathbf{S}}(\gamma(\varepsilon))$ is known and transverse for $\varepsilon > 0$ sufficiently small, and we are interested in $D_{\mathbf{S}}(\gamma(t))$ as t increases. Note that $D_{\mathbf{S}}(\gamma(0))$ is not assumed to be transverse and that reaching $\gamma(t_{\text{target}})$ is the subject of Section 2.6. In this section, $\varepsilon > 0$ always denotes a sufficiently small number, where the meaning of “sufficiently small” should be clear from context.

Conceptually, our path tracking works exactly as in [Jen16b]: We track a mixed cell $\mathbf{s} \in D_{\mathbf{S}}(\gamma(\varepsilon))$ from $\gamma(\varepsilon)$ to $\gamma(t_{\text{target}})$, and update it accordingly when $\gamma(t)$ breaches the mixed cell cone $C_{\mathbf{S}}(\mathbf{s})$.

Unfortunately, computing the mixed cell cone $C_{\mathbf{S}}(\mathbf{s})$ in our setting is impractical as it involves the linear support S_{lin} . Fortunately, as discussed in Section 2.2.3, the support of the Bergman fan can also be equipped with the fine structure $\Sigma_{S_{\text{lin}}}^{\text{fine}}$ that is easier to work with locally. Instead of identifying when $\gamma(t)$ breaches $C_{\mathbf{S}}(\mathbf{s})$, we therefore track the following two times:

1. The time $t_{\text{Bergman}} \in (0, t_{\text{target}}]$ at which the tropical intersection point $\sigma_{\mathbf{S}}(\mathbf{s}, \gamma(t))$ breaches a maximal cone of the fine structure. This time can be computed using the induced chain of flats.
2. Replacing $\sigma_{S_{\text{lin}}}(s_{\text{lin}}, 0)$ by $\text{span}(\sigma_{S_{\text{lin}}}(s_{\text{lin}}, 0))$, the time $t_{\text{Jensen}} \in (0, t_{\text{target}}]$ at which the tropical intersection point crosses a lower dimensional polyhedron of one of the hypersurfaces $\Sigma_{S_i}(c_i)$. As $\text{span}(\sigma_{S_{\text{lin}}}(s_{\text{lin}}, 0))$ can be written as a stable intersection of hypersurfaces $\Sigma_{S_1}(0) \wedge \cdots \wedge \Sigma_{S_k}(0)$, this time can be computed using mixed cell cones of hypersurfaces as in [Jen16b].

We will now explain how to compute the times t_{Bergman} and t_{Jensen} , as well as the potential change in the mixed cell \mathbf{s} .

2.5.1 Time until Bergman failure

Definition 2.5.1. Let \mathbf{s} be a mixed cell induced by $\gamma(\varepsilon)$. Let $\sigma_{\text{fine}} \in \Sigma_{S_{\text{lin}}}^{\text{fine}}(0)$ be the cone of the fine structure containing $\sigma_{\mathbf{S}}(\mathbf{s}, \mathbf{c})$. We define the *time of Bergman failure* to be

$$t_{\text{Bergman}}(\mathbf{s}, \mathbf{c}) := \inf \left(\left\{ t \in (0, t_{\text{target}}] \mid \sigma_{\mathbf{S}}(\mathbf{s}, \gamma(t)) \notin \sigma_{\text{fine}} \right\} \cup \{\infty\} \right).$$

To explain how t_{Bergman} can be computed, we require the following notion:

Definition 2.5.2. Let \mathbf{s} be a mixed cell induced by $\gamma(\varepsilon)$. The *tropical drift* of \mathbf{s} along γ is

$$u_{\mathbf{s}}(\mathbf{s}, \gamma) := \lim_{t \rightarrow 0} \frac{\sigma_{\mathbf{s}}(\mathbf{s}, \gamma(t)) - \sigma_{\mathbf{s}}(\mathbf{s}, \gamma(0))}{t} \in \mathbb{R}^n.$$

Similar to Lemma 2.2.12 for tropical intersection points, tropical drifts may be computed also using only the chain of flats and the active hypersurface supports:

Lemma 2.5.2 *Let \mathbf{s} be a mixed cell induced by $\mathbf{c} = \gamma(\varepsilon)$. Let $A_{\mathbf{s}, \mathbf{c}}$ and $b_{\mathbf{c}}$ be the matrix and vector from Lemma 2.2.12, and let $A_{\mathbf{s}, \mathbf{c}}^{-1}$ be the left-inverse of $A_{\mathbf{s}, \mathbf{c}}$. Then $u_{\mathbf{s}}(\mathbf{s}, \gamma) = -A_{\mathbf{s}, \mathbf{c}}^{-1} b_{\mathbf{u}_{\gamma}}$.*

Proof. As \mathbf{c} is assumed to be strongly generic by Convention 2.5.1, we have $\sigma_{\mathbf{s}}(\mathbf{s}, \gamma(t)) \in \sigma_{\text{fine}}$ for $t > 0$ sufficiently small. Moreover, by Lemma 2.3.1, we have $\gamma(t) \in C_{\mathbf{s}}(\mathbf{s})$ for $t > 0$ sufficiently small, which in turn implies $A_{\mathbf{s}, \mathbf{c}} = A_{\mathbf{s}, \gamma(t)}$. As such, we have $A_{\mathbf{s}, \mathbf{c}} \sigma_{\mathbf{s}}(\mathbf{s}, \mathbf{c}) = b_{\mathbf{c}}$ and $A_{\mathbf{s}, \gamma(t)} \sigma_{\mathbf{s}}(\mathbf{s}, \gamma(t)) = A_{\mathbf{s}, \mathbf{c}} \sigma_{\mathbf{s}}(\mathbf{s}, \gamma(t)) = b_{\gamma(t)}$. We have

$$\begin{aligned} b_{\mathbf{c}} - b_{\gamma(t)} &= \gamma(\varepsilon)_{ij} - \gamma(\varepsilon)_{i1} - (\gamma(t)_{ij} - \gamma(t)_{i1}) \\ &= (\gamma(t) - \gamma(\varepsilon))_{ij} - (\gamma(t) - \gamma(\varepsilon))_{i1} = t \cdot b_{\mathbf{u}_{\gamma}}. \end{aligned}$$

Thus

$$\begin{aligned} A_{\mathbf{s}, \mathbf{c}} u(\mathbf{s}, \mathbf{c}) &= A_{\mathbf{s}, \mathbf{c}} \left(\frac{\sigma_{\mathbf{s}}(\mathbf{s}, \gamma(t)) - \sigma_{\mathbf{s}}(\mathbf{s}, \gamma(\varepsilon))}{t} \right) = \frac{1}{t} (A_{\mathbf{s}, \mathbf{c}} \sigma_{\mathbf{s}}(\mathbf{s}, \gamma(t)) - A_{\mathbf{s}, \mathbf{c}} \sigma_{\mathbf{s}}(\mathbf{s}, \gamma(\varepsilon))) \\ &= \frac{1}{t} (b_{\gamma(t)} - b_{\mathbf{c}}) = -b_{\mathbf{u}_{\gamma}}. \end{aligned}$$

We know $A_{\mathbf{s}, \mathbf{c}}$ is left-invertible from Lemma 2.2.6. The result follows. \square

Combining Lemma 2.2.12 and Lemma 2.5.2 gives the following algorithm:

Algorithm 2.5.3 (tropical_intersection_point_and_drift)

Input: (\mathbf{s}, γ) , where γ as in Convention 2.5.1 and \mathbf{s} is a mixed cell induced by $\gamma(\varepsilon)$.

Output: $(\sigma_{\mathbf{s}}(\mathbf{s}, \gamma(\varepsilon)), u_{\mathbf{s}}(\mathbf{s}, \gamma))$.

- 1: Let $A_{\mathbf{s}, \mathbf{c}}$ be the matrix from Lemma 2.2.12 for $\mathbf{c} := \gamma(\varepsilon)$.
- 2: Compute its left-inverse $A_{\mathbf{s}, \mathbf{c}}^{-1}$.

3: **return** $(A_{\mathbf{s},\mathbf{c}}^{-1} \cdot b_{\mathbf{c}}, -A_{\mathbf{s},\mathbf{c}}^{-1} \cdot b_{\mathbf{u}_\gamma})$.

Computing t_{Bergman} now simply boils down to computing when the tropical intersection point leaves the Bergman cone in the fine structure:

Algorithm 2.5.4 (t_{Bergman})

Input: (\mathbf{s}, γ) , where $\mathbf{s} \in D_{\mathbf{S}}(\gamma(\varepsilon))$ is a mixed cell induced by $\gamma(\varepsilon)$.

Output: $t_{\text{Bergman}} \in (0, 1]$ the time of Bergman failure as in Definition 2.5.1.

1: Use Algorithm 2.5.3 to compute the tropical intersection point and tropical drift

$$(w, u) := \text{tropical_intersection_point_and_drift}(\mathbf{s}, \gamma).$$

2: Construct the chain of flats induced by $w = (w_1, \dots, w_n)$, i.e.,

$$\emptyset \subsetneq F_1 \subsetneq \dots \subsetneq F_k = [n] \quad \text{where } F_j := \{i \in [n] \mid w_i \leq v_j\}$$

for $v_1 < \dots < v_k$ with $\{v_1, \dots, v_k\} = \{w_1, \dots, w_n\}$.

3: Compute

$$t_{\text{Bergman}} := \inf \left(\left\{ t \in (0, t_{\text{target}}] \mid w + t \cdot u \notin \text{cone}(-e_{F_1}, \dots, -e_{F_{r+1}}) \right\} \cup \{\infty\} \right),$$

where $e_{F_i} := \sum_{j \in F_i} e_j$.

4: **return** t_{Bergman} .

2.5.2 Time until Jensen failure

Definition 2.5.3. Let $\mathbf{s} = (s_{\text{lin}}, s_{k+1}, \dots, s_n) \in D_{\mathbf{S}}(\gamma(\varepsilon))$ be a mixed cell induced by $\gamma(\varepsilon)$, and let $\sigma_{\text{lin}} \in \Sigma_{S_{\text{lin}}}(0)$ be the maximal cone of dual to s_{lin} . Pick binomial supports $S_1, \dots, S_k \subseteq \mathbb{Z}^n$, i.e., $|S_i| = 2$, such that

$$|\Sigma_{S_1}(0) \wedge \dots \wedge \Sigma_{S_k}(0)| = \text{Span}(\sigma_{\text{lin}}).$$

Consider the mixed support $\mathbf{S}' := \sqcup_{i=1}^n S_i$, and the mixed height path in $\mathbb{T}^{\mathbf{S}'}$ that is zero on $\sqcup_{i=1}^k S_k$ coordinates and coincides with γ on the $\sqcup_{i=k+1}^n S_k$ coordinates:

$$\gamma' : [0, t_{\text{target}}] \rightarrow \mathbb{T}^{\mathbf{S}'}, t \mapsto (0, \dots, 0, \gamma_{k+1}(t), \dots, \gamma_n(t)).$$

Then $\mathbf{s}' := (S_1, \dots, S_k, s_{k+1}, \dots, s_n) \in D_{\mathbf{S}'}(\gamma'(\varepsilon))$ and we define the *time until Jensen-failure* to be

$$t_{\text{Jensen}}(\mathbf{s}) := \inf \left(\left\{ t \in (0, t_{\text{target}}] \mid \gamma'(t) \notin C_{\mathbf{S}'}(\mathbf{s}') \right\} \cup \{\infty\} \right).$$

We first show that t_{Jensen} is well-defined, which is a straightforward consequence of Corollary 2.2.5.

Lemma 2.5.5 *Given \mathbf{S}' , γ' , and t_{Jensen} as in Definition 2.5.3. Then $\mathbf{s}' \in D_{\mathbf{S}'}(\gamma'(\varepsilon))$ and the definition of t_{Jensen} is independent of the choice of S_1, \dots, S_k .*

Proof. The fact that $\mathbf{s}' \in D_{\mathbf{S}'}(\gamma'(\varepsilon))$ follows from $\sigma_{S_1}(S_1, 0) \cap \dots \cap \sigma_{S_k}(S_k, 0) = \text{Span}(\sigma_{\text{lin}})$. Moreover, as $D_{\mathbf{S}}(\gamma(\varepsilon))$ is assumed to be transverse in Convention 2.5.1, the varieties

$$\Sigma_{S_1}(0), \dots, \Sigma_{S_k}(0), \Sigma_{S_{k+1}}(\gamma_{k+1}(\varepsilon)), \dots, \Sigma_{S_n}(\gamma_n(\varepsilon))$$

intersect transversally. Hence $D_{\mathbf{S}'}(\gamma'(0))$ is transverse and so is $D_{\mathbf{S}'}(\gamma'(t))$ for $t \in [0, t_{\text{Jensen}})$. In particular, $D_{\mathbf{S}'}(\gamma'(t))$ is uniquely determined by $\Sigma_{\mathbf{S}'}(\gamma'(t))$ by Corollary 2.2.5 which is independent of the choice of S_i in Definition 2.5.3. \square

Thanks to Lemma 2.3.1, computing t_{Jensen} is straightforward:

Algorithm 2.5.6 (t_{Jensen})

Input: (\mathbf{s}, γ) , where $\mathbf{s} \in D_{\mathbf{S}}(\gamma(\varepsilon))$ is a mixed cell induced by $\gamma(\varepsilon)$.

Output: $t_{\text{Jensen}} \in (0, 1]$ the time of Jensen failure as in Definition 2.5.3.

1: Let \mathbf{S}' and \mathbf{s}' be as in Definition 2.5.3.

2: Compute

$$t_{\text{Jensen}}(\mathbf{s}) := \inf \left(\left\{ t \in (0, t_{\text{target}}] \mid \gamma'(t) \notin C_{\mathbf{S}'}(\mathbf{s}') \right\} \cup \{\infty\} \right).$$

3: **return** t_{Jensen} .

We conclude with a lemma that explains the tropical intuition behind t_{Bergman} and t_{Jensen} . They are the times at which the tropical intersection point $\sigma_{\mathbf{s}}(\mathbf{s}, \gamma(t))$ breaches a cone in the fine structure of the Bergman fan $\Sigma_{\text{lin}}^{\text{fine}}(0)$ or a polyhedron in a tropical hypersurface $\Sigma_{S_i}(\gamma_i(t))$, respectively:

Lemma 2.5.7 *Let t_{Bergman} and t_{Jensen} be as in Definitions 2.5.1 and 2.5.3. Then*

1. *If $t_{\text{Bergman}} < t_{\text{Jensen}}$, then*

$$t_{\text{Bergman}}(\mathbf{s}) := \inf \left(\left\{ t \in (0, t_{\text{target}}] \mid \sigma_{\mathbf{s}}(\mathbf{s}, \gamma(t)) \notin \sigma_{\text{fine}} \right\} \right),$$

where $\sigma_{\text{fine}} \in \Sigma_{\text{lin}}^{\text{fine}}(0)$ is the cone in the fine structure of the Bergman fan containing $\sigma_{\mathbf{s}}(\mathbf{s}, \gamma(\varepsilon))$.

2. *If $t_{\text{Jensen}} < t_{\text{Bergman}}$, then*

$$t_{\text{Jensen}}(\mathbf{s}) := \inf \left(\left\{ t \in (0, t_{\text{target}}] \mid \sigma_{\mathbf{s}}(\mathbf{s}, \gamma(t)) \notin \sigma_{S_i}(s_i, \gamma_i(t)) \right. \right. \\ \left. \left. \text{for some } k+1 \leq i \leq n \right\} \right).$$

2.5.3 Bergman flip

In this section, we explain how a mixed cell \mathbf{s} changes along γ when $t_{\text{Bergman}} < t_{\text{Jensen}}$.

Lemma 2.5.8 *Let $\mathbf{s} =: (s_{\text{lin}}, s_{k+1}, \dots, s_n) \in D_{\mathbf{s}}(\gamma(\varepsilon))$ be a mixed cell induced by $\gamma(\varepsilon)$ such that $t_{\text{Bergman}} := t_{\text{Bergman}}(\mathbf{s}, \gamma) < t_{\text{Jensen}}(\mathbf{s}, \gamma)$. Consider:*

1. F'_{\bullet} the non-maximal chain of flats induced by $\sigma_{\mathbf{s}}(\mathbf{s}, \gamma(t_{\text{Bergman}}))$,
2. F_{\bullet} any maximal chain of flats refining F'_{\bullet} .

Suppose that $\text{length}(F_{\bullet}) = \text{length}(F'_{\bullet}) + 1$. Then

$$\sigma_{\text{lin}}(F_{\bullet}) \cap |\Sigma_{\mathbf{s}}(\gamma(t_{\text{Bergman}} + \varepsilon))| \neq \emptyset \text{ for } \varepsilon > 0 \text{ sufficiently small}$$

$$\iff \text{Span}(e_{F_1}, \dots, e_{F_k}) \cap \{w \in \mathbb{R}^n \mid w \cdot v \geq 0\} \cap \left(u + \bigcap_{i=k+1}^n s_i^\perp\right) \neq \emptyset$$

which is equivalent to the condition

$$\text{Span}(e_{F_1}, \dots, e_{F_k}) \cap \left(\bigcap_{i=k+1}^n s_i^\perp\right) = \{0\} \text{ and } \pi(u) \cdot v > 0 \quad (2.5.1)$$

where

1. $e_{F_i} := \sum_{\ell \in F_i} e_\ell$ is the indicator vector of F_i for $i = 1, \dots, k$,
2. F_j is the unique flat in F_\bullet but not in F'_\bullet ,
3. $s_i^\perp := \{w \in \mathbb{R}^n \mid w \cdot (\alpha_i - \beta_i) = 0\}$ is the hyperplane of normal vectors on the affine span of $s_i =: \{\alpha_i, \beta_i\}$,
4. $u := u_{\mathbf{s}}(\mathbf{s}, \gamma) \in \mathbb{R}^n$ is the tropical drift of \mathbf{s} under γ ,
5. $v := (\sum_{\ell \in F_j \setminus F_{j-1}} e_\ell) - (\sum_{\ell \in F_{j+1} \setminus F_j} e_\ell)$, F_j being the unique flat in F_\bullet and not in F'_\bullet , is the inner normal vector of facet $\sigma_{\text{lin}}(F'_\bullet)$ of $\sigma_{\text{lin}}(F_\bullet)$,
6. $\pi : \left(\bigcap_{i=k+1}^n s_i^\perp\right)^\perp \rightarrow \text{Span}(e_{F_1}, \dots, e_{F_k})$ is the oblique projection.

Proof. In the following, let $\mathbf{c}_\varepsilon := (0, c_{k+1, \varepsilon}, \dots, c_{n, \varepsilon}) := \gamma(t_{\text{Bergman}} + \varepsilon)$ for $\varepsilon \in \mathbb{R}$. As $t_{\text{Bergman}} < t_{\text{Jensen}}(\mathbf{s}, \gamma)$, we have

1. dual cells $s_i \in D_{S_i}(c_{i,0})$ remain dual cells $s_i \in D_{S_i}(c_{i,\varepsilon})$ for $|\varepsilon|$ sufficiently small,
2. these $s_i \in D_{S_i}(c_{i,\varepsilon})$ are the only dual cells whose tropical polyhedra $\sigma_{S_i}(s_i, c_{i,\varepsilon})$ intersect $\Sigma_{S_{\text{lin}}}(0)$ around the tropical intersection point $\sigma_{\mathbf{s}}(\mathbf{s}, \mathbf{c}_0)$.

Locally around $\sigma_{\mathbf{s}}(\mathbf{s}, \mathbf{c}_0)$, the stable intersection $\bigwedge_{i=k+1}^n \Sigma_{S_i}(c_{i,0})$ therefore looks like the subspace $\bigcap_{i=k+1}^n s_i^\perp$ and moving in direction of drift u for $\varepsilon > 0$, while the maximal Bergman cone $\sigma_{\text{lin}}(F_\bullet)$ looks like the intersection of the subspace $\text{Span}(e_{F_1}, \dots, e_{F_k})$ with the halfspace $\{w \in \mathbb{R}^n \mid w \cdot v \geq 0\}$. Combining both, we get

$$\sigma_{\text{lin}}(F_\bullet) \cap |\Sigma_{\mathbf{s}}(\gamma(t_{\text{Bergman}} + \varepsilon))| \neq \emptyset \iff \sigma_{\text{lin}}(F_\bullet) \cap \left(\bigcap_{i=k+1}^n \sigma_{S_i}(s_i, c_{i,\varepsilon})\right) \neq \emptyset$$

$$\iff \underbrace{\text{Span}(e_{F_1}, \dots, e_{F_k})}_{=:V_1} \cap \underbrace{\{w \in \mathbb{R}^n \mid w \cdot v \geq 0\}}_{=:V_2} \cap \left(u + \underbrace{\bigcap_{i=k+1}^n s_i^\perp}_{=:V_3=:u+H} \right) \neq \emptyset.$$

Suppose the intersection above is nonempty, with a common point w . Let A be the matrix with columns given by the e_{F_i} . Since $w \in \text{Span}(e_{F_1}, \dots, e_{F_k})$, then $w = Ax$ for some $x \in \mathbb{R}^k$. Hence since $w \in u + \bigcap_{i=k+1}^n s_i^\perp$, letting B be the matrix whose columns are given by the s_i , we have $B^t(Ax - u) = 0$ and hence $x = (B^tA)^{-1}B^tu$ where we know the left-inverse exists since A and B have full column rank. The intersection point of these two linear spaces is therefore

$$w = A(B^tA)^{-1}B^tu$$

where $A(B^tA)^{-1}B^t$ can be understood as the matrix of the oblique projection $\pi : \left(\bigcap_{i=k+1}^n s_i^\perp\right)^\perp \rightarrow \text{Span}(e_{F_1}, \dots, e_{F_k})$. Hence we have $\pi(u) \cdot v \geq 0$, which is exactly the condition in Equation (2.5.1). The converse is similar. \square

Algorithm 2.5.9 (Bergman_flip)

Input: (\mathbf{s}, γ) , where

1. $\gamma: [0, t_{\text{target}}] \rightarrow \mathbb{H}^{\mathbf{S}}$ a linear path as in Convention 2.5.1,
2. $\mathbf{s} =: (s_{\text{lin}}, s_{k+1}, \dots, s_n) \in D_{\mathbf{S}}(\gamma(\varepsilon))$ a mixed cell induced by $\gamma(\varepsilon)$,

such that

1. $t_{\text{Bergman}} := t_{\text{Bergman}}(\mathbf{s}, \gamma) < t_{\text{Jensen}}(\mathbf{s}, \gamma)$,
2. $\sigma_{\mathbf{S}}(\mathbf{s}, \gamma(t_{\text{Bergman}})) \in \tau$ for $\tau \in \Sigma_{\text{lin}}^{\text{fine}}(0)$ a facet of the fine structure.

Output: The mixed cells induced by $\gamma(t_{\text{Bergman}} + \varepsilon)$ sharing facet τ :

$$\left\{ (s'_{\text{lin}}, s_{k+1}, \dots, s_n) \in D_{\mathbf{S}}(\gamma(t_{\text{Bergman}} + \varepsilon)) \mid \sigma_{S_{\text{lin}}}(s_{\text{lin}}, 0) \cap \sigma_{S_{\text{lin}}}(s'_{\text{lin}}, 0) = \tau \right\}$$

- 1: Use Algorithm 2.5.3 to compute the tropical intersection point and tropical drift

$$(w, u) := \text{tropical_intersection_point_and_drift}(\mathbf{s}, \gamma).$$

2: Use Algorithm 2.5.4 to compute the time of Bergman failure

$$t_{\text{Bergman}} := t_{\text{Bergman}}(\mathbf{s}, \gamma)$$

3: Let F'_\bullet be the chain of flats induced by $\sigma_{\mathbf{S}}(\mathbf{s}, \gamma(t_{\text{Bergman}})) = w + t_{\text{Bergman}} \cdot u$.

4: Initialise a list of maximal chains of flats $\mathcal{F} := \emptyset$.

5: **for** $F_\bullet = (F_1, \dots, F_k)$ maximal chain of flats refining F'_\bullet **do**

6: Let F_j be the unique flat in F_\bullet and not in F'_\bullet .

7: **if** $\text{Span}(e_{F_1}, \dots, e_{F_k}) \cap \left(\bigcap_{i=k+1}^n s_i^\perp \right) = \{0\}$ and $\pi(u) \cdot v > 0$ as in Lemma 2.5.8

then

8: Add F_\bullet to \mathcal{F} .

9: **end if**

10: **end for**

11: Construct a set of corresponding dual cells $\mathcal{S} := \{\mathbf{s}(F_\bullet) \mid F_\bullet \in \mathcal{F}\}$.

12: **return** \mathcal{S} .

Remark 2.5.10 By Lemma 2.5.7, t_{Bergman} marks the time when the tropical intersection point $\sigma_{\mathbf{S}}(\mathbf{s}, \gamma(t))$ crosses a cone in the fine structure of the Bergman fan $\Sigma_{S_{\text{lin}}}^{\text{fine}}(0)$. In particular, $\sigma_{\mathbf{S}}(\mathbf{s}, \gamma(t))$ need not necessarily cross a cone in the Bergman fan $\Sigma_{S_{\text{lin}}}(0)$, which implies that s_{lin} need not necessarily change under Algorithm 2.5.9. In practise, our implementation keeps track of chains of flats F_\bullet instead of dual cells s_{lin} , so Algorithm 2.5.9 will change the data we are tracking.

Example 2.5.4. Consider from Example 2.2.12

1. $\mathbf{S} := (S_{\text{lin}}, S_3, S_4)$ with $S_{\text{lin}} = \binom{[4]}{2}$, $S_3 = \{e_4, 0\}$, and $S_4 = \{e_1 + e_2, 0\}$,

2. $\mathbf{c}_t := (0, c_3, c_{4,t})$ with $c_3 = (0, 0)$ and $c_{4,t} = (0, t)$,

and the path $\gamma: [-3, 1] \rightarrow \mathbb{T}^{\mathbf{S}}, t \mapsto \mathbf{c}_t$.

For $t = -2$, $D_{\mathbf{S}}(\gamma(-2))$ consists of a single mixed cell $\mathbf{s} = (s_{\text{lin}}, S_3, S_4)$ with $s_{\text{lin}} = \{-e_{14}, -e_{24}, -e_{34}\}$ where $e_{ij} := e_i + e_j$.

The resulting matrix $A_{\mathbf{s}}$, its right-inverse $A_{\mathbf{s}}^{-1}$, and vector $b_{\mathbf{s}}$ from the tropical point and drift computations in Lemma 2.2.6 and Lemma 2.5.2 are

$$A_{\mathbf{s}} = \begin{pmatrix} -1 & 1 & 0 & 0 \\ -1 & 0 & 1 & 0 \\ 0 & 0 & 0 & 1 \\ 1 & 1 & 0 & 0 \end{pmatrix}, \quad A_{\mathbf{s}}^{-1} = \frac{1}{2} \begin{pmatrix} -1 & 0 & 0 & 1 \\ 1 & 0 & 0 & 1 \\ -1 & 2 & 0 & 1 \\ 0 & 0 & 2 & 0 \end{pmatrix}, \quad b_{\mathbf{c}_{-2}} = \begin{pmatrix} 0 \\ 0 \\ 0 \\ -2 \end{pmatrix}. \quad (2.5.2)$$

The data above yields the tropical point and tropical drift

$$\sigma_{\mathbf{S}}(\mathbf{s}, \mathbf{c}_{-2}) = A_{\mathbf{s}}^{-1} \cdot b_{\mathbf{c}_{-2}} = -(1, 1, 1, 0), \quad u_{\mathbf{s}}(\mathbf{s}, \boldsymbol{\gamma}) = -A_{\mathbf{s}}^{-1} \cdot (0, 0, 0, 1) = \frac{1}{2}(1, 1, 1, 0).$$

Alternatively, we could have noted that the chain of flats in the initial mixed cell is $\emptyset \subsetneq \{4\} \subsetneq [4]$, which we can use to construct the same matrices and vector in Equation (2.5.2) but using Lemma 2.2.6 and without the need to consider s_{lin} .

One sees that $t_{\text{Bergman}}(\mathbf{s}, \boldsymbol{\gamma}) = 2$, as $\sigma_{\mathbf{S}}(\mathbf{s}, \mathbf{c}_{-2}) + 2 \cdot u_{\mathbf{s}}(\mathbf{s}, \mathbf{c}_{-2}) = 0$ induces a different chain of flats $F'_{\bullet}: \emptyset \subsetneq [4]$. To compute the chain of flats after the Bergman-flip, notice that all extended chains of flats F'_{\bullet} are:

$$\begin{aligned} F_{\bullet}^{(1)}: \emptyset \subsetneq \{1\} \subsetneq [4], & & F_{\bullet}^{(2)}: \emptyset \subsetneq \{2\} \subsetneq [4], \\ F_{\bullet}^{(3)}: \emptyset \subsetneq \{3\} \subsetneq [4], & & F_{\bullet}^{(4)}: \emptyset \subsetneq \{4\} \subsetneq [4]. \end{aligned}$$

First note that the intersection condition of the criteria in Lemma 2.5.8 means that $F_{\bullet}^{(3)}$ will not be involved post Bergman-flip. Looking at what remains, we get the following normal vectors v and drift projections $\pi(u)$:

$$v^{(1)} = e_1 - (e_2 + e_3 + e_4), \quad v^{(2)} = e_2 - (e_1 + e_3 + e_4), \quad v^{(4)} = e_4 - (e_1 + e_2 + e_3),$$

and

$$\pi^{(1)}(u) = (1, 0, 0, 0), \quad \pi^{(2)}(u) = (0, 1, 0, 0), \quad \pi^{(4)}(u) = \frac{1}{2}(1, 1, 1, 0).$$

Using the remaining criterion in Lemma 2.5.8, we can now see that $F_{\bullet}^{(1)}$ and $F_{\bullet}^{(2)}$ are the two chains post Bergman-flip.

2.5.4 Jensen flip

If $t_{\text{Jensen}} < t_{\text{Bergman}}$, then we can be sure that s_{lin} appears both in \mathbf{s} and in all mixed cells after crossing the corresponding facet of $C_{\mathbf{S}}(\mathbf{s})$. As such, we can replace s_{lin} with a tuple (s_1, \dots, s_k) of binomial hypersurface dual supports whose intersection is equal to $\text{Span}(\sigma_{S_{\text{lin}}}(s_{\text{lin}}, 0))$. This reduces us to computing bistellar flips for the hypersurface dual supports (s_1, \dots, s_n) . The same idea was considered by Anders Jensen [Jen16b], so we simply retell it in our language.

We have

1. An ambient support $\mathbf{S}' = (s_1, \dots, s_k, S_{k+1}, \dots, S_n)$.
2. A transverse mixed cell candidate $\mathbf{s} = (s_1, \dots, s_n)$ with mixed cell cone $C_{\mathbf{S}'}(\mathbf{s})$.
3. A linear path $\gamma : [0, t_{\text{target}}] \rightarrow \mathbb{T}^{\mathbf{S}'}$ with $\gamma(t)$ inducing the same mixed subdivision for all $t < t_{\text{Jensen}}$ and crossing a unique facet F of $C_{\mathbf{S}'}(\mathbf{s})$ generically (i.e. with $\gamma(t_{\text{Jensen}}) \in \text{relint}(F)$, and such that $\gamma(t_{\text{Jensen}})$ is not in the codimension 2 skeleton of the secondary fan of $\text{Cayley}_{\mathbf{S}'}$).

This implies that $\gamma(t_{\text{Jensen}} + \varepsilon)$ and $\gamma(t_{\text{Jensen}} - \varepsilon)$ both induce a regular triangulation on $\text{Cayley}_{\mathbf{S}'}$ for $\varepsilon > 0$ sufficiently small, and all the s_i consist of exactly two points. The regular subdivision of $\text{Cayley}_{\mathbf{S}'}$ changes locally at the points where the facet inequality corresponding to F is nonzero.

Lemma 2.5.11 *Let $p \notin \mathbf{s}$ be the point defining the mixed cell cone facet F . This is defined by an inequality $\kappa_p \cdot \mathbf{c} \leq 0$. Let D_+ be the points in κ_p with a positive coefficient and $D_- \ni p$ the points in κ_p with a negative coefficient. Then, locally at $D = D_+ \sqcup D_-$,*

1. *The maximal simplicies before crossing F are given by $\{D \setminus \{d\} \mid d \in D_-\}$,*
2. *The maximal simplicies after crossing F are given by $\{D \setminus \{d\} \mid d \in D_+\}$.*

Proof. We know that $\gamma(t_{\text{Jensen}}) = w$ is a generic point of F . Crossing the facet to a lift $w + \varepsilon \cdot \kappa_p$ for $\varepsilon > 0$ sufficiently small, we get

$$\kappa_p \cdot (w + \varepsilon \cdot \kappa_p) = \kappa_p \cdot w + \varepsilon |\kappa_p|^2 > 0$$

which means lifting the points with positive coefficient in κ_p lower higher breaks the mixed cell cone. In other words, those points are not involved after crossing F , which is exactly the condition we wrote down. The argument is similar for the maximal simplicies before crossing F . \square

Lemma 2.5.12 (*Bistellar flip.*) *Let \mathbf{s} be a transverse mixed cell candidate and suppose $\gamma : [0, t_{\text{target}}] \rightarrow \mathbb{T}^{\mathbf{S}'}$ crosses the relative interior of a unique facet F of $C_{\mathbf{S}'}(\mathbf{s})$ corresponding to a non active point $p \in s_i$, $p \notin \mathbf{s}$. Suppose further that this crossing point $\gamma(t_{\text{Jensen}})$ is sufficiently generic (i.e. not in the codimension 2 skeleton of $\text{Cayley}_{\mathbf{S}'}$). Let $s_i^+ \subseteq s_i$ be the points with positive coefficient in κ_p . Then immediately after crossing F , the new mixed cells corresponding to \mathbf{s} are given, for each $q \in s_i^+$, by swapping s_i for*

$$s'_i := s_i \cup \{p\} \setminus \{q\}.$$

Proof. Since \mathbf{s} is a transverse mixed cell candidate, it involves exactly two vertices from each hypersurface dual support s_1, \dots, s_n . Then, as maximal simplicies after crossing F , appealing to Lemma 2.5.11, we know that any new mixed cells corresponding to \mathbf{s} must now involve p , and any new mixed cells will remain transverse by genericity. Hence they are defined by not involving exactly one of the points of s_i . The points not involved (and hence the number of new mixed cells) can be determined by their sign in κ_p , since that point is now lifted too high (and arbitrarily high lifts are therefore permitted). This is exactly the condition specified in the lemma. \square

Example 2.5.5. We compute the first Jensen flip encountered in Example 2.2.13, see the top arrow of Figure 2.5. The path γ is tracked from $t = -3$ to $t = 3$. At

$t = -3$, the mixed cell σ dual to the intersection point inside the ray spanned by e_3 in $\Sigma_{\text{lin}}(0)$ is given by

$$\mathbf{s} = (\{e_{13}, e_{23}, e_{43}\}, S_3, \{(0, 2, 2, 0), (0, 2, 0, 0)\}) \subseteq \mathbf{S} = S_{\text{lin}} \sqcup S_3 \sqcup S_4$$

Its tropical drift along γ is 0, which is why its Bergman time is ∞ . One can check that its Jensen time is smaller than the Bergman times and Jensen times from all other mixed cells, which is why \mathbf{s} is Jensen-flipped first.

We replace S_{lin} by the two hypersurface dual supports $S_1 = \{(1, -1, 0, 0), (0, 0, 0, 0)\}$ and $S_2 = \{(1, 0, 0, -1), (0, 0, 0, 0)\}$. One can verify that $S_1^\perp \cap S_2^\perp = \text{Span}(\sigma_{\text{lin}})$. The Cayley matrix of these four supports is given by

$$\text{Cayley}_{(S_3, S_4, S_1, S_2)} = \begin{pmatrix} 0 & 0 & 0 & 0 & 0 & 0 & 0 & 1 & 0 & 1 & 0 \\ 0 & 0 & 1 & 0 & 2 & 0 & 2 & -1 & 0 & 0 & 0 \\ 0 & 0 & 1 & 2 & 2 & 0 & 0 & 0 & 0 & 0 & 0 \\ 1 & 0 & 0 & 0 & 0 & 0 & 0 & 0 & 0 & -1 & 0 \\ 1 & 1 & 0 & 0 & 0 & 0 & 0 & 0 & 0 & 0 & 0 \\ 0 & 0 & 1 & 1 & 1 & 1 & 1 & 0 & 0 & 0 & 0 \\ 0 & 0 & 0 & 0 & 0 & 0 & 0 & 1 & 1 & 0 & 0 \\ 0 & 0 & 0 & 0 & 0 & 0 & 0 & 0 & 0 & 1 & 1 \end{pmatrix}.$$

In the above we have highlighted the columns indexed by σ . For each of the three points not involved, we get a facet of the mixed cell cone. The normals to these facets are given using the procedure described in Algorithm 2.3.5. The reader can verify that the facet that is broken first (at time $t = -1$) corresponds to the point $(0, 1, 1, 0) \in S_4$, with facet normal

$$\kappa_{(0,1,1,0)} = (-2, 2, -1, 0, 0, 0, 1, -2, 2, 2, -2).$$

Both of the points in s_4 have positive coefficient in $\kappa_{(0,1,1,0)}$, so we get two new mixed

cells after crossing this facet, obtained by swapping each of them for $(0, 1, 1, 0)$:

$$\mathbf{s}' := (\{e_{13}, e_{23}, e_{43}\}, S_3, \{(0, 2, 0, 0), (0, 1, 1, 0)\}) \subseteq \mathbf{S},$$

$$\mathbf{s}'' := (\{e_{13}, e_{23}, e_{43}\}, S_3, \{(0, 2, 2, 0), (0, 1, 1, 0)\}) \subseteq \mathbf{S}.$$

The new mixed cells after the flip are $\mathbf{s}', \mathbf{s}''$. These correspond to the two new intersection points as we move from the top left to the top right of Figure 2.5.

We now introduce a lemma that serves to verify whether a perturbation is indeed sufficiently small.

Lemma 2.5.13 *Suppose \mathbf{s} is a transverse mixed cell induced by \mathbf{c} . Suppose \mathbf{c}' is another mixed height such that*

1. $\sigma_{\mathbf{S}'}(\mathbf{s}', \mathbf{c}')$ induces the same chain of flats in M as $\sigma_{\mathbf{S}}(\mathbf{s}, \mathbf{c})$, and
2. $\mathbf{c}' \in \text{relint}(C_{\mathbf{S}'}(\mathbf{s}'))$ for every mixed cell candidate \mathbf{s}' where we replace s_{lin} with the binomial hypersurfaces s_1, \dots, s_k .

Then $\mathbf{c}' \in \text{relint}(C_{\mathbf{S}}(\mathbf{s}))$.

Proof. We need to show that $\mathbf{s} = (s_{\text{lin}}, s_{k+1}, \dots, s_n)$ remains a mixed cell induced by \mathbf{c}' . By (2) and Lemma 2.2.4, we know that s_{k+1}, \dots, s_n remain dual cells induced by c'_{k+1}, \dots, c'_n , respectively, dual to transversally intersecting tropical polyhedra $\sigma_{S_{k+1}}(s_{k+1}, c'_{k+1}), \dots, \sigma_{S_n}(s_n, c'_n)$. By (1), the tropical polyhedra $\sigma_{S_{\text{lin}}}(s_{\text{lin}}, 0), \sigma_{S_{k+1}}(s_{k+1}, c'_{k+1}), \dots, \sigma_{S_n}(s_n, c'_n)$ also intersect transversally. Applying Lemma 2.2.4 again gives $\mathbf{c}' \in \text{relint}(C_{\mathbf{S}}(\mathbf{s}))$. \square

Algorithm 2.5.14 (Jensen_flip)

Input: (\mathbf{s}, γ) , where

1. $\gamma: [0, t_{\text{target}}] \rightarrow \mathbb{H}^{\mathbf{S}}$ a linear path as in Convention 2.5.1,
2. $\mathbf{s} \in D_{\mathbf{S}}(\gamma(\varepsilon))$ a mixed cell induced by $\gamma(\varepsilon)$,

such that

1. $t_{\text{Jensen}}(\mathbf{s}, \gamma) < t_{\text{Bergman}}(\mathbf{s}, \gamma)$
2. $\gamma'(t_{\text{Jensen}}) \in \text{relint}(\tau)$

where $\tau \subseteq C_{\mathbf{S}'}(\mathbf{s}')$ is a facet of the mixed cell cone and \mathbf{S}' , \mathbf{s}' , γ' are as in Definition 2.5.3.

Output: The mixed cells induced by $\gamma(t_{\text{Jensen}} + \varepsilon)$ with mixed cell cone facet τ :

$$\{\mathbf{s}' \in D_{\mathbf{s}}(\gamma(t_{\text{Jensen}} + \varepsilon)) \mid C_{\mathbf{S}'}(\mathbf{s}') \cap C_{\mathbf{S}}(\mathbf{s}) = \tau\}.$$

- 1: Replace \mathbf{s} by $\mathbf{s}' = (s_1, \dots, s_k, s_{k+1}, \dots, s_n)$ as in Definition 2.5.3.
- 2: Let κ_p for $p \in s_i$ be the linear functional cutting out the mixed cell cone facet F .
- 3: Set $A = \{s_i \cup \{p\} \setminus \{q\} \mid q \in s_i, q \text{ has positive coefficient in } \kappa_p\}$.
- 4: **return** $\{\mathbf{s}' = (s_{\text{lin}}, s_{k+1}, \dots, s'_i, \dots, s_n) \mid s'_i \in A\}$.

2.6 Endgame and Timeouts

In this section, we discuss the task of reaching $\gamma(t_{\text{target}})$ in the two cases it is important:

Endgame If $D_{\mathbf{S}}(\mathbf{c}_{\text{target}})$ is the target mixed subdivision we want to compute.

Timeout If $D_{\mathbf{S}}(\mathbf{c}_{\text{target}})$ lies in a different strata of $\mathbb{H}^{\mathbf{S}}$ as described in Remark 2.2.11.

In the following, we assume without loss of generality that $\mathbf{c} = \gamma(0)$.

2.6.1 Endgame

One way for computing $D_{\mathbf{S}}(\mathbf{c}_{\text{target}})$ or $\Sigma_{\mathbf{S}}(\mathbf{c}_{\text{target}})$ in the case that $\mathbf{c}_{\text{target}} \in C_{\mathbf{S}}(\mathbf{s})$ for all $\mathbf{s} \in D_{\mathbf{S}}(\gamma(\varepsilon))$ for $\varepsilon > 0$ sufficiently small, but $D_{\mathbf{S}}(\mathbf{c}_{\text{target}})$ not necessarily transverse, is by following Definition 2.2.7 and using tropical points and tropical drifts.

Lemma 2.6.1 *Let $\gamma: [0, t_{\text{target}}] \rightarrow \mathbb{H}^{\mathbf{S}}$ be a linear mixed height path such that for $\varepsilon > 0$ sufficiently small $D_{\mathbf{S}}(\gamma(\varepsilon))$ is transverse and $\gamma(t_{\text{target}}) \in C_{\mathbf{S}}(\mathbf{s})$ for all $\mathbf{s} \in D_{\mathbf{S}}(\gamma(\varepsilon))$. Then*

$$\Sigma_{\mathbf{S}}(\gamma(t_{\text{target}})) = \left\{ \sigma_{\mathbf{S}}(\mathbf{s}, \gamma(0)) + t_{\text{target}} \cdot u(\mathbf{s}, \gamma) \mid \mathbf{s} \in D_{\mathbf{S}}(\gamma(0)) \right\}$$

where $u(\mathbf{s}, \gamma) \in \mathbb{H}_{\mathbb{R}}^{\mathbf{S}}$ denotes the tropical drift of \mathbf{s} along γ .

Proof. Follows directly from Proposition 2.2.8. □

Lemma 2.6.1 justifies following algorithm:

Algorithm 2.6.2 (endgame_tracker)

Input: $(D_{\mathbf{S}}(\mathbf{c}), \gamma)$, where $D_{\mathbf{S}}(\mathbf{c})$ transverse and $\gamma: [0, t_{\text{target}}] \rightarrow \mathbb{T}^{\mathbf{S}}$ is a linear path in the mixed height space with $\gamma(0) = \mathbf{c}$ and $\gamma(t_{\text{target}}) =: \mathbf{c}^{\circ}$.

Output: $D_{\mathbf{S}}(\mathbf{c}^{\circ})$.

- 1: Initialise $D_{\mathbf{S}}(\mathbf{c}^{\circ}) := \emptyset$
- 2: **for** $\mathbf{s} \in D_{\mathbf{S}}(\mathbf{c})$ **do**
- 3: **if** $\mathbf{c} \in \text{relint}(C_{\mathbf{S}}(\mathbf{s}))$ **then**
- 4: Add \mathbf{s} to $D_{\mathbf{S}}(\mathbf{c}^{\circ})$.
- 5: **else**
- 6: Use Algorithm 2.5.3 to compute the tropical intersection point and drift

$$(w, u) := \text{tropical_intersection_point_and_drift}(\mathbf{s}, \gamma).$$
- 7: Set $w^{\circ} := w + t_{\text{target}} \cdot u$.
- 8: Construct \mathbf{s}° from w° .
- 9: Add \mathbf{s}° to $D_{\mathbf{S}}(\mathbf{c}^{\circ})$.
- 10: **end if**
- 11: **end for**
- 12: **return** $D_{\mathbf{S}}(\mathbf{c}^{\circ})$.

2.6.2 Timeouts

We now explain what happens to the mixed cells for unbounded paths γ that move to a strata at infinity of $\mathbb{H}^{\mathbf{S}}$ as per Remark 2.2.11. Whilst a variation of Algorithm 2.6.2 could be used, the situation of an unbounded path is actually much easier. The following lemma explains which mixed cells get deleted and which stay:

Lemma 2.6.3 *Let $\gamma = (0, \gamma_{k+1}, \dots, \gamma_n): [0, \infty] \rightarrow \mathbb{T}^{\mathbf{S}}$ be an unbounded linear path such that $\gamma(t) \in C_{\mathbf{S}}(D_{\mathbf{S}}(\mathbf{c}))$ for all $t \in [0, \infty)$, where $\mathbf{c} := \gamma(\varepsilon)$ for $\varepsilon > 0$ sufficiently small. Then*

$$D_{\mathbf{S}}(\gamma(\infty)) = \left\{ (s_{\text{lin}}, s_{k+1}, \dots, s_n) \in D_{\mathbf{S}}(\mathbf{c}) \mid (\gamma_i(\infty))_{\alpha} \neq \infty \text{ for all } \alpha \in s_i \text{ for all } i \right\}.$$

In particular, if $D_{\mathbf{S}}(\mathbf{c})$ is transverse, then so is $D_{\mathbf{S}}(\gamma(\infty))$.

Proof. The lemma follows from the explicit duality between mixed cells and tropical intersection points in Lemma 2.2.4, which implies that as t diverges to ∞ , the tropical intersection point $\sigma_{\mathbf{S}}(\mathbf{s}, \gamma(t))$ diverges if and only if the mixed cell \mathbf{s} does not satisfy the equation above. \square

Algorithm 2.6.4 (timeout_tracker)

Input: $(D_{\mathbf{S}}(\mathbf{c}), \gamma)$, where $D_{\mathbf{S}}(\mathbf{c})$ is transverse and $\gamma: [0, \infty] \rightarrow \mathbb{T}^{\mathbf{S}}$ is an infinite linear path with $\mathbf{c} = \gamma(0)$ and $\gamma(t) \in C_{\mathbf{S}}(D_{\mathbf{S}}(\mathbf{c}))$ for all $t \in [0, \infty)$.

Output: $D_{\mathbf{S}}(\gamma(\infty))$.

1: **return** $\{(s_{\text{lin}}, s_{k+1}, \dots, s_n) \in D_{\mathbf{S}}(\mathbf{c}) \mid (\gamma_i(\infty))_{\alpha} \neq \infty \text{ for all } \alpha \in s_i\}$.

2.7 The homotopy algorithm

In this section, we combine the previous algorithms to formulate the main algorithm for tropical homotopy continuation, beginning with the path tracking algorithm for a linear path.

Note that Algorithm 2.7.1 only tracks the mixed subdivision to a mixed height $\mathbf{c}_{\text{target}}$ close to the target $\gamma(t_{\text{target}})$. This is because we do not require $D_{\mathbf{S}}(\gamma(t_{\text{target}}))$ to be transverse, as it is difficult to test a priori. We remark now that Algorithm 2.7.1 may raise an error if γ is not generic. In theory, this is not possible if the starting mixed height is chosen generically. In application, this can be corrected for using symbolic perturbations as in [Jen16b, Section 6.1].

Algorithm 2.7.1 (`linear_tracker`)

Input: $(D_{\mathbf{S}}(\mathbf{c}), \gamma)$, where $D_{\mathbf{S}}(\mathbf{c})$ transverse and $\gamma: [0, t_{\text{target}}] \rightarrow \mathbb{T}^{\mathbf{S}}$ is a linear path in the mixed height space with $D_{\mathbf{S}}(\mathbf{c}) = D_{\mathbf{S}}(\gamma(\varepsilon))$ for $\varepsilon > 0$ sufficiently small.

Output: $(D_{\mathbf{S}}(\mathbf{c}_{\text{target}}), \mathbf{c}_{\text{target}})$, where $D_{\mathbf{S}}(\mathbf{c}_{\text{target}})$ transverse and $\mathbf{c}_{\text{target}}$ sufficiently close to $\gamma(t_{\text{target}})$ in the sense that

$$\gamma(t_{\text{target}}) \in C_{\mathbf{S}}(\mathbf{s}) \text{ for all } \mathbf{s} \in D_{\mathbf{S}}(\mathbf{c}_{\text{target}}).$$

1: Use Algorithm 2.5.4 to identify the minimal time of Bergman failure:

$$t_{\text{Bergman}} := \min\{t_{\text{Bergman}}(\mathbf{s}, \gamma) \mid \mathbf{s} \in D_{\mathbf{S}}(\mathbf{c})\}.$$

2: Use Algorithm 2.5.6 to identify the minimal time of Jensen failure:

$$t_{\text{Jensen}} := \min\{t_{\text{Jensen}}(\mathbf{s}, \gamma) \mid \mathbf{s} \in D_{\mathbf{S}}(\mathbf{c})\}.$$

3: Set $t_{\min} := \min(t_{\text{Bergman}}, t_{\text{Jensen}})$.

4: **if** $t_{\text{target}} \leq t_{\min}$ **then**

5: **return** $(D_{\mathbf{S}}(\mathbf{c}), \mathbf{c})$

6: **end if**

7: Initialise $D' := D_{\mathbf{S}}(\mathbf{c})$.

8: **for** $\mathbf{s} \in D_{\mathbf{S}}(\mathbf{c})$ **do**

9: **if** $t_{\text{Bergman}}(\mathbf{s}, \gamma) = t_{\min} = t_{\text{Jensen}}(\mathbf{s}, \gamma)$ **then**

10: **Error:** γ not generic.

11: **end if**

12: **if** $t_{\text{Bergman}}(\mathbf{s}, \gamma) = t_{\min}$ **then**

```

13:   if  $\sigma_{\mathbf{S}}(\mathbf{c}, \gamma(t_{\text{Bergman}}))$  induces a chain of flats of length less than  $k - 2$ , then
14:       Error:  $\gamma$  not generic.
15:   end if
16:   Use Algorithm 2.5.9 to compute the Bergman flipped mixed cells

            $\{\mathbf{s}'_1, \dots, \mathbf{s}'_\ell\} := \text{Bergman\_flip}(\mathbf{s}, \gamma)$ 

17:   Update  $D' := D_{\mathbf{S}}(\mathbf{c}) \setminus \{\mathbf{s}\} \cup \{\mathbf{s}'_1, \dots, \mathbf{s}'_\ell\}$ .
18:   end if
19:   if  $t_{\text{Jensen}}(\mathbf{s}, \gamma) = t_{\min}$  then
20:       if  $\gamma(t_{\text{Jensen}})$  does not lie in the relative interior of a facet of  $C'_{\mathbf{S}}(\mathbf{s}')$ , then
21:           Error:  $\gamma$  not generic.
22:       end if
23:       Use Algorithm 2.5.14 to compute the Jensen flipped mixed cells

            $\{\mathbf{s}'_1, \dots, \mathbf{s}'_\ell\} := \text{Jensen\_flip}(\mathbf{s}, \gamma)$ 

24:       Update  $D' := D_{\mathbf{S}}(\mathbf{c}) \setminus \{\mathbf{s}\} \cup \{\mathbf{s}'_1, \dots, \mathbf{s}'_\ell\}$ .
25:   end if
26: end for
27: Let  $\gamma': [0, t_{\text{target}} - t_{\min}] \rightarrow \mathbb{H}^{\mathbf{S}}, t \mapsto \gamma(t + t_{\min})$ .
28: return linear_tracker( $D', \gamma'$ ).

```

Note that the recursive Algorithm 2.7.1 indeed terminates in finite time:

Lemma 2.7.2 *Algorithm 2.7.1 terminates in finite time with probability 1.*

Proof. Note that whenever we run `Bergman_flip` or `Jensen_flip` we make a change to the combinatorial structure of the mixed subdivision $D_{\mathbf{S}}(\mathbf{c})$. As there are only finitely many such combinatorial types and we are decreasing the distance to $\gamma(t_{\text{target}})$ with each flip, we will reach termination in Line 5 after finitely many calls to `Bergman_flip` and `Jensen_flip`. Moreover, `perturbation` returns with probability 1 a perturbed path γ' for whom $t_{\text{Jensen}} \neq t_{\text{Bergman}}$. Consequently, the probability of

being stuck endlessly in the case $t_{\text{Jensen}} = t_{\text{Bergman}}$ is 0. \square

Next we need the following algorithm for adjusting homotopy paths γ to facilitate the fact that Algorithm 2.7.1 does not necessarily reach the potentially degenerate target mixed height. Note that Algorithm 2.7.3 returns a path with the same target mixed height if $t_{\text{target}} \neq \infty$, which is important to guarantee that the main algorithm reaches the desired target mixed height.

Algorithm 2.7.3 (path_rebase)

Input: (γ, \mathbf{c}') , where $D_{\mathbf{S}}(\mathbf{c}')$ transverse and $\gamma: [0, t_{\text{target}}] \rightarrow \mathbb{T}^{\mathbf{S}}$ is a linear path in the mixed height space with $\gamma(0) \in C_{\mathbf{S}}(D_{\mathbf{S}}(\mathbf{c}))$.

Output: $\gamma': [0, t_{\text{target}}] \rightarrow \mathbb{H}^{\mathbf{S}}$ linear with $\gamma'(0) = \mathbf{c}'$ and

1. $\gamma(t_{\text{target}}) = \gamma'(t_{\text{target}})$ if $t_{\text{target}} \neq \infty$, or
 2. $\gamma(t_{\text{target}}) \in C_{\mathbf{S}}(\mathbf{s})$ for all $\mathbf{s} \in D_{\mathbf{S}}(\gamma'(t_{\text{target}}))$.
- 1: Suppose $\gamma: [0, t_{\text{target}}] \rightarrow \mathbb{H}^{\mathbf{S}}, t \mapsto \mathbf{c} + t \cdot \mathbf{u}$ for $\mathbf{c}, \mathbf{u} \in \mathbb{H}_{\mathbb{R}}^{\mathbf{S}}$.
 - 2: **if** $t_{\text{target}} = \infty$ **then**
 - 3: Set $\gamma': [0, t_{\text{target}}] \rightarrow \mathbb{H}^{\mathbf{S}}, t \mapsto \mathbf{c}' + t \cdot \mathbf{u}$.
 - 4: **else**
 - 5: Set $\gamma': [0, t_{\text{target}}] \rightarrow \mathbb{H}^{\mathbf{S}}, t \mapsto \mathbf{c}' + t \cdot (\mathbf{u} + \frac{\mathbf{c} - \mathbf{c}'}{t_{\text{target}}})$.
 - 6: **end if**
 - 7: **return** γ'

We now have all necessary parts for the main tropical homotopy continuation algorithm.

Algorithm 2.7.4 (Stable intersection via tropical homotopy continuation)

Input: $(A_M, f_{k+1}^{\circ}, \dots, f_n^{\circ})$, where

1. $A_M \in K^{k \times n}$, the realisation matrix of a matroid M ,
2. $f_i^{\circ} =: \sum_{\alpha \in S_1^{\circ}} c_{i,\alpha}^{\circ} \odot x^{\alpha} \in \mathbb{T}[x^{\pm}]$ tropical Laurent polynomials.

Output: The stable intersection

$$\text{Trop}(M) \wedge \text{Trop}(f_{k+1}^\circ) \wedge \cdots \wedge \text{Trop}(f_n^\circ),$$

where $\text{Trop}(M)$ is the Bergman fan of M in \mathbb{R}^n and the $\text{Trop}(f_i^\circ)$ are the tropical hypersurfaces of f_i° in \mathbb{R}^n .

1: Use Algorithm 2.4.3 to construct the randomised starting data

$$D_{\mathbf{S}}(\mathbf{c}) = \text{starting_data}(A_M, \mathbf{S}^\circ).$$

where $\mathbf{S}^\circ := (S_{\text{lin}}, S_{k+1}, \dots, S_n)$.

2: Follow Definition 2.4.4 and pick a piecewise linear path $\gamma^\bullet := (\gamma^{(1)}, \dots, \gamma^{(\ell)})$ connecting $\mathbf{c} \in \mathbb{H}^{\mathbf{S}}$ to $\mathbf{c}^\circ := (0, c_{k+1}^\circ, \dots, c_n^\circ) \in \mathbb{H}^{\mathbf{S}^\circ}$, say

$$\gamma^{(i)} : [0, t_{\text{target}}^{(i)}] \longrightarrow \mathbb{T}^{\mathbf{S}^{(i)}},$$

where $\mathbf{S}^{(i)} \subseteq \mathbf{S}$ such that $\gamma^{(i)}(0) \in \mathbb{H}_{\mathbb{R}}^{\mathbf{S}^{(i)}}$ (which means $\mathbf{S}^{(\ell)} = \mathbf{S}^\circ$).

3: **for** $(\gamma, t_{\text{target}}) = (\gamma^{(1)}, t_{\text{target}}^{(1)}), \dots, (\gamma^{(\ell)}, t_{\text{target}}^{(\ell)})$ **do**

4: Translate γ to make it start at \mathbf{c} by Algorithm 2.7.3.

5: Use Algorithm 2.7.1 to track $D_{\mathbf{S}}(\mathbf{c})$ from \mathbf{c} to around $\gamma(t_{\text{target}})$

$$(D_{\mathbf{S}}(\mathbf{c}), \mathbf{c}) := \text{linear_tracker}(D_{\mathbf{S}}(\mathbf{c}), \gamma).$$

6: **if** $t_{\text{target}} = \infty$ **then**

7: Use Algorithm 2.6.4 to prune the mixed cells

$$D_{\mathbf{S}}(\gamma(\infty)) := \text{timeout_tracker}(D_{\mathbf{S}}(\mathbf{c}), \gamma).$$

8: Update $\mathbf{c} := \gamma(\infty)$.

9: **end if**

10: **end for**

11: Let $\gamma^{(\ell+1)}$ be the path connecting \mathbf{c} to \mathbf{c}° in $\mathbb{H}_{\mathbb{R}}^{(\ell)}$.

12: Use Algorithm 2.6.2 to compute the target mixed subdivision

$$D_{\mathbf{S}}(\mathbf{c}^\circ) := \text{endgame_tracker}(D_{\mathbf{S}}(\mathbf{c}), \gamma^{(\ell+1)}).$$

13: Use Corollary 2.2.5 to construct the stable intersection $\Sigma_{\mathcal{S}^\circ}(\mathbf{c}^\circ)$.

14: **return** $\Sigma_{\mathcal{S}^\circ}(\mathbf{c}^\circ)$.

2.8 Applications

In this section, we discuss two applications which prominently feature stable intersections that can be computed using tropical homotopy continuation. Section 2.8.1 explains how to incorporate inverted tropical linear spaces on a small example from graph rigidity. Section 2.8.2 describes a more involved example from chemical reaction networks.

2.8.1 Graph Rigidity

Graph rigidity studies graphs that have a rigid embedding into \mathbb{R}^d for some d and various notions of rigidity; see [Sou24] for a recent overview. We focus on generically rigid graphs for $d = 2$, also known as Laman graphs, and we are concerned with their realisation number, which is the number of embeddings these graphs have modulo some natural transformations. We will use the tropical characterisation of realisation number from [Cla+25].

Definition 2.8.1. A *Laman graph* is a simple graph $G = ([n], E)$ on n vertices and $2n - 3$ edges such that any k -vertex subgraph has at most $2k - 3$ edges. The *realisation number* of G is the tropical intersection number

$$\frac{1}{2} \cdot \text{Trop}(G) \cdot (-\text{Trop}(G)),$$

where

1. $\text{Trop}(G)$ denotes the Bergman fan of the graphic matroid of G [MS15, Example 4.2.14],
2. $\text{Trop}(G)$ is regarded as a balanced polyhedral complex in the tropical torus $\mathbb{R}^{|E|}/(1, \dots, 1) \cdot \mathbb{R}$ as in [MS15, Section 4.4] and [Jos21, Section 10],

3. $-\text{Trop}(G)$ denotes the image of $\text{Trop}(G)$ under the linear transformation $\mathbb{R}^{|E|}/(1, \dots, 1) \cdot \mathbb{R} \rightarrow \mathbb{R}^{|E|}/(1, \dots, 1) \cdot \mathbb{R}, \bar{w} \mapsto -\bar{w}$,
4. $\text{Trop}(G) \cdot (-\text{Trop}(G))$ denotes the number of points in their stable intersection (counted with multiplicity).

Note that as we are working in the tropical torus, intersection points can be regarded as affine lines in $\mathbb{R}^{|E|}$ parallel to $(1, \dots, 1) \cdot \mathbb{R}$.

The following example exemplifies how we can use tropical homotopy continuation to work with inverted tropical linear spaces like $-\text{Trop}(G)$:

Example 2.8.2. Let G be the complete graph with 4 vertices minus an edge as illustrated in Figure 2.12. It has 5 edges. To compute its realisation number, we consider in \mathbb{R}^{5+5} with coordinates

$$e_{x_{12}}, e_{x_{13}}, e_{x_{23}}, e_{x_{24}}, e_{x_{34}}, \quad e_{y_{12}}, e_{y_{13}}, e_{y_{23}}, e_{y_{24}}, e_{y_{34}}$$

the stable intersection of

1. the Bergman fan $\Sigma_G \times \Sigma_G$
2. the tropical hypersurfaces $\text{Trop}(x_{ij}y_{ij} \oplus 0)$ for $\{ij\} \in E$.

Note that the tropical linear space $\Sigma_G \times \Sigma_G$ is the tropicalisation of a linear ideal that can be read of its signed incidence matrix M_G in Figure 2.12:

$$\Sigma_G \times \Sigma_G = \text{Trop} \left(\langle M_G \cdot (x_{12}, \dots, x_{34})^t \rangle + \langle M_G \cdot (y_{12}, \dots, y_{34})^t \rangle \right),$$

where for example $\langle M_G \cdot (x_{12}, \dots, x_{34})^t \rangle$ stands for the linear ideal generated by the four entries of the vector $M_G \cdot (x_{12}, \dots, x_{34})^t$.

Applying our starting data algorithm yields the starting dual supports $S_{ij} = \{2e_{x_{ij}}, e_{x_{ij}} + e_{y_{ij}}, 2e_{y_{ij}}, 0\}$ for $\{ij\} \in E(G)$. A total of 7 mixed cells diverge as we track the mixed height to the target mixed height $0 \in \mathbb{H}^{\mathbb{S}^\circ}$. On average we track a maximum of 6 mixed cells at a time, and after the endgame we are left with a single mixed cell corresponding to the tropical intersection point $\bar{0}$ with multiplicity 4.

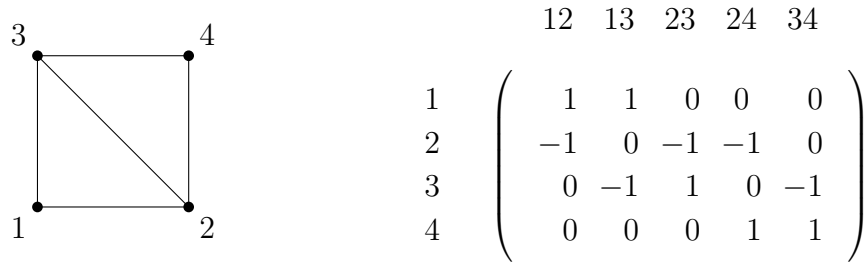


Figure 2.12: A Laman graph G and (one of) its signed incidence matrix M_G .

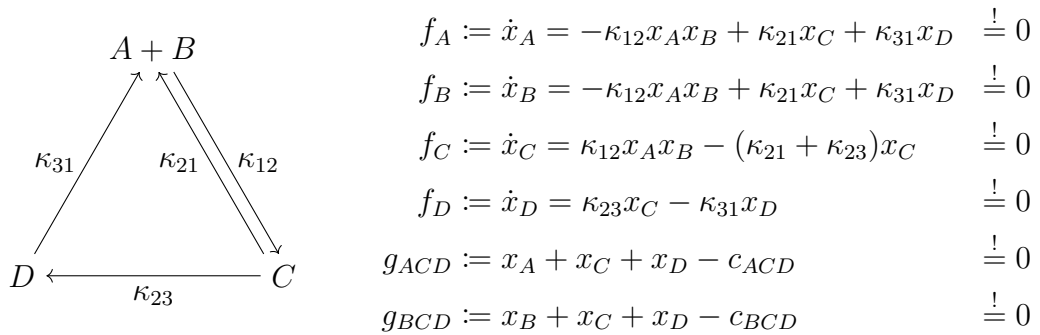


Figure 2.13: A chemical reaction networks, and its steady state and conservation equations.

2.8.2 Chemical Reaction Networks

Chemical reaction network theory studies the dynamics of chemical systems. We refer the reader to [Dic16] for an introduction to the algebraic geometry in chemical reaction network theory. Figure 2.13 shows the simple reaction network from [Dic16, Section 2], as well as the steady state system $\{f_A, f_B, f_C, f_D\}$ and the conservation equations $\{g_{ACD}, g_{BCD}\}$ arising from it. After removing redundant equations, polynomial systems arising from chemical reaction networks are parametrised polynomial systems of the following form:

Definition 2.8.3. A *vertically parametrised polynomial system* is a parametrised polynomial system $\{f_1, \dots, f_n\} \subseteq K[a][x]$ of the form

$$f_i = \sum_{\alpha \in S_i} c_{i,\alpha} \cdot a_\alpha \cdot x^\alpha \in K[a][x] := K[a_\alpha \mid \alpha \in S][x_1, \dots, x_n]$$

for some coefficients $c_{i,\alpha} \in K$, finite supports $S_1, \dots, S_n \subseteq \mathbb{Z}^n$ and $S := \bigcup_{i=1}^n S_i$. Letting $I := \langle f_1, \dots, f_n \rangle \subseteq K[a][x]$ denote the ideal they generate, the *generic root*

count of I is the vector space dimension

$$\ell_{I,K(a)} := \dim_{K(a)} K(a)[x] / I \otimes_{K[a]} K(a),$$

where $K(a) := K(a_\alpha \mid \alpha \in S)$ is the rational function field in the parameters.

While the systems arising from chemical reaction networks can be quite complicated, their structure allows for special insight into their solution sets, such as generic dimension [FHP23] or smoothness of existing positive solutions [FHP24]. Of particular interest to us is the fact that the generic root count can be expressed as a tropical intersection number, which means we can apply the techniques introduced in this chapter:

Corollary 2.8.1 *Let $I = \langle f_1, \dots, f_n \rangle \subseteq K[a][x]$ be as in Definition 2.8.3. Then*

$$\ell_{I,K(a)} := \text{Trop}(\langle \hat{f}_1, \dots, \hat{f}_n \rangle) \cdot \prod_{\alpha \in S} \text{Trop}(\hat{g}_\alpha),$$

where

$$\hat{f}_i := \sum_{\alpha \in S_i} c_{i,\alpha} \cdot y_\alpha \quad \text{and} \quad \hat{g}_\alpha := y_\alpha - x^\alpha \in K[x_i, y_\alpha \mid i \in [n], \alpha \in S].$$

Proof. Follows from [HHR24, Lemma 4.2]. □

Moreover, not only does the tropical intersection number in Corollary 2.8.1 give us the generic root count $\ell_{I,K(a)}$, computing the tropical intersection points for a generic perturbation allows us to construct homotopies for computing $V(I_Q)$ for some given choice of parameters $Q \in K^S$ [HHR24, Algorithm 3.1].

Note that we regard steady state systems of chemical reaction networks as vertically parametrised systems as in Definition 2.8.3 even though the conservation laws lack parameters. The fact that this does not change the generic root count is subject to ongoing work.

Chapter 3

Finite Cluster Structures on E_n Homogeneous Spaces

3.1 Overview

In this chapter we discuss finite type cluster structures on the homogeneous varieties associated to representations of the type E_n Lie groups. The main result concerns a finite type cluster structure on the (complex) Cayley plane, which is the cominuscule homogeneous space $\mathbb{O}\mathbb{P}^2 = E_6/P_6$. Along the way we will introduce Laurent phenomenon algebras and discuss relevant aspects of toric and birational geometry. Laurent phenomenon algebras (LPAs) are a generalisation of Fomin and Zelevinsky's cluster algebras [FZ02a] [FZ02b] [BFZ05] [FZ07] introduced by Lam and Pylyavskyy in [LP16]. They are defined in terms of essentially arbitrary exchange polynomials, with the caveat that mutation of seeds admits a more involved description. The advantage of Laurent phenomenon algebras is that the theory of cluster varieties (as we discuss later) looks essentially the same for them as it does for Fomin and Zelevinsky's cluster algebras, but transition maps between torus charts are no longer constrained to be in terms of binomials.

The existence of cluster algebra structures (cluster structures) on the coordinate rings of homogeneous spaces have been an active area of study for some time,

beginning with the case of Grassmannians [Sco06] and followed by the case of partial flag varieties by Geiß, Leclerc & Schröer [GLS08]. Their construction provides cluster algebra structures for both the Cayley plane and the Freudenthal variety E_7/P_7 , albeit not ones of finite type. Given the non-uniqueness of LPA structures in general, it is quite possible (as we show for the Cayley plane in this chapter) that a homogeneous variety may admit a finite type LPA structure, even when it only has cluster algebra structures that are not of finite type.

A cluster structure (or more generally, as we consider in this chapter, a LPA structure) on the coordinate ring of an algebraic variety \mathcal{V} need not be uniquely determined, since it depends on a choice of anticanonical divisor $\mathcal{D} \subset \mathcal{V}$, on which a set of *frozen coefficients* vanish. The simplest examples of cluster structures are *finite type cluster structures*, in which the cluster algebra has only finitely many seeds, although these are rather uncommon since cluster algebras are typically not of finite type.

The *Cayley plane* is the main homogeneous space we study in this chapter. It is a 16-dimensional algebraic variety, with a projective ‘octonic spinor’ embedding $\mathbb{O}\mathbb{P}^2 \subset \mathbb{P}^{26}$ of codimension 10. As stated earlier, it can be realised as the cominiscule homogeneous space E_6/P_6 . Despite the name, the Cayley plane was first discovered by Ruth Moufang in 1933 [Mou33]. It was named after Cayley since it can also be realised as the projective plane over the octonions.

The work in this chapter was joint with Tom Ducat, and is largely based on the joint publication [DD24]. The proof of the main result relies on the author’s open source SageMath package, freely available at

[https://github.com/oliverdaisey/sage/blob/develop/src/sage/combinat/
lp_algebra_seed.py](https://github.com/oliverdaisey/sage/blob/develop/src/sage/combinat/lp_algebra_seed.py)

3.2 Preliminaries

We first recall the basic notions that define Lam and Pylyavskyy's Laurent phenomenon algebras. A more detailed treatment is available in [LP16].

3.2.1 Seeds

Let A be a commutative ring, which we assume to be a unique factorisation domain. We view A as a *coefficient ring*. One typically takes A to be \mathbb{Z} , any polynomial ring over \mathbb{Z} , or even a polynomial ring over \mathbb{Q} , but throughout this section we will take A to be the \mathbb{C} -algebra freely generated by indeterminates a_1, a_2, \dots, a_m for some $m \in \mathbb{N}$. Denote $\mathcal{F} = \text{Frac}(A[x_1, \dots, x_n])$.

Definition 3.2.1. A *seed* S is a tuple (\mathbf{x}, \mathbf{f}) , where $\mathbf{x} = \{x_1, \dots, x_n\}$ is a transcendence basis for \mathcal{F} over $\text{Frac}(A)$, and $\mathbf{f} = \{f^1, \dots, f^n\}$ is a collection of polynomials in $A[x_1, \dots, x_n]$ satisfying the following conditions:

1. (LP1) Each f^ℓ is irreducible and not divisible by any variable x_t ,
2. (LP2) f^ℓ does not involve the variable x_ℓ .

We call \mathbf{x} the *cluster* of S . Each element of \mathbf{x} is called a *cluster variable*. Each element of \mathbf{f} is called an *exchange polynomial*.

Note the cluster variables and the exchange polynomials are unordered, but the exchange polynomial f^ℓ corresponds to the cluster variable x_ℓ . Since we have n cluster variables, we say that S is of *rank* n .

We let $\mathcal{L} = \mathcal{L}(S)$ denote the Laurent polynomial ring $A[x_1^{\pm 1}, \dots, x_n^{\pm 1}]$ in the cluster variables of S .

Definition 3.2.2. Let $S = (\mathbf{x}, \mathbf{f})$ be a seed. We define the collection $\hat{\mathbf{f}} = \{\hat{f}^1, \dots, \hat{f}^n\} \subset \mathcal{L}$ of *exchange Laurent polynomials* by the following conditions:

1. $\hat{f}^\ell = \frac{f^\ell}{M}$, where $M = x_1^{c_1} \dots x_n^{c_n}$ is a monomial in the cluster variables x_t , $t \neq \ell$,

2. For each $t \neq \ell$, we have that

$$\hat{f}^\ell|_{x_t \leftarrow f^t/x} \in A[x_1^{\pm 1}, \dots, x_{t-1}^{\pm 1}, x_t^{\pm 1}, x_{t+1}^{\pm 1}, \dots, x_n^{\pm 1}],$$

and $\hat{f}^\ell|_{x_t \leftarrow f^t/x}$ is not divisible by f^t as an element of this ring.

Remark 3.2.3. The \hat{f}^ℓ are well-defined, since their definition tells us how to obtain them uniquely. Indeed, the power of x_t in the monomial M is equal to the largest power of f^t that divides f^ℓ upon the substitution $x_t \leftarrow f^\ell/x$.

Lemma 3.2.4. *If f^ℓ/\hat{f}^ℓ involves x_t , then f^t does not use the variable x_ℓ .*

Proof. Viewing f^ℓ as a polynomial in x_t , we can write $f^\ell = f^\ell|_{x_t \leftarrow 0} + Cx_t$. By the above remark, we see that f^t divides $f^\ell|_{x_t \leftarrow f^t/x}$. Hence f^t must divide $f^\ell|_{x_t \leftarrow 0}$. By (LP1), we have $f^\ell|_{x_t \leftarrow 0} \neq 0$. By (LP2), f^ℓ does not depend on x_ℓ . Hence the constant term $f^\ell|_{x_t \leftarrow 0}$ does not depend on x_ℓ . Since f^t is a factor of the constant term, it follows that f^t also does not depend on x_ℓ . \square

3.2.2 Mutation

We now move on to the definition of seed mutation. The most important point is that, whilst mutation in cluster algebras is fully deterministic, in the setting of LP algebras the mutation is only defined up to a collection of units.

Definition 3.2.5. Let $S = (\mathbf{x}, \mathbf{f})$ be a seed. Let $i \in \{1, \dots, n\}$. Then we define a *mutation* $\mu_i(S) = S_i = (\mathbf{y}_i, \mathbf{f}_i)$ of S at index i as follows:

1. The cluster variables of S_i are the same, except we replace x_i according to its exchange relation. That is, $\mathbf{y}_i = \{x_1, \dots, y_i, \dots, x_n\}$, where

$$x_i y_i = \hat{f}^i.$$

Note that we use the exchange *Laurent* polynomial in this relation.

2. The exchange polynomial f_i^i corresponding to y_i remains the same, that is $f_i^i := f^i$. The exchange polynomials f_i^ℓ for $\ell \neq i$ are defined through the

following procedure: If f^ℓ does not depend on x_i , then we set f_i^ℓ to be any polynomial satisfying $f_i^\ell = u f^\ell$, where u is a unit in A . If f^ℓ does depend on x_i , then we execute the following:

- **Substitution step.** We set

$$(f_i^\ell)' = f^\ell \Big|_{x_i \leftarrow \frac{\hat{f}^i|_{x_\ell \leftarrow 0}}{y_i}}.$$

- **Cancellation step.** We divide out by any common factors $(f_i^\ell)'$ shares with $\hat{f}^i|_{x_\ell \leftarrow 0}$. This then defines f_i^ℓ up to a monomial multiplier.
- **Normalisation step.** We multiply through by a monomial in the variables $x_1, \dots, y_i, \dots, x_n$ to make f_i^ℓ satisfy (LP1) and (LP2) as an exchange polynomial in S_i . Such a monomial will be uniquely defined only up to a unit. Thus f_i^ℓ is only defined up to a unit multiplier.

We denote a sequence of mutations $\mu_{s_1 s_2 \dots s_k}(S) := \mu_{s_k} \circ \mu_{s_{k-1}} \circ \dots \circ \mu_{s_1}(S) = S_{s_1 s_2 \dots s_k}$.

Remark 3.2.6. We note that when we are mutating an exchange polynomial that does depend on x_i , the substitution step is well-defined, since the denominator of the exchange Laurent polynomial \hat{f}^i cannot involve x_ℓ , by Lemma 3.2.4.

We summarise the main properties of mutation in the following:

Proposition 3.2.7. *Let S be a seed and $S_i = \mu_i(S)$ a mutation of S at index i .*

Then:

1. *Mutation of S produces a valid seed*

$$S_i = (\mathbf{y}_i, \mathbf{f}_i) = (\{x_1, \dots, y_i, \dots, x_n\}, \{f_i^1, \dots, f_i^n\}).$$

2. *Mutation is involutive, so we can choose a mutation $\mu_i(S_i)$ of S_i so that $S = \mu_i(S_i)$.*
3. *f^ℓ depends on x_i if and only if f_i^ℓ depends on y_i .*
4. *For each index i , we have $\hat{f}_i^i = \hat{f}^i$.*

Of course, the most striking property of LP seed mutation is that every cluster variable we can get is a Laurent polynomial in the original cluster.

Proposition 3.2.8. (*Laurent phenomenon*). *Let $S = (\mathbf{x}, \mathbf{f})$ be a seed. Then for any sequence of indices s_1, \dots, s_k , any cluster variable in the mutated seed $\mu_{s_1, \dots, s_k}(S) = (\mathbf{y}_{s_1, \dots, s_k}, \mathbf{f}_{s_1, \dots, s_k})$ is a Laurent polynomial in the cluster variables $x_t \in \mathbf{x}$.*

Example 3.2.9. Consider the initial seed with exchange variables $\{x_1, x_2\}$ and corresponding exchange polynomials $\{f^1, f^2\} = \{1 + x_2, 1 + x_1\}$. One checks that the exchange Laurent polynomials have trivial denominators, so that $\{f^1, f^2\} = \{\hat{f}^1, \hat{f}^2\}$. Mutating at x_1 replaces x_1 with

$$x_3 := \frac{1 + x_2}{x_1}$$

and leaves x_2 invariant. The exchange polynomial at x_2 is changed by this mutation. The substitution step yields

$$(f_1^2)' = 1 + \frac{1}{x_3}.$$

There are no common factors to cancel out. Finally, multiplying by x_3 gives an exchange polynomial that satisfies (LP1) and (LP2), so the mutated exchange polynomial $f_1^2 = 1 + x_3$. The mutation of the seed is therefore

$$(\{x_1, x_2\}, \{1 + x_2, 1 + x_1\}) \mapsto \left(\left\{ x_3 = \frac{1 + x_2}{x_1}, x_2 \right\}, \{1 + x_2, 1 + x_3\} \right).$$

We noted earlier that seed mutation is only well-defined up to units, so we introduce an equivalence relation to ensure mutation returns a unique object.

Definition 3.2.10. (Seed equivalence). Let $S = (\mathbf{x}, \mathbf{f}), S' = (\mathbf{x}', \mathbf{f}')$ be seeds of rank n . We say that S and S' are *equivalent* if there exists units u_ℓ, v^ℓ such that

$$x_\ell = u_\ell x'_\ell, \quad f^\ell = v^\ell f'^\ell$$

for every $1 \leq \ell \leq n$. Seed equivalence forms an equivalence relation. Denote $[S]$ for the equivalence class of S .

Mutation is compatible with equivalence of seeds, so we have $[S] = [S']$ if and only if $[\mu_i(S)] = [\mu_i(S')]$. We will often identify two seeds if they are equivalent. Thus we can speak of *the* mutation of a seed at index i .

3.2.3 Laurent phenomenon algebras

To get a commutative ring from a seed $S = (\mathbf{x}, \mathbf{f})$, one starts with the A -algebra generated by the elements of \mathbf{x} , and iteratively mutates S in all possible directions, appending the cluster variables we get to the generating set. Of course, since mutation is defined only up to units, any cluster variable we append to the generating set will also be defined only up to a unit multiple. But this does not affect the resulting A -algebra, and thus the Laurent phenomenon algebra is a well-defined construction. We state the formal definition:

Definition 3.2.11. Let A be a coefficient ring and \mathcal{F} the rational function field in n independent variables over $\text{Frac}(A)$. A *Laurent phenomenon algebra* (LP algebra) $\mathcal{A} = (\mathcal{A}, \mathbf{S})$ over A consists of a subring $\mathcal{A} \subset \mathcal{F}$, together with a distinguished collection of seeds $\mathbf{S} = \{(\mathbf{x}, \mathbf{f})\}$, such that \mathbf{S} is closed (up to equivalence) with respect to seed mutations, and \mathcal{A} is generated as an A -algebra by all cluster variables in all seeds of \mathbf{S} . We say \mathcal{A} is *normalised* if no two seeds in \mathbf{S} lie in the same equivalence class.

Suppose \mathcal{A} is an LP algebra whose distinguished collection of seeds contains two equivalent seeds. Then one of these seeds does not add any linearly independent generators to \mathcal{A} and, up to equivalence, is redundant with respect to the mutation dynamics. So we introduce a notion to remove these extra seeds from the collection:

Definition 3.2.12. Given any LP algebra $\mathcal{A} = (\mathcal{A}, \mathbf{S})$, one defines a *normalisation* \mathcal{A}' of \mathcal{A} as the LP algebra $\mathcal{A}' = (\mathcal{A}, \mathbf{S}')$, where \mathbf{S}' is the collection of seeds formed

by choosing a set of representatives from the set of equivalence classes

$$\{[S] \mid S \in \mathbf{S}\}.$$

The commutative ring \mathcal{A} is the same for both \mathcal{A} and \mathcal{A}' , and there is a canonical surjective map $p: \mathcal{S} \rightarrow \mathcal{S}'$ fitting into a commutative diagram

$$\begin{array}{ccc} \mathbf{S} & \xrightarrow{p} & \mathbf{S}' \\ \mu \downarrow & & \downarrow \mu \\ \mathbf{S} & \xrightarrow{p} & \mathbf{S}' \end{array}$$

where μ is mutation at any index, defined by sending every seed in \mathbf{S} to the chosen equivalence class representative in \mathbf{S}' .

Any two normalisations of \mathcal{A} have the same mutation dynamics, only differing by the choice of equivalence class representatives, so we will often talk about *the* normalisation of an LP algebra, with the understanding that all our constructions are invariant upon multiplying by units.

Remark 3.2.13. From a more geometrical point of view we consider a LPA \mathcal{A} as the ring of regular functions on an affine algebraic variety $U = \text{Spec } \mathcal{A}$. Each seed S corresponds to the inclusion of a torus chart

$$S = (\mathbf{x}, \mathbf{f}), \quad \mathbb{T}_S := \text{Spec } A[x_1^{\pm 1}, \dots, x_n^{\pm 1}] \hookrightarrow U,$$

by the Laurent phenomenon $\mathcal{A} \subseteq A[x_1^{\pm 1}, \dots, x_n^{\pm 1}]$. Each mutation then corresponds to a birational map, e.g.

$$\mu_1: \mathbb{T}_S \dashrightarrow \mathbb{T}_{\mu_1 S}, \quad \mu_1^*(x'_1, x_2, \dots, x_n) = (x_1^{-1} \hat{f}^1, x_2, \dots, x_n),$$

and these torus charts are glued together by identifying points according to these mutations. The LPA (as we have defined it) is then the ring of regular functions on the union of all these seed tori, and $U = \text{Spec } \mathcal{A}$ is the ‘affinisation’ of $\bigcup_S \mathbb{T}_S$. This geometrical point of view is described in the context of cluster algebras in [GHK15, §3], and more generally in [Duc23, §2.2] (see [Duc23, Remark 2.7] in particular). We

will also discuss this point of view again shortly.

3.2.4 Finite type

Let us denote $\mathcal{A}(S)$ for the normalised Laurent phenomenon algebra $\mathcal{A} = (\mathcal{A}, \mathbf{S})$, where $S \in \mathbf{S}$. If \mathbf{S} is a finite set, then we say that $\mathcal{A}(S)$ is *finite-type*. A rank two LP algebra $\mathcal{A}(S)$ is finite-type if and only if the product of the degrees of the exchange polynomials in S is less than 4 [LP16, Theorem 6.4].

Finite type implies finite mutation type, but not conversely, as shown by Lam & Pylyavskyy in their two-layer brick wall example [LP16, Section 7.2]. This recovers the situation we see in the cluster algebra case, in which exceptional quivers arise of infinite type, but finite mutation type.

Borrowing terminology from cluster algebras, we may construct the *exchange graph* of a given seed S . The vertices of this graph are given by all seeds obtainable by mutation of S , and any two vertices are connected by an edge if one may be obtained from the other (up to similarity) by a single mutation.

3.2.5 Frozen variables

If $S = (\mathbf{x}, \mathbf{f})$ is a rank n seed, *freezing* at index i produces a rank $n - 1$ seed S' with coefficient ring $A[x_i, x_i^{\pm 1}]$ by discarding (x_i, f^i) from the seed S . Furthermore, we update exchange polynomials f^ℓ for $\ell \neq i$ in S' by dividing through by the same power of x_i as in the exchange Laurent polynomial for f^ℓ in S .

Lemma 3.2.14. *Let $S = (\mathbf{x}, \mathbf{f})$ be a seed. Without loss of generality, let S' be the restricted seed obtained by considering x_1 to be frozen and x_2, \dots, x_n mutable. Let s_1, s_2, \dots, s_k be a sequence of indices with $s_j \neq 1$ for any $1 \leq j \leq k$. Then*

$$\mu_{s_1 s_2 \dots s_k}(S') = S' \iff \mu_{s_1 s_2 \dots s_k}(S) = S.$$

Proof. The right hand side implies the left hand side [LP16, Proposition 3.7], so suppose $\mu_{s_1 s_2 \dots s_k}(S') = S'$. We need to show that the cluster variables and corresponding exchange polynomials for the original seed S and its mutation $\mu_{s_1 s_2 \dots s_k}(S)$ agree. If $\ell > 1$, the calculation for the mutation of f^ℓ is exactly the same in both S and S' , which implies all exchange polynomials f^ℓ agree. Similarly all the cluster variables remain the same, and clearly not mutating at index 1 implies x_1 remains the same. We are therefore reduced to showing that $f_{12\dots k}^1 = f^1$, as was shown in [DL22, Theorem 3.1]. \square

It is clear how this lemma extends to an arbitrary number of frozen variables.

3.2.6 Log Calabi-Yau varieties

We will present a high level summary of the main ideas of mirror symmetry, which will serve as a motivation for the main results of this chapter.

Definition 3.2.15. Let U be a smooth complex affine variety, such that U admits a compactification to a smooth projective variety X by a reduced effective integral anticanonical divisor D with simple normal crossings. We call the pair (X, D) a *log Calabi-Yau pair* and $U = X \setminus D$ a *log Calabi-Yau variety*.

Note that in the literature, (X, D) is treated more generally with divisorial log terminal singularities. For our purposes, the smooth case suffices. We also note that a log Calabi-Yau variety U comes naturally equipped with a nonvanishing holomorphic differential form ω_U in the following way: Take a divisor $\text{div } \omega_X = -D$ and set $\omega_U := \omega_X|_U$. Moreover, this divisor is uniquely determined up to scaling, so we can take a representative with $\int_U \omega_U = 1$.

Definition 3.2.16. A birational map $\mu : U \rightarrow V$ between log Calabi-Yau varieties is said to be *volume preserving* if $\mu^* \omega_V = \omega_U$.

This brings us to the appropriate category in which we wish to work. The objects are log Calabi-Yau varieties, and the morphisms are volume preserving birational maps.

Example 3.2.17. Probably the easiest example of a log Calabi-Yau variety is an elliptic curve X (or any variety X with $K_X = 0$). The corresponding log Calabi-Yau pair is $(X, 0)$ and $U = X$.

Example 3.2.18. Compact toric varieties with their boundary divisors form log Calabi-Yau pairs. The dense open torus $(\mathbb{C}^\times)^n$ is log Calabi-Yau.

3.2.7 A short interlude on toric geometry

Let $M \cong \mathbb{Z}^n$ be a lattice (the *character lattice*) and let $N := \text{Hom}(M, \mathbb{Z})$ denote the dual lattice (the *cocharacter lattice*). Recall that a *toric variety* X is an algebraic variety of dimension d containing a dense open torus $\mathbb{T}_N \subset X$, such that the standard group action $\mathbb{T}_N \times \mathbb{T}_N \rightarrow \mathbb{T}_N$ extends to an action $\mathbb{T}_N \times X \rightarrow X$. Except in the most general case, toric varieties occur as the toric variety X_Σ associated to a fan Σ in $N(\mathbb{R})$. Indeed, any normal separated toric variety can be obtained in this way [CLS24]. Thus the reader should keep in mind the correspondence

$$\text{toric varieties} \longleftrightarrow \text{fans}.$$

Affine toric varieties

We now briefly recall how an affine toric variety is obtained from a rational polyhedral cone $\sigma \in N(\mathbb{R})$. Recall from Section 1.1.2 the *dual cone*

$$\sigma^\vee = \{m \in M(\mathbb{R}) \mid \langle n, m \rangle \geq 0 \text{ for all } n \in \sigma\} \subset M(\mathbb{R}).$$

The *dual semigroup* of σ is the monoid $S_\sigma := \sigma^\vee \cap M$. It is finitely generated by Gordan's lemma. Therefore, define the subalgebra

$$\mathbb{C}[S_\sigma] := \bigoplus_{s \in S_\sigma} \mathbb{C}t^s \subset \mathbb{C}[M]$$

which is also finitely generated since S_σ is. Hence $\text{Spec } \mathbb{C}[S_\sigma]$ is an affine algebraic variety; in fact, a toric variety, of dimension d with maximal torus \mathbb{T}_N .

Open affine subsets and faces

We first note the correspondence between affine open subsets of X_σ and faces of the cone σ . Indeed, if $\tau \subseteq \sigma$ is a face of $\sigma \subset N(\mathbb{R})$, then we have $\tau = \sigma \cap m^\perp$ for some $m \in M$ (i.e. m^\perp is the *supporting hyperplane* of τ). One can show that

$$\tau^\vee = \sigma^\vee + \mathbb{Z}(-m)$$

which, on the level of rings, corresponds to the equality with the localisation

$$\mathbb{C}[S_\tau] = \mathbb{C}[S_\sigma]_{t^m}.$$

On the level of varieties, this is the statement that $X_\tau = X_\sigma \setminus \mathbb{V}(t^m)$. Hence we have an open inclusion $X_\tau \hookrightarrow X_\sigma$ for each face $\tau \subseteq \sigma$.

Glueing construction

Recall that a collection of cones $\Sigma = \{\sigma_i \subset N(\mathbb{R}) \mid i \in I\}$ closed under taking faces is a polyhedral fan if, given any $\sigma_i, \sigma_j \in \Sigma$, the intersection $\tau = \sigma_i \cap \sigma_j$ is a face of both σ_i and σ_j (and hence contained in Σ). We can pick $m \in M$ such that m^\perp is a supporting hyperplane for τ in both σ_i and σ_j . As such, τ corresponds to the inclusion of open affine torus invariant subsets

$$X_{\sigma_i} \xleftarrow{f_1} X_\tau \xrightarrow{f_2} X_{\sigma_j} .$$

We can glue X_{σ_i} and X_{σ_j} together along X_τ by forming the quotient space

$$X := X_{\sigma_i} \sqcup X_{\sigma_j} \setminus (f_1(x) \sim f_2(x), \forall x \in X_\tau)$$

equipped with the quotient topology. Since any point $x \in X$ belongs to either X_{σ_i} or X_{σ_j} , X is an algebraic variety. Any normal separated toric variety arises by using this construction to glue all the affine varieties $\{X_\sigma \mid \sigma \in \Sigma\}$ together [Sum74].

The upshot of all this discussion is that one can view $N(\mathbb{R})$ as describing compactifications of the torus $(\mathbb{C}^\times)^d$. Indeed, each ray in the fan Σ corresponds to a divisor in the compactification, and each full-dimensional cone corresponds to an affine toric chart. Glueing these together according to the combinatorics of Σ gives the compactification.

3.2.8 Cluster varieties

We begin by describing a generalised way of looking at mutations.

Definition 3.2.19. Let $N \cong \mathbb{Z}^d$ have skew bilinear form $(\cdot, \cdot) : N \times N \rightarrow \mathbb{Z}$. A *seed* is a choice of integral basis $\{e_1, \dots, e_d\}$ for N .

Definition 3.2.20. Let $A \cong \mathbb{Z}^d$ and $B = A^\vee$ be dual lattices, and denote $\langle \cdot, \cdot \rangle : A \times B \rightarrow \mathbb{Z}$ the standard intersection pairing. Suppose $a \in A$ and $b \in B$ are two vectors with $\langle a, b \rangle = 0$. The *mutation* $\mu_{a,b} : \mathbb{T}_A \dashrightarrow \mathbb{T}_A$ is the birational map whose corresponding map of rings $\mu_{a,b}^* : \mathbb{C}[B] \rightarrow \mathbb{C}[B]$ is given (in the setting of Fomin and Zelevinsky) as

$$\mu_{a,b}^*(t^{b'}) = t^{b'}(1 + t^b)^{-\langle a, b' \rangle}.$$

We note an analogous definition applies when considering LP mutations. Now we define the *cluster variety* as the abstract scheme $A = \bigcup_{i \in \mathcal{I}} \mathbb{T}_{S_i}$ defined by glueing the torus charts $\mathbb{T}_S := \mathbb{T}_N$ along their common open subsets, with the glueing maps given by the mutations. The fact this is possible follows from [GHK15, Proposition 2.4]. Hence cluster varieties are log Calabi-Yau. The (upper) cluster algebra \mathcal{A} is the ring of regular functions on A , and it is better behaved than the ring A_0 generated by all the cluster variables.

3.2.9 Mirror symmetry

We now sketch the notion of the *tropicalisation* of a log Calabi-Yau variety $U^{\text{trop}}(\mathbb{R})$ as introduced in [GHKK18]. It is defined as an integral affine manifold with singu-

larities. Roughly speaking, the tropicalisation plays the same role for log Calabi-Yau varieties that the cocharacter lattice $N(\mathbb{R})$ plays for a torus.

There is a conjectured duality for log Calabi-Yau varieties satisfying a certain positivity condition, which works by taking a log Calabi-Yau variety U to its *mirror* log Calabi-Yau U^\vee . This duality operates on the level of tori by exchanging the open torus $\mathbb{T}_N = \mathbb{C}^\times \otimes_{\mathbb{Z}} N$ with its dual $\mathbb{T}_N^\vee = \mathbb{T}_M = \mathbb{C}^\times \otimes_{\mathbb{Z}} M$. In general, a maximal log Calabi-Yau pair (X, D) admits a mirror dual

$$\hat{\mathfrak{X}} \rightarrow \mathrm{Spf} \mathbf{k}[[NE(X)]]$$

whose coordinate ring of a general fibre $\mathbb{C}[V]$ admits an additive basis of *theta functions*

$$\mathcal{B}_V = \{\vartheta \in \mathbb{C}[V] \mid n \in N_{X \setminus D}(\mathbb{Z}) \text{ integral tropical point}\}.$$

The coefficients of the ϑ can be found by counting *broken lines* in an object called the *scattering diagram* $\mathcal{D}_{(X,D)}$. The computation of the theta functions is usually intractable and involves an infinite number of broken lines.

Remark 3.2.1 We have mentioned cluster varieties as examples of log Calabi-Yau varieties. When we apply the Gross-Siebert program in the case that the corresponding LP algebra is of finite type, the resulting scattering diagram will have finitely many walls and chambers, and thus a mirror can be explicitly computed. This means that finding interesting such examples serves as a cornerstone for building a portfolio of evidence towards the mirror symmetry conjecture. In particular, Spacek & Wang [SW23] recently studied mirrors for both the Cayley plane and the Freudenthal variety using the cluster algebra structures of [GLS08].

3.2.10 Simple algebraic groups

Throughout this section, let G be a simply connected simple complex algebraic group. A standard reference for the material in this section is [FH13], particularly

§23.3, Homogeneous spaces, p. 382-395.

Definition 3.2.21. A *Borel* subgroup $H \subset G$ of G is a maximal Zariski closed solvable algebraic subgroup. Any subgroup of G containing a Borel subgroup is called *parabolic*.

Parabolic subgroups may be characterised as those subgroups of G for which the homogeneous space G/P has the structure of a projective variety. Moreover, Borel subgroups may be seen as the parabolic subgroups for which this projective variety is as large as possible.

Definition 3.2.22. Let V be an irreducible representation of G with highest weight λ . Let $v \in V$ be any vector in the corresponding 1-dimensional subspace V_λ of V . The homogeneous space given by the unique closed orbit $\mathcal{X} = G \cdot v \subset \mathbb{P}(V)$ is called a *homogeneous variety*.

Note that in the above definition, the stabiliser $P = G_v$ of v by the action of G on V is a parabolic subgroup. For the classical Lie groups, one can put the points of \mathcal{X} in correspondence with partial flags in their standard representation, which explains the alternate nomenclature *partial flag variety* one finds in the literature.

Example 3.2.23. Let $G = \mathrm{SL}_n(\mathbb{C})$ and consider its standard representation on \mathbb{C}^n . Each of the standard basis vectors e_i forms a weight vector, and we can take e_1 to be a highest weight vector. The orbit of $e_1 \in \mathbb{C}^n$ is equal to \mathbb{P}^{n-1} . The corresponding parabolic subgroup is the stabiliser of e_i , which is given by the span of the matrix

$$P_i = \begin{pmatrix} 1 & * & * & \dots \\ 0 & * & * & \dots \\ \vdots & \vdots & \vdots & \ddots \\ 0 & * & * & \dots \end{pmatrix}.$$

The prototypical partial flag varieties are Grassmannians $\mathrm{Gr}(k, n)$. They may be realised for $\mathrm{SL}_n(\mathbb{C})$ by considering maximal parabolic subgroups; these are the

subgroups preserving exactly one subspace of dimension k . We will see later a similar construction for the exceptional simple Lie groups E_4, E_5, E_6, E_7 .

3.2.11 Enumerative geometry of del Pezzo surfaces

In this subsection we briefly recall the relationship between del Pezzo surfaces and type E_n Dynkin diagrams, with the final goal to understand how the classes of the lines in $\text{NS}(\text{dP}_n)$ arise as vertices of the semiregular Gosset polytope Ξ_n .

Definition 3.2.24. A *del Pezzo surface* dP_n of degree n is the blowup of $9 - n$ points P_1, P_2, \dots, P_{9-n} in \mathbb{P}^2 in general position.

In this chapter we concentrate on the case $3 \leq n \leq 7$. Here “general position” means that no three of the points are collinear and no six lie on a conic.

Definition 3.2.25. An *exceptional curve* on a variety X is a smooth rational curve with self-intersection index -1 .

It is simple to describe how the exceptional curves arise on a del Pezzo surface:

1. the exceptional divisors ℓ_i that arise from the blowups at each point P_i ,
2. the strict transforms $\ell_{i,j}$ of lines between P_i and P_j for $i \neq j$,
3. the strict transforms c_i of the conics through five of the P_j for $i \neq j$.

It is well known [Dol06], [Man86] that the symmetry group of the lines in dP_n is given by the Weyl group E_n . Recall the *Picard group* $\text{Pic}(X)$ of divisors on X modulo linear equivalence, equipped with the intersection pairing. By the blowup description of dP_n , we have

$$\text{Pic dP}_n = \mathbb{Z}\ell \oplus \mathbb{Z}\ell_1 \oplus \dots \oplus \mathbb{Z}\ell_n.$$

where ℓ is the class of a line in \mathbb{P}^2 . Consider the convex polytope Ξ_n in $\text{Pic dP}_n \otimes_{\mathbb{Z}} \mathbb{Q}$ whose vertices are given by the classes of the lines ℓ in dP_n . It is well known that

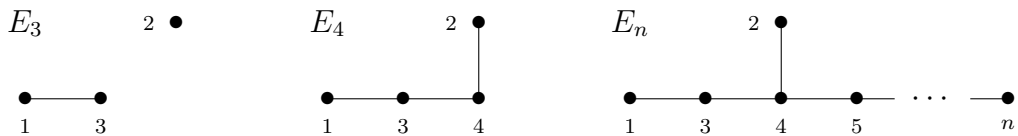
this polytope is exactly the semiregular Gosset polytope $(d - 4)_{21}$ [Cox73, §11.8]. To see how the lines have E_n symmetry, recall that the intersection product is negative-definite in $K_{\text{dP}_n}^\perp$. We assign the root system

$$R_n = \{D \in \text{Pic dP}_n \mid D \cdot D = -2, D \cdot K_{\text{dP}_n} = 0\}$$

with the simple roots given by $e_0 = \ell - \ell_1 - \ell_2 - \ell_3$, $e_i = \ell_i - \ell_{i+1}$ for $1 \leq i \leq n - 1$. The roots correspond to reflections $r_\phi(D) := D + (D \cdot \phi)\phi$ for every $D \in \text{Pic dP}_n$. It is clear that the corresponding Weyl group is equal to $W(E_n)$. The action of $W(E_n)$ on R_n extends to $\text{Pic dP}_n \otimes \mathbb{Q}$, and we claim it acts on (the classes of) the lines on dP_n by reflections. Indeed, the lines live in the hyperplane section $-D \cdot K_{\text{dP}_n} = 1$ of $\text{Pic dP}_n \otimes \mathbb{Q}$. Since $-K_{\text{dP}_n}$ is ample, the intersection pairing induces a negative-definite inner product on this hyperplane section by the Hodge index theorem. We get an induced norm by fixing $\frac{1}{n}K_{\text{dP}_n}$ as the origin of the hyperplane section. Finally, we observe that this choice of origin is fixed by all the reflections r_ϕ for $\phi \in R_n$. Hence $W(E_n)$ acts on the lines as a reflection group.

3.3 Giving the coordinate rings an LPA structure

The main result of this chapter concerns the existence of a finite type LPA, which we view as the $n = 6$ case in a sequence of homogeneous varieties indexed by type E_n Dynkin diagrams. As such, we write down the Dynkin diagrams of type E_n for $3 \leq n \leq 8$ (where $E_3 = A_1 \oplus A_2$, $E_4 = A_4$ and $E_5 = D_5$) with the nodes labelled according to the convention adopted by Bourbaki.



We can associate a number of mathematical objects to this sequence:

1. a smooth del Pezzo surface dP_n of degree $9 - n$, obtained by blowing up n general points in \mathbb{P}^2 ,

2. the homogeneous space $\mathcal{V}_n := E_n/P_n$, where P_n is the parabolic subgroup associated to the n th node of the Dynkin diagram,
3. the n -dimensional semiregular Gosset polytope Ξ_n with Coxeter symbol $(n - 4)_{21}$.

3.3.1 Numerical invariants

We collect some numerical invariants associated to this sequence in Table 3.1.

n	\mathcal{V}_n	$\dim \mathcal{V}_n$	Coxeter number h	$\gamma_{n,1}$	$\gamma_{n,2}$	$\gamma_{n,3}$	$\gamma_{n,2} + \gamma_{n,3}$
3	$\mathbb{P}^2 \times \mathbb{P}^1$	3	3	6	3	2	5
4	$\text{Gr}(2, 5)$	6	5	10	5	5	10
5	$\text{OGr}(5, 10)$	10	8	16	10	16	26
6	$\mathbb{O}\mathbb{P}^2$	16	12	27	27	72	99
7	Freudenthal variety	27	18	56	126	576	702

Table 3.1: Numerical invariants associated to the E_n root systems for $3 \leq n \leq 7$.

According to the three different points of view, for $3 \leq n \leq 7$ these numbers can be interpreted in the following ways.

1. The del Pezzo surface dP_n contains $\gamma_{n,1}$ lines, $\gamma_{n,2}$ conic classes ξ (which correspond to conic fibrations $\xi: dP_n \rightarrow \mathbb{P}^1$), and $\gamma_{n,3}$ cubic classes η (which correspond to contractions $\eta: dP_n \rightarrow \mathbb{P}^2$).
2. The homogeneous space $\mathcal{V}_n \subset \mathbb{P}^{\gamma_{n,1}-1}$ has an embedding into a projective space of dimension $\gamma_{n,1} - 1$ and is cut out by $\gamma_{n,2}$ quadratic equations. It is a Fano variety of the specified dimension and Fano index h (or in other words, $-K_{\mathcal{V}_n} = \mathcal{O}_{\mathcal{V}_n}(h)$ for the given embedding).
3. The effective cone $\text{Eff}(dP_n)$ is the cone over $\Xi_n \subset \text{NS}(dP_n) \cong \mathbb{R}^{n+1}$, where the polytope Ξ_n is obtained as the convex hull of the classes of the lines

in $\text{NS}(\text{dP}_n)$. It has $\gamma_{n,1}$ vertices and $\gamma_{n,2} + \gamma_{n,3}$ facets, of which $\gamma_{n,2}$ facets are $(n - 1)$ -dimensional orthoplexes and $\gamma_{n,3}$ facets are $(n - 1)$ -dimensional simplexes.

3.3.2 Coxeter projection of Ξ_n

In Figure 3.1 we draw the projection of the polytope Ξ_n onto the Coxeter plane for the cases $n = 4, 5, 6, 7$. The action of the Coxeter rotation of order h is plainly visible. In these four cases, the vertices of the polytopes are split into orbits of the following sizes:

$$(10) = 2 \times (5), \quad (16) = 2 \times (8), \quad (27) = 2 \times (12) + (3), \quad (56) = 3 \times (18) + (2).$$

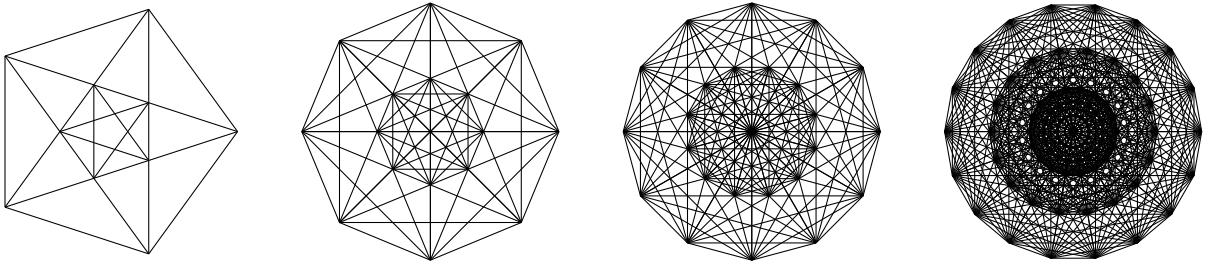


Figure 3.1: Coxeter projections of the polytopes Ξ_n for $n = 4, 5, 6, 7$.

3.3.3 A family of log Calabi–Yau varieties

Following interpretations (2) and (3) from §3.3.1, the $\gamma_{n,1}$ coordinates on the homogeneous space $\mathcal{V}_n \subset \mathbb{P}^{\gamma_{n,1}-1}$ can be placed in one-to-one correspondence with vertices of Ξ_n . Given that the Fano index of \mathcal{V}_n is equal to the Coxeter number h , we can make a natural choice of anticanonical boundary divisor $\mathcal{D}_n \subset \mathcal{V}_n$ by taking

$$\mathcal{D}_n = \mathbb{V}(a_1) + \mathbb{V}(a_2) + \cdots + \mathbb{V}(a_h) \in |-K_{\mathcal{V}_n}|$$

where a_1, \dots, a_h are the coordinates on \mathcal{V}_n corresponding to the ‘outside ring’ of the Coxeter projection (Figure 3.1).

Definition 3.3.1. We let $\mathcal{A}_n := \mathbb{C}[\mathcal{V}_n]$ be the homogeneous coordinate ring of \mathcal{V}_n , with respect to the given embedding, and consider the affine cone $C\mathcal{V}_n = \text{Spec } \mathcal{A}_n$.

We consider the fibration induced by the projection

$$\pi: C\mathcal{V}_n \rightarrow \mathbb{A}_{a_1, \dots, a_h}^h.$$

and let $U_n := \pi^{-1}(\alpha_1, \dots, \alpha_h)$ denote a general fibre.

This log Calabi–Yau variety U_n is simply the affine variety obtained by substituting the value $\alpha_1, \dots, \alpha_h \in \mathbb{C}$ for each coordinate a_1, \dots, a_h in \mathcal{A}_n respectively. This projection π spreads out the components of $C\mathcal{D}_n$ over the coordinate hyperplanes of \mathbb{A}^h , giving a degenerating family of log Calabi–Yau varieties.

Remark 3.3.2. In the language of cluster algebras, the coordinates a_1, \dots, a_h are *frozen variables* and we will interpret the remaining coordinates as *cluster variables* in a LPA. Moreover, a LPA structure for \mathcal{A}_n over the base ring $A = \mathbb{C}[a_1, \dots, a_h]$ must have rank $r = \dim \mathcal{V}_n + 1 - h$, since the cluster of each seed will correspond to the inclusion of a torus chart

$$\text{Spec } A[x_1^{\pm 1}, \dots, x_r^{\pm 1}] = \mathbb{A}_{a_1, \dots, a_h}^h \times (\mathbb{C}^\times)_{x_1, \dots, x_r}^r \hookrightarrow C\mathcal{V}_n$$

that birationally cover $C\mathcal{V}_n$.

Remark 3.3.3. We do not extend our discussion to include the E_8 case, since the numerology of Table 3.1 breaks down for the homogeneous space $\mathcal{V}_8 = E_8/P_8$. In particular, the Fano index of \mathcal{V}_8 is 29 [Sno89], rather than the Coxeter number $h = 30$, and thus we do not obtain an anticanonical divisor $\mathcal{D}_8 \subset \mathcal{V}_8$ in the same way.

3.3.4 Type E_4

The LPA in this case is given by the famous example of the A_2 cluster algebra.

It is convenient to name the frozen variables a_1, \dots, a_5 and the non-frozen variables x_1, \dots, x_5 according to the labelling of Ξ_4 shown in Figure 3.2. Then the Grassman-

nian $\mathcal{V}_4 = \text{Gr}(2, 5) \subset \mathbb{P}^9$ is cut out by five quadratic Plücker equations corresponding to the five octahedral faces of Ξ_4 .

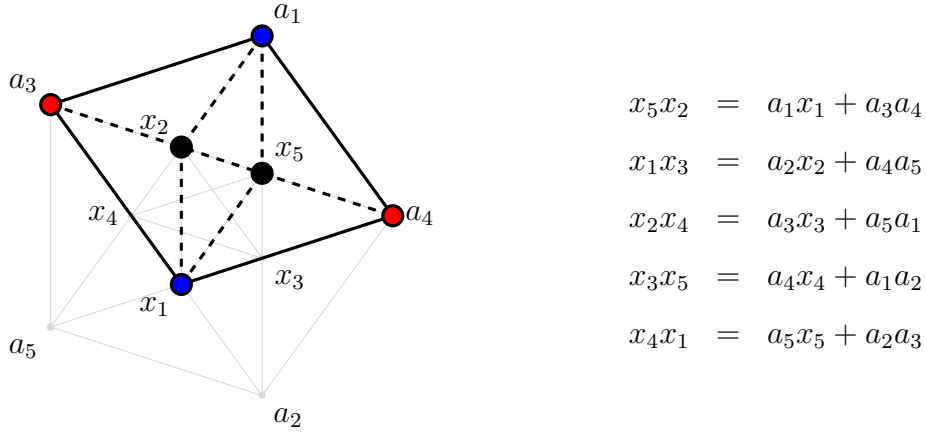


Figure 3.2: The equations of \mathcal{V}_4 .

Structure of the equations

The five quadratic equations have a common structure in that they are comprised of three monomials, each one of which is a product of two opposite vertices in the corresponding octahedron. A coherent choice of signs for these equations is determined by the following *positivity rule*

$$x_i x_{i+2} = \text{positive sum of the other monomials}, \quad (3.3.1)$$

where $x_i x_{i+2}$ is the monomial corresponding to the pair of ‘internal’ vertices of the projected octahedron, and the right hand side comprises of the monomials corresponding to all pairs of ‘external’ vertices.

We let $A = \mathbb{C}[a_1, \dots, a_5]$ be the ring generated by the frozen variables and, by Remark 3.3.2, a LPA structure on \mathcal{A}_4 will have rank 2. As is well-known, each of the following Plücker coordinates

$$x_3 = \frac{a_2 x_2 + a_4 a_5}{x_1}, \quad x_4 = \frac{a_5 a_1 x_1 + a_2 a_3 x_2 + a_3 a_4 a_5}{x_1 x_2}, \quad x_5 = \frac{a_1 x_1 + a_3 a_4}{x_2}$$

can be expressed as Laurent polynomials in $A[x_1^{\pm 1}, x_2^{\pm 1}]$.

Initial seed

An initial seed for the corresponding LPA structure on \mathcal{A}_4 is given by

$$S = \begin{cases} x_1, & a_2x_2 + a_4a_5, \\ x_2, & a_1x_1 + a_3a_4. \end{cases}$$

Mutating S at x_1 gives an almost identical seed (up to reordering) where the only difference is that all the indices of all the variables x_i and a_i have been shifted by $i \mapsto i + 1 \pmod{5}$.

Exchange graph

The exchange graph of \mathcal{A}_4 is a pentagon, with vertices labelled by the five possible clusters $\{x_i, x_{i+1}\}$ for all $i \in \mathbb{Z}/5\mathbb{Z}$ and edges by the five possible mutations $\{x_{i-1}, x_i\} \rightarrow \{x_i, x_{i+1}\}$. Moreover, the ring \mathcal{A}_4 exhibits a curious property known as the *positivity phenomenon*: every coefficient in the Laurent expansion of every cluster variable is positive, as well as every coefficient in the exchange polynomials of every seed.

3.3.5 Type E_5

This is the LPA studied in [Duc23]. In this case we label the variables a_1, \dots, a_8 and x_1, \dots, x_8 with $i \in \mathbb{Z}/8\mathbb{Z}$, as in Figure 3.3. The orthogonal Grassmannian $\mathcal{V}_5 = \text{OGr}(5, 10) \subset \mathbb{P}^{15}$ is cut out by ten quadratic equations which correspond to the ten octahedral faces of Ξ_5 . However this time the equations of \mathcal{V}_5 split into one orbit (a) of size eight and one orbit (b) of size two.

Structure of the equations

We can make a coherent choice of minus signs in the equations by asking that the eight (a) equations obey the analogous positivity rule to equation (3.3.1). Doing that uniquely determines the signs in the remaining two (b) equations.

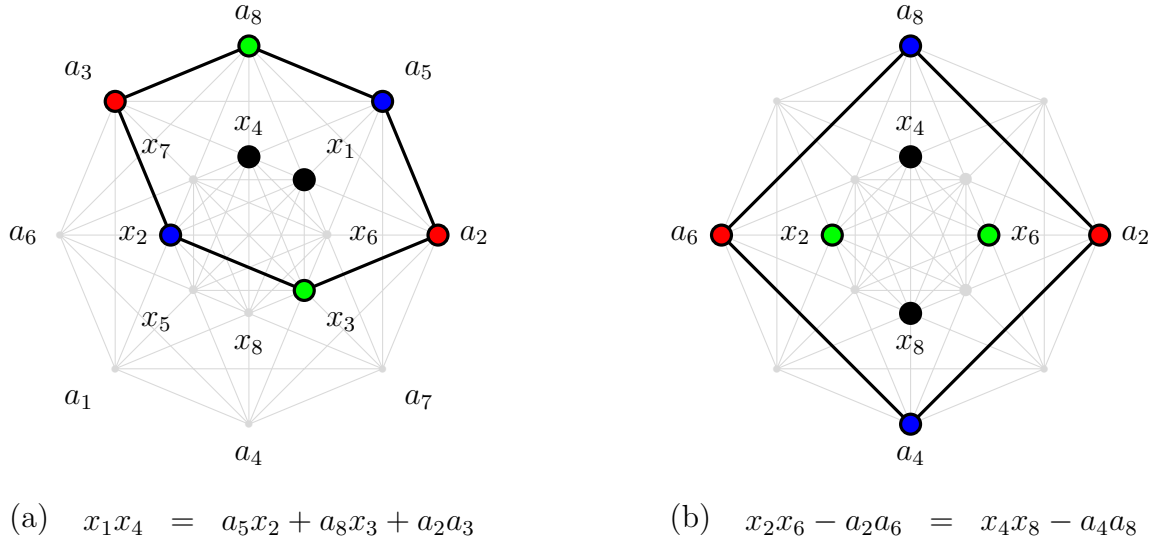


Figure 3.3: The equations of \mathcal{V}_5 .

Initial seed

By Remark 3.3.2, a LPA structure on \mathcal{A}_5 will have rank 3. Beginning with $\{x_1, x_2, x_3\}$ as a candidate for an initial cluster, we can check that each of the other x_i can be written as a Laurent polynomial in x_1, x_2, x_3 . Thus we proceed with the hope that this initial cluster can be used to get an LPA structure on \mathcal{V}_5 which is analogous to the LPA structure on \mathcal{V}_4 .

To promote this cluster into a seed, we have to specify what the exchange polynomial f^i corresponding to x_i should be for $i = 1, 2, 3$. The two equations $x_1x_4 = \dots$ and $x_3x_8 = \dots$ give easy and obvious candidates for the exchange polynomials f^1 and f^2 :

$$f^1 = a_5x_2 + a_8x_3 + a_2a_3, \quad f^3 = a_4x_1 + a_7x_2 + a_1a_2.$$

However, it is not immediately clear how to write down the exchange polynomial f^2 .

Since we would like mutation in the LPA to be compatible with the Coxeter symmetry (as it was in the previous case), we can easily work out what f^2 should be by considering the mutation $\mu_1: \{x_1, x_2, x_3\} \mapsto \{x_2, x_3, x_4\}$, writing down the exchange polynomial $\mu_1 f^2 = a_6x_3 + a_1x_4 + a_3a_4$ that we expect to see for x_2 with respect to this seed, and then mutating back to get $f^2 = \mu_1^{-1}(\mu_1 f^2)$.

As seen in [Duc23], this gives an initial seed

$$S = \begin{cases} x_1, & a_5x_2 + a_8x_3 + a_2a_3, \\ x_2, & a_6x_1x_3 + a_3a_4x_1 + a_8a_1x_3 + a_1a_2a_3, \\ x_3, & a_4x_1 + a_7x_2 + a_1a_2, \end{cases}$$

and, incredibly, the mutation of this LPA seed is compatible with the Dih_8 -symmetry, in the sense that mutating S at x_1 returns an identical seed (up to reordering) with all indices shifted by $i \mapsto i + 1 \pmod 8$.

Moreover, mutating x_2 gives a quantity $q_1 = x_2^{-1}f^2$ which can be expressed as a quadratic $q_1 = x_1x_5 - a_1a_5 = x_3x_7 - a_3a_7$ in the other variables. If we also let $q_2 = x_2x_6 - a_2a_6 = x_4x_8 - a_4a_8$, then we get a finite type LPA structure with sixteen clusters:

$$\begin{aligned} & \{x_1, x_2, x_3\}, \{x_2, x_3, x_4\}, \{x_3, x_4, x_5\}, \dots, \{x_7, x_8, x_1\}, \\ & \{x_1, x_3, q_1\}, \{x_2, x_4, q_2\}, \{x_3, x_5, q_1\}, \dots, \{x_8, x_2, q_2\}. \end{aligned}$$

Exchange graph

The exchange graph is the 1-skeleton of a 3-dimensional polytope with sixteen vertices, eight pentagonal faces (corresponding to x_1, \dots, x_8) and two square faces (corresponding to q_1, q_2). The exchange graph is shown in Figure 3.4.

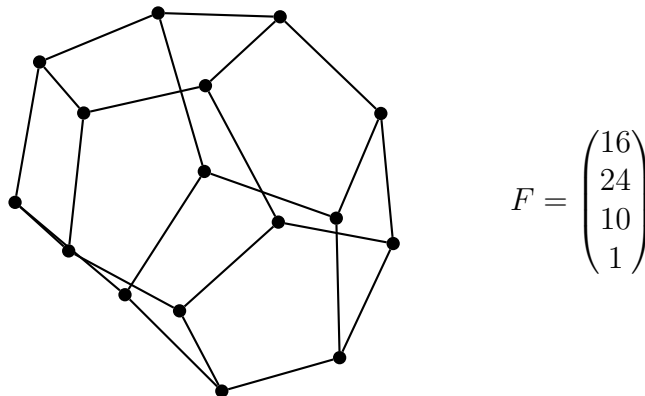


Figure 3.4: The exchange graph for the LPA in the \mathcal{V}_5 case with f-vector F .

Positivity

The reader may be a little bit disturbed by the fact that the two equations of type (b) appear to have negative coefficients. However, after we introduced the two new cluster variables q_1, q_2 , these equations can be rewritten as exchange relations with positive coefficients, e.g.

$$x_1x_5 - a_1a_5 = x_3x_7 - a_3a_7 \implies x_1x_5 = q_1 + a_1a_5.$$

As with the previous case, \mathcal{A}_5 also has the positivity phenomenon. By an explicit calculation one can check that every Laurent expansion of a cluster variable, as well as every exchange polynomial in every seed, has positive coefficients.

3.3.6 Type E_6

To describe the projective embedding of the Cayley plane, we must first understand the equations of the projective embedding $\mathcal{V}_6 \subset \mathbb{P}^{26}$. We do this by thinking of the 27-dimensional representation of E_6 in terms of the 27 lines on a cubic surface.

The equations of the Cayley plane

We fix a birational model $\pi: \mathrm{dP}_6 \rightarrow \mathbb{P}^2$ for the smooth cubic surface $\mathrm{dP}_6 \subset \mathbb{P}^3$ obtained as the blowup of six points $p_1, \dots, p_6 \in \mathbb{P}^2$, and we name the 27 lines in dP_6 according to the following conventions:

1. let e_i be the line corresponding to the exceptional divisor over p_i ,
2. let ℓ_{ij} be the line corresponding to the line through p_i, p_j and
3. let c_i be the line corresponding to the conic through the five points other than p_i .

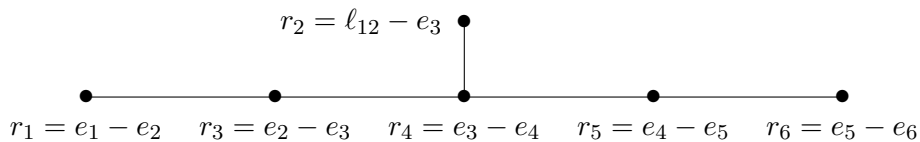
The polytope Ξ_6

As mentioned in §3.3.1, the polytope $\Xi_6 \subset \text{NS}(\text{dP}_6)$ has 27 vertices, corresponding to the 27 lines of dP_6 , and $99 = 27 + 72$ facets which are one of two types:

1. There are 27 5-dimensional orthoplex facets, corresponding to the 27 extremal rays $\xi \in \text{Nef}(\text{dP}_6)$ that define conic fibrations $\pi_\xi: \text{dP}_6 \rightarrow \mathbb{P}^1$. Each face has ten vertices $\ell_1, \dots, \ell_5, \ell'_1, \dots, \ell'_5$ appearing in five ‘opposite’ pairs ℓ_i, ℓ'_i such that $\xi \sim \ell_i + \ell'_i$ for $i = 1, \dots, 5$.
2. There are 72 5-dimensional simplex facets, corresponding to the 72 extremal rays $\eta \in \text{Nef}(\text{dP}_6)$ that define contractions $\pi_\eta: \text{dP}_6 \rightarrow \mathbb{P}^2$. Each face has six vertices ℓ_1, \dots, ℓ_6 ; the six lines that are contracted by π_η .

3.3.7 Action of a Coxeter rotation

The 72 roots of the E_6 root system in $\text{NS}(\text{dP}_6)$ are given by all possible differences $\ell_i - \ell_j$, where ℓ_i, ℓ_j are a pair of non-intersecting lines in dP_6 . Each root r_i specifies a reflection $\rho_i(r_j) = r_j + (r_i \cdot r_j)r_i$, and a Coxeter rotation is an element $\sigma = \rho_1\rho_2\rho_3\rho_4\rho_5\rho_6$ of order 12, obtained as a product of the reflections over a set of simple roots. For example, if σ is the Coxeter rotation obtained from the following choice of simple roots



then the action of σ on the set of the 27 lines has (ordered) orbits of length 12, 12, 3, as shown in the rows of Table 3.2. The 27 lines correspond to 27 spinor coordinates of $\mathcal{V}_6 \subset \mathbb{P}^{26}$, and we name these coordinates a_i, x_j, z_k for $i, j \in \mathbb{Z}/12\mathbb{Z}$ and $k \in \mathbb{Z}/3\mathbb{Z}$ according to which of these three orbits they belong to, as in Table 3.2. We have labelled the Coxeter projection of Ξ_6 with these coordinate names, as shown in

Table 3.2: The frozen variables a_i and cluster variables x_i, z_i for \mathcal{A}_6 .

i	1	2	3	4	5	6	7	8	9	10	11	12
a_i	e_3	l_{34}	l_{56}	e_6	c_2	e_4	c_6	l_{16}	l_{23}	c_3	e_5	c_1
x_i	l_{26}	l_{24}	l_{46}	e_1	l_{45}	e_2	l_{35}	l_{15}	l_{13}	c_4	l_{12}	c_5
z_i	l_{14}	l_{36}	l_{25}									

Figure 3.5(i) (where the orbit $\{z_1, z_2, z_3\}$ of size three has been squished together in the centre).

The equations of the Cayley plane

The 27 octahedral faces of Ξ_6 also split up into two orbits of size 12 and one orbit of size three under the action of the rotation σ . These three types of octahedral face are shown in Figure 3.5(ii), and a representative equation from each of these three Dih_{12} -orbits is given by

$$x_1x_6 = a_6x_3 + a_1z_2 + a_8x_4 + a_3a_{11}, \quad (\text{a})$$

$$x_1x_5 = x_3z_3 - a_3x_2 - a_{10}x_4 + a_1a_{12}, \quad (\text{b})$$

$$z_1z_2 = x_3x_9 + x_6x_{12} + a_2a_8 + a_5a_{11}. \quad (\text{c})$$

The choice of \pm sign in front of each monomial in each of these equations is uniquely determined by specifying that all of the equations in orbit (a) obey the analogous positivity rule to equation (3.3.1). Indeed, Macaulay2 agrees that these equations define an irreducible Gorenstein variety $\mathcal{V}_6 \subset \mathbb{P}^{26}$ which has codimension 10 and a Gorenstein resolution with Betti numbers $(1, 27, 78, 351, 650, 702, 650, 351, 78, 27, 1)$.

3.3.8 Finding an initial seed

We now describe how we found an initial seed for an LPA structure on \mathcal{A}_6 . We do this in three steps:

1. First find a candidate for an initial cluster (e.g. an appropriately sized subset of

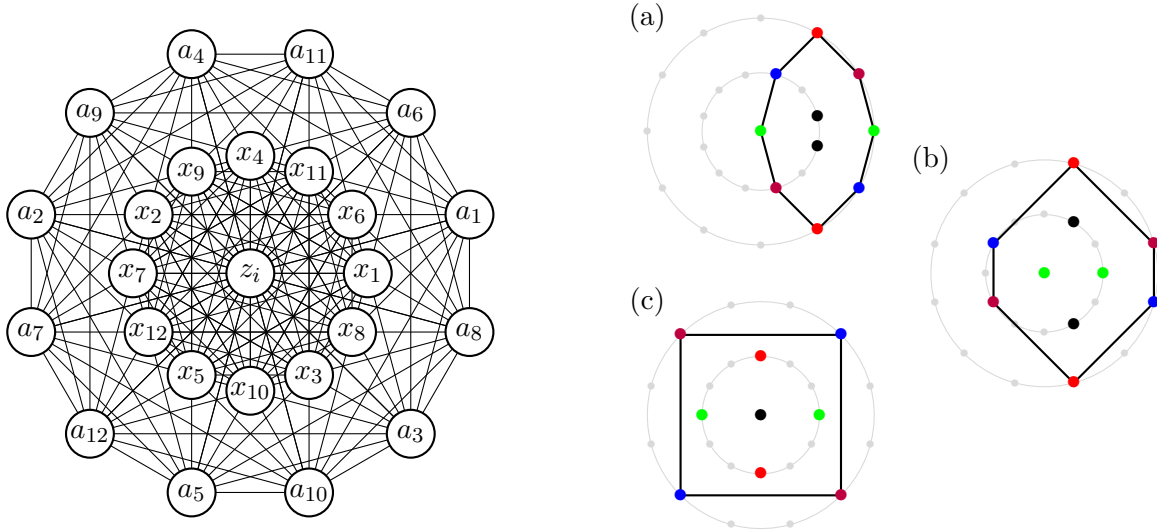


Figure 3.5: (i) A labelling of the vertices of Ξ_6 , and (ii) the three types of octahedral face.

the spinor coordinates for which all other spinor coordinates can be expressed as Laurent polynomials).

2. Work out corresponding exchange polynomials for this cluster.
3. Check that the corresponding LPA is of finite type and contains all (non-frozen) spinor coordinates on \mathcal{V}_6 as cluster variables.

We first note that we expect such a LPA structure to have rank 5, by Remark 3.3.2.

Finding an initial cluster

We describe three attempts we made in order to find an initial cluster.

Attempt 1. As with the previous cases, our first thought was to take $\{x_1, x_2, x_3, x_4, x_5\}$ as an initial cluster. Unfortunately however, we have the equation

$$x_1x_5 = x_3z_3 - a_3x_2 - a_{10}x_4 + a_1a_{12}$$

that looks like it could make x_5 redundant as a cluster variable. It also does not account for the variable z_3 appearing in the corresponding exchange polynomial.

Attempt 2. Next we replaced x_5 with z_3 , hoping that $\{x_1, x_2, x_3, x_4, z_3\}$ would work as an initial cluster. Using computer algebra to eliminate variables from the ring \mathcal{A}_6 we discover that all of the other x_i and z_i variables can be written as rational functions in this cluster, but not, unfortunately, as *Laurent polynomials*.

Attempt 3. Finally, although the rational functions obtained in attempt 2 were not Laurent polynomials, a closer inspection reveals that they are ‘almost’ Laurent polynomials. Indeed, the denominators are always monomials in the five terms

$$x_1, x_2, x_3, x_4, x_3z_3 - a_3x_2 - a_{10}x_4.$$

Therefore we introduce $y_3 := x_3z_3 - a_3x_2 - a_{10}x_4$ as a new cluster variable.

Definition 3.3.4. We let y_i be defined by the expression

$$y_i := x_i z_i - a_i x_{i-1} - a_{i+7} x_{i+1} \quad i \in \mathbb{Z}/12\mathbb{Z}.$$

We conclude that we have the following result.

Lemma 3.3.5. *We can expand all of the spinors variables x_i, z_i as Laurent polynomials in $\{x_1, x_2, x_3, x_4, y_3\}$, and thus we can use this as a candidate for an initial cluster. Moreover, the new variables y_1, \dots, y_{12} are also all Laurent polynomials in our chosen initial cluster, and they are all distinct. By symmetry we find that both*

$$\{x_{i-1}, x_i, x_{i+1}, x_{i+2}, y_i\} \quad \text{and} \quad \{x_{i-1}, x_i, x_{i+1}, x_{i+2}, y_{i+1}\}$$

are clusters for any value of i .

Finding the exchange polynomials

From the equations of type (b) above we immediately have the relation

$$x_1 x_5 = y_3 + a_1 a_{12}.$$

Moreover, by manipulations with the equations of all the types (a, b, c), we can write the product $y_2 y_3$ as a positive sum of monomials in terms of the frozen coefficients

and x_1, x_2, x_3, x_4 . Indeed we get

$$\begin{aligned} y_2 y_3 &= (x_2 z_2 - a_2 x_1 - a_9 x_3)(x_3 z_3 - a_3 x_2 - a_{10} x_4) \\ &= x_1 x_4 (a_5 x_2 + a_7 x_3 + a_2 a_{10}) + a_{12} x_3 (a_4 x_1 + a_1 a_9) + a_{12} x_2 (a_6 x_3 + a_8 x_4 + a_3 a_{11}). \end{aligned}$$

Thus we can use these as exchange relations in the following sequence of mutations, together with the expected Dih_{12} symmetry, to work out what all of the other exchange polynomials should be.

$$\dots \longleftrightarrow \left\{ \begin{array}{cccc} x_1 & x_2 & x_3 & x_4 \\ & y_2 & & \end{array} \right\} \longleftrightarrow \left\{ \begin{array}{cccc} x_1 & x_2 & x_3 & x_4 \\ & & y_3 & \end{array} \right\} \longleftrightarrow \left\{ \begin{array}{cccc} x_2 & x_3 & x_4 & x_5 \\ & y_3 & & \end{array} \right\} \longleftrightarrow \left\{ \begin{array}{cccc} x_2 & x_3 & x_4 & x_5 \\ & & & y_4 \end{array} \right\} \longleftrightarrow \dots$$

Doing this, we arrive at the following candidate for our the initial seed.

Proposition 3.3.6. *The following seed S is an initial seed for a LPA structure on $\mathcal{A}_6 = \mathbb{C}[\mathcal{V}_6]$, which is compatible with the Dih_{12} -symmetry:*

$$S = \left\{ \begin{array}{ll} x_1, & y_3 + a_{12} a_1 \\ x_2, & a_2 x_1 (y_3 + a_{10} x_4) + a_9 x_3 (y_3 + a_1 a_{12}) + x_1 x_3 (a_7 x_4 + a_4 a_{12}) \\ x_3, & y_3 + a_3 x_2 + a_{10} x_4 \\ x_4, & a_{11} (y_3 + a_3 x_2) + x_3 (a_4 x_1 + a_6 x_2 + a_1 a_9) \\ y_3, & x_1 x_4 (a_5 x_2 + a_7 x_3 + a_2 a_{10}) + a_{12} x_3 (a_4 x_1 + a_1 a_9) + a_{12} x_2 (a_6 x_3 + a_8 x_4 + a_3 a_{11}). \end{array} \right.$$

3.3.9 Summary of the LPA structure

Number of seeds and the exchange graph

Once we are given the right initial seed it is easy to plug into the code and verify that it generates a LPA of finite type.

Theorem 3.3.7. *The LPA structure on \mathcal{A}_6 , generated by the initial seed of Proposition 3.3.6, has finite type. In particular it has 264 seeds and 32 cluster variables.*

The cluster variables consist of the 15 spinor coordinates $x_1, \dots, x_{12}, z_1, z_2, z_3$ on \mathcal{V}_6 , plus 17 additional cluster variables $y_1, \dots, y_{12}, t_1, t_2, t_3, u_1, u_2$ where

1. y_1, \dots, y_{12} are quadratics in the spinor variables introduced above,
2. t_1, t_2, t_3 are quartics in the spinor variables determined by the Dih_{12} -conjugates of the equation

$$x_1x_4x_7x_{10} = t_1 + a_3a_6a_9a_{12},$$

3. u_1, u_2 are cubics in the spinor variables determined by the Dih_{12} -conjugates of the equation¹

$$x_1x_5x_9 = u_1 + a_4a_5x_1 + a_8a_9x_5 + a_{12}a_1x_9 + a_1a_5a_9 + a_4a_8a_{12}.$$

Up to the Dih_{12} -symmetry there are 15 different orbits of seeds; seven orbits have length 24, which we label A, \dots, G , and eight orbits have length 12, which we name H, \dots, O . They are related by mutation according to Table 3.3, and the Dih_{12} -quotient of the exchange graph is presented in Figure 3.6.

We can also check various things about the structure of the exchange graph, such as the fact that every x (resp. y, z, t, u) variable belongs to 60 (resp. 32, 40, 8, 36) seeds.

Positivity

By inspecting the output of our computation, which consists of all of the seeds for \mathcal{A}_6 (including the Laurent expansion of all of the cluster variables), we have the following result.

Corollary 3.3.8. *The positivity phenomenon holds for \mathcal{A}_6 . In other words, all of the coefficients in the Laurent expansions of the cluster variables and all the coefficients in exchange polynomials of each seed are positive.*

¹It is clear from the equation that u_1 is invariant under the shift $i \mapsto i + 4$ for $i \in \mathbb{Z}/12\mathbb{Z}$, but in fact, as a consequence of the other relations, it turns out that it is invariant under $i \mapsto i + 2$ too.

A	$x_1 \ x_2 \ x_3 \ x_4 \ y_2$	F	$x_1 \ x_2 \ x_4 \ y_{12} \ z_3$	K	$x_1 \ x_7 \ y_5 \ y_{11} \ z_2$
	$y_4 \ z_2 \ y_{12} \ x_{12} \ y_3$		$y_6 \ x_{10} \ x_{11} \ y_3 \ y_2$		$x_9 \ x_3 \ x_{10} \ x_4 \ u_2$
	D B C A A		L E B B C		L L E E O
B	$x_1 \ x_2 \ x_4 \ y_3 \ z_3$	G	$x_1 \ x_4 \ x_7 \ y_3 \ y_5$	L	$x_1 \ x_3 \ y_5 \ y_{11} \ z_2$
	$x_5 \ x_7 \ x_{11} \ y_{12} \ x_3$		$x_5 \ u_1 \ x_3 \ z_2 \ z_3$		$x_9 \ x_7 \ x_{12} \ x_4 \ u_1$
	B E F F A		C N C E E		K K F F M
C	$x_1 \ x_2 \ x_4 \ y_{12} \ y_2$	H	$x_1 \ x_3 \ y_3 \ y_5 \ u_1$	M	$x_1 \ x_3 \ y_5 \ y_{11} \ u_1$
	$u_2 \ x_{10} \ x_{12} \ x_3 \ z_3$		$x_5 \ x_7 \ y_{11} \ y_1 \ x_4$		$x_9 \ x_7 \ y_1 \ y_3 \ z_2$
	H G D A F		I N M I C		O O H H L
D	$x_1 \ x_2 \ x_3 \ y_1 \ y_3$	I	$x_1 \ x_3 \ y_1 \ y_3 \ u_1$	N	$x_1 \ x_7 \ y_3 \ y_5 \ u_1$
	$x_5 \ u_1 \ x_{11} \ x_4 \ x_{12}$		$x_5 \ x_{11} \ y_5 \ y_{11} \ x_2$		$x_5 \ x_3 \ y_{11} \ y_9 \ x_4$
	C I C A A		H H H H D		H H O O G
E	$x_1 \ x_4 \ x_7 \ y_3 \ z_3$	J	$x_1 \ x_4 \ x_7 \ z_2 \ t_1$	O	$x_1 \ x_7 \ y_5 \ y_{11} \ u_1$
	$x_5 \ y_9 \ x_2 \ t_1 \ y_5$		$x_{10} \ x_{10} \ x_{10} \ z_3 \ y_5$		$x_9 \ x_3 \ y_9 \ y_3 \ z_2$
	F K B J G		J J J J E		M M N N K

Table 3.3: Representatives for each of the 15 orbits of seeds A, . . . , O. The top row of each entry contains the five cluster variables in the seed. The second row records which cluster variable is obtained by mutating the seed at the variable directly above it, leading to a seed in the orbit given by the label on the third row.

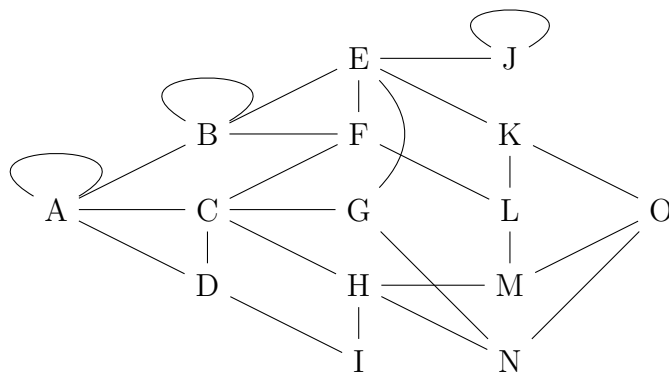


Figure 3.6: The Dih_{12} -quotient of the exchange graph of \mathcal{A}_6 . Beginning with the initial seed S of Proposition 3.3.6, which is in the orbit A, the remaining orbits are named alphabetically, according to the order in which they were found during a breadth-first search of the exchange graph.

This is somewhat unexpected, since enforcing the positivity rule in equation (3.3.1) on the equations of type (a) necessarily creates minus signs in some of the other spinor equations defining the Cayley plane, e.g.

$$x_1x_5 = x_3z_3 - a_3x_2 - a_{10}x_4 + a_1a_{12}.$$

However, in order to get a Laurent phenomenon we needed to introduce the new cluster variable $y_3 = x_3z_3 - a_3x_2 - a_{10}x_4$ and this allows us to rewrite this equation with positive coefficients as $x_1x_5 = y_3 + a_1a_{12}$.

Remark 3.3.9. Positivity was proved for cluster algebras by Gross, Hacking, Keel & Kontsevich [GHKK18] by associating a *consistent scattering diagram* to a cluster algebra. The proof follows by interpreting the coefficients in the Laurent expansion of each cluster monomial as a count of broken lines in the scattering diagram. The consistent scattering diagram for the LPA structure on \mathcal{A}_5 was constructed in [Duc23], and it should be possible to construct one for \mathcal{A}_6 in a similar manner.

A final remark

We recall that the definition of mutation in an LPA uses the exchange Laurent polynomials \hat{f}^i , rather than the exchange polynomials f^i . We always have $f^i = \hat{f}^i$ in the case of cluster algebras, and it is tempting to think we might be able to dispense with the \hat{f}^i in the general case of an LPA. However, it is crucial to work with the \hat{f}^i in order for the LPA structure on \mathcal{A}_6 to have finite type. Moreover, this LPA provides an example for which every seed has at least one direction i in which $f^i \neq \hat{f}^i$.

3.3.10 Limited progress on type E_7

We conjecture the existence of a similar LPA structure on the homogeneous coordinate ring of the Freudenthal variety \mathcal{V}_7 .

Conjecture 3.3.10. *There is a finite type LPA structure of rank 10 on $\mathcal{A}_7 = \mathbb{C}[\mathcal{V}_7]$, which has the positivity phenomenon.*

The LPA should have rank 10 by Remark 3.3.2. We get as far as writing down the equations for \mathcal{V}_7 (as we did for \mathcal{V}_6 in §3.3.6).

The equations of the Freudenthal variety

The Freudenthal variety has an embedding $\mathcal{V}_7 \subset \mathbb{P}^{55}$ where the 56 variables

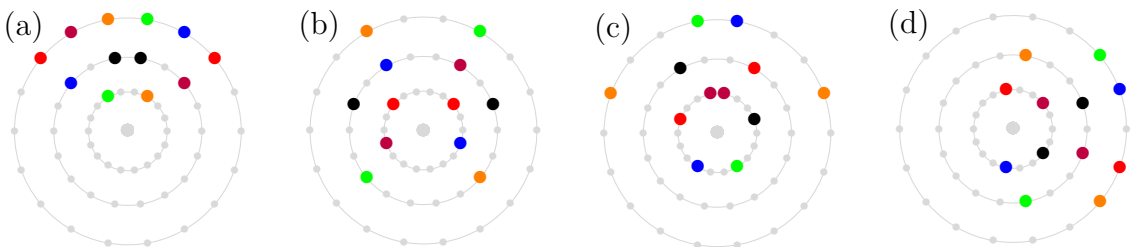
$$a_1, \dots, a_{18}, x_1, \dots, x_{18}, y_1, \dots, y_{18}, z_1, z_2$$

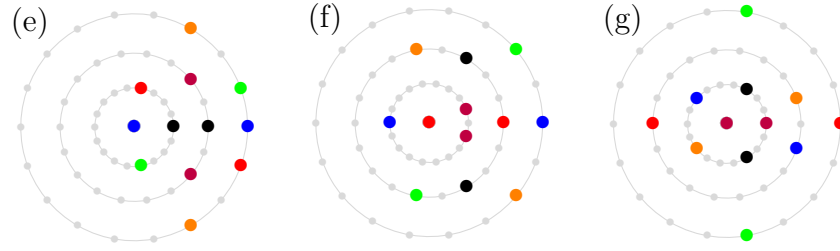
can be put into one-to-one correspondence with the 56 lines on a del Pezzo surface of degree 2. The Coxeter rotation has order 18 and the action on the variables is on the labels.

There are seven orbits of equations:

- $x_1x_2 = a_3x_{17} + a_2y_0 + a_1y_3 + a_0x_4 + a_{17}a_4$ (a)
- $y_{14}y_1 = x_{15}y_4 - a_0x_{10} - a_{15}x_5 + x_0y_{11} + x_{13}x_2$ (b)
- $y_2y_1 = a_2y_{12} + y_5x_0 + y_{16}x_3 + a_1y_9 + a_5a_{16}$ (c)
- $x_4y_1 = x_2y_5 + a_5x_{17} + a_4y_{16} - a_2y_8 - a_1x_7$ (d)
- $x_2x_6 = x_4y_4 \mp a_4z_2 - a_5y_0 - a_3y_8 + a_1a_7$ (e)
- $y_1y_3 = x_{17}x_5 \pm x_2z_1 + a_0x_7 + a_4x_{15} - a_2y_{11}$ (f)
- $y_4y_{16} = \pm y_1z_2 - y_8x_0 - y_{12}x_2 - a_1x_{10} + a_5a_{15}$ (g)

corresponding to the diagrams





and some additional quadratic equations

$$z_1 z_2 = y_3 y_{12} + y_7 y_{16} + y_8 y_{17} + x_1 x_{10} + x_3 x_{12} + x_5 x_{14} + a_0 a_9 + a_2 a_{11} - a_3 a_{12} + a_4 a_{13} + a_6 a_{15}$$

that are implied by the others. Here the choice of \pm sign in the equations is due to the fact that the z_i variables do not appear in the equations of type (a), and thus the positivity rule of equation (3.3.1) does not determine the signs in front of the monomials containing exactly one z_i .

From our observations on the previous cases, it seems like it will be constructive to introduce new cluster variables which will allow us to rearrange the equations so that they satisfy the positivity phenomenon, such as

$$t_? := y_{14} y_1 - x_0 y_{11} - x_{13} x_2 = x_{15} y_4 - a_0 x_{10} - a_{15} x_5$$

$$u_? := x_4 y_1 - a_5 x_{17} - a_4 y_{16} = x_2 y_5 - a_2 y_8 - a_1 x_7$$

and so on.

However, at this point we get stuck. Trying to follow our previous approach of identifying an initial cluster, by using computer algebra to eliminate variables in a ring of codimension 28, proves to be a step too far.

List of Figures

1.1	A point set and its convex hull.	20
1.2	A cone σ (in red) and its associated dual cone σ^\vee (in blue).	21
1.3	A polyhedral fan.	21
1.4	A plane polytope P with its lifted polytope, whose lower envelope defines a regular subdivision of P	22
1.5	An illustration of the duality between regular subdivisions and tropical hypersurfaces. The blue tropical hypersurface is dual to the regular subdivision shown in Figure 1.4.	25
1.6	The matroid polytope associated to the uniform matroid $U_{2,4}$. The picture is drawn on the hyperplane $x_4 = 0$	28
2.1	The matroid polytope P_M for the uniform matroid $U_{4,2}$ (left) with minimal loopless faces shaded in blue, and its Bergman fan (right). The pictures show the projection of the matroid polytope onto the hyperplane $x_4 = 0$, and the intersection of the Bergman fan with the hyperplane $x_4 = 0$	38
2.2	The dual subdivision $D_{S_4}(c_{4,t})$ and tropical hypersurface $\Sigma_{S_4}(c_{4,t})$ of Example 2.2.5 (4). Not illustrated is the invariance of $\Sigma_{S_4}(c_{4,t})$ under translation by $\text{Span}(e_1, e_4)$ as $D_{S_4}(c_{4,t})$ is contained in $\text{Span}(e_1, e_4)^\perp$. The illustrated rays of $\Sigma_{S_4}(c_{4,t})$ have multiplicity 2.	39

2.3	$\Sigma_{S_{\text{lin}}}(0) \cap \Sigma_{S_3}(c_3) \cap \Sigma_{S_4}(c_{4,t})$ from Example 2.2.11. The rays represent $\Sigma_{S_{\text{lin}}}(0) \cap \Sigma_{S_3}(c_3)$ while the shaded area represents $\Sigma_{S_4}(c_{4,t})$ for various t . The white points are stable intersection points.	42
2.4	$\Sigma_{S_{\text{lin}}}(0) \cap \Sigma_{S_3}(c_3) \cap \Sigma_{S_4}(c_{4,t})$ from Example 2.2.12. The rays represent $\Sigma_{S_{\text{lin}}}(0) \cap \Sigma_{S_3}(c_3)$ while the shaded area represents $\Sigma_{S_4}(c_{4,t})$ for various t . The white points are stable intersection points. At $t = 0$ the ray $\mathbb{R}_{\geq 0} \cdot e_3$ lies on $\Sigma_{S_4}(c_{4,t})$	43
2.5	$\Sigma_{S_{\text{lin}}}(0) \cap \Sigma_{S_3}(c_3) \cap \Sigma_{S_4}(c_{4,t})$ from Example 2.2.13. The rays represent $\Sigma_{S_{\text{lin}}}(0) \cap \Sigma_{S_3}(c_3)$ while the shaded area represents $\Sigma_{S_4}(c_{4,t})$ for various t . The white points are stable intersection points.	45
2.6	Bergman fan and hypersurface with two intersection points and mixed cells.	47
2.7	The Cayley trick. The mixed subdivision of P and Q arises by taking a horizontal slice of the Cayley polytope (left). The mixed cells are in correspondence with maximal Cayley cells (middle and right).	53
2.8	The arrangement of the tropical hypersurfaces dual to P and Q	54
2.9	Starting dual supports and dual heights from Example 2.4.2	60
2.10	Straight line homotopy from Example 2.4.5 and the corresponding change in dual subdivision (axes inverted) and tropical hypersurface (multiplicities omitted).	63
2.11	Coordinatewise homotopy from Example 2.4.5 and the corresponding change in dual subdivision (axes inverted) and tropical hypersurface (multiplicities omitted).	64
2.12	A Laman graph G and (one of) its signed incidence matrix M_G	87
2.13	A chemical reaction networks, and its steady state and conservation equations.	87
3.1	Coxeter projections of the polytopes Ξ_n for $n = 4, 5, 6, 7$	107

3.2	The equations of \mathcal{V}_4	109
3.3	The equations of \mathcal{V}_5	111
3.4	The exchange graph for the LPA in the \mathcal{V}_5 case with f-vector F	112
3.5	(i) A labelling of the vertices of Ξ_6 , and (ii) the three types of octahedral face.	116
3.6	The Dih_{12} -quotient of the exchange graph of \mathcal{A}_6 . Beginning with the initial seed S of Proposition 3.3.6, which is in the orbit A, the remaining orbits are named alphabetically, according to the order in which they were found during a breadth-first search of the exchange graph.	120

List of Tables

3.1	Numerical invariants associated to the E_n root systems for $3 \leq n \leq 7$.	106
3.2	The frozen variables a_i and cluster variables x_i, z_i for \mathcal{A}_6 .	115
3.3	Representatives for each of the 15 orbits of seeds A, ..., O. The top row of each entry contains the five cluster variables in the seed. The second row records which cluster variable is obtained by mutating the seed at the variable directly above it, leading to a seed in the orbit given by the label on the third row.	120

Bibliography

- [AEP24] Federico Ardila-Mantilla, Christopher Eur and Raul Penaguião. *The Tropical Critical Points of an Affine Matroid*. 2024.
doi:10.48550/arXiv.2212.08173.
arXiv:arXiv:2212.08173.
- [AHK18] Kareem Adiprasito, June Huh and Eric Katz. ‘Hodge Theory for Combinatorial Geometries’. In: *Annals of Mathematics* 188.2 (2018).
doi:10.4007/annals.2018.188.2.1.
- [AHR16] Lars Allermann, Simon Hampe and Johannes Rau. ‘On Rational Equivalence in Tropical Geometry’. In: *Canadian Journal of Mathematics* 68.2 (2016), pp. 241–257.
doi:10.4153/CJM-2015-036-0.
- [AK06] Federico Ardila and Caroline J. Klivans. ‘The Bergman Complex of a Matroid and Phylogenetic Trees’. In: *Journal of Combinatorial Theory, Series B* 96.1 (Jan. 2006), pp. 38–49. (Visited on 16/02/2025)
doi:10.1016/j.jctb.2005.06.004.
- [BFZ05] Arkady Berenstein, Sergey Fomin and Andrei Zelevinsky. ‘Cluster algebras III: Upper bounds and double Bruhat cells’. In: (2005).
- [BO17] Some Body and An Other. ‘An example article’. In: *J. Ex.* (1 2017), pp. 1–2.
doi:10something/fakedoi.
arXiv:notreal/1234.

- [BT18] Paul Breiding and Sascha Timme. ‘HomotopyContinuation.jl: A Package for Homotopy Continuation in Julia’. In: *International Congress on Mathematical Software*. Springer, 2018, pp. 458–465.
- [Cap+18] Jose Capco, Matteo Gallet, Georg Grasegger, Christoph Koutschan, Niels Lubbes and Josef Schicho. ‘The number of realizations of a Laman graph’. English. In: *SIAM J. Appl. Algebra Geom.* 2.1 (2018), pp. 94–125.
doi:10.1137/17M1118312.
- [Cla+25] Oliver Clarke, Sean Dewar, Daniel Green Tripp, James Maxwell, Anthony Nixon, Yue Ren and Ben Smith. *A Tropical Approach to Rigidity: Counting Realisations of Frameworks*. 2025.
doi:10.48550/arXiv.2502.10255.
arXiv:arXiv:2502.10255.
- [CLS24] David A Cox, John B Little and Henry K Schenck. *Toric varieties*. Vol. 124. American Mathematical Society, 2024.
- [Cox73] H.S.M. Coxeter. *Regular polytopes*. 3rd. New York: Dover, 1973.
- [Dai] O. Daisey. *Laurent Phenomenon Algebra Seed Cell*. Available online at <https://oliverdaisey.github.io/code.html>.
- [DD24] Oliver Daisey and Tom Ducat. ‘A Laurent phenomenon for the Cayley plane’. In: *Symmetry, Integrability and Geometry: Methods and Applications* 20.0 (2024), pp. 33–18.
- [Dic16] Alicia Dickenstein. ‘Biochemical reaction networks: an invitation for algebraic geometers’. English. In: *Mathematical congress of the Americas. First mathematical congress of the Americas, Guanajuato, México, August 5–9, 2013*. Providence, RI: American Mathematical Society (AMS), 2016, pp. 65–83.
doi:10.1090/conm/656/13076.

- [DL22] Qiuning Du and Fang Li. ‘Some elementary properties of Laurent phenomenon algebras’. In: *arXiv preprint arXiv:2201.02917* (2022).
- [Dol06] Igor Dolgachev. ‘Topics in classical algebraic geometry, Part I’. In: *page web personnelle* (2006).
- [Dol12] I. Dolgachev. *Classical Algebraic Geometry: A Modern View*. Cambridge University Press, 2012.
- [Duc23] T. Ducat. ‘The 3-dimensional Lyness map and a self-mirror log Calabi-Yau 3-fold’. In: *manuscripta math.* (2023).
<https://doi.org/10.1007/s00229-023-01497-0>
[doi:10.1007/s00229-023-01497-0](https://doi.org/10.1007/s00229-023-01497-0).
- [FH13] William Fulton and Joe Harris. *Representation theory: a first course*. Vol. 129. Springer Science & Business Media, 2013.
- [FHP23] Elisenda Feliu, Oskar Henriksson and Beatriz Pascual-Escudero. *Generic consistency and nondegeneracy of vertically parametrized systems*. 2023.
[arXiv:\href{https://arxiv.org/abs/2304.02302}](https://arxiv.org/abs/2304.02302){arXiv:2304.02302}.
- [FHP24] Elisenda Feliu, Oskar Henriksson and Beatriz Pascual-Escudero. *The generic geometry of steady state varieties*. 2024.
[arXiv:\href{https://arxiv.org/abs/2412.17798}](https://arxiv.org/abs/2412.17798){arXiv:2412.17798}.
- [FZ02a] Sergey Fomin and Andrei Zelevinsky. ‘Cluster algebras I: foundations’. In: *Journal of the American mathematical society* 15.2 (2002), pp. 497–529.
- [FZ02b] Sergey Fomin and Andrei Zelevinsky. ‘Cluster algebras II: Finite type classification’. In: *arXiv preprint math/0208229* (2002).
- [FZ07] Sergey Fomin and Andrei Zelevinsky. ‘Cluster algebras IV: coefficients’. In: *Compositio Mathematica* 143.1 (2007), pp. 112–164.

- [GHK15] M. Gross, P. Hacking and S. Keel. ‘Birational geometry of cluster algebras’. In: *Algebraic Geometry 2.2* (2015), pp. 137–175.
- [GHKK18] M. Gross, P. Hacking, S. Keel and M. Kontsevich. ‘Canonical bases for cluster algebras’. In: *J. Amer. Math. Soc.* 31 (2018), pp. 497–608.
- [GHR16] Elizabeth Gross, Heather A. Harrington, Zvi Rosen and Bernd Sturmfels. ‘Algebraic systems biology: a case study for the Wnt pathway’. English. In: *Bull. Math. Biol.* 78.1 (2016), pp. 21–51.
doi:10.1007/s11538-015-0125-1.
- [GI24] Michael Gekhtman and Anton Izosimov. ‘Integrable systems and cluster algebras’. In: *arXiv preprint arXiv:2403.07287* (2024).
- [GLS08] C. Geiß, B. Leclerc and J. Schröer. ‘Partial flag varieties and preprojective algebras’. In: *Ann. Inst. Fourier (Grenoble)* 58.3 (2008), pp. 825–876.
- [HHR24] Paul Alexander Helminck, Oskar Henriksson and Yue Ren. *A tropical method for solving parametrized polynomial systems*. 2024.
arXiv:arXiv:2409.13288.
- [HR24] Paul Alexander Helminck and Yue Ren. *Generic Root Counts and Flatness in Tropical Geometry*. 2024.
doi:10.48550/arXiv.2206.07838.
arXiv:arXiv:2206.07838.
- [HS95] Birkett Huber and Bernd Sturmfels. ‘A polyhedral method for solving sparse polynomial systems’. English. In: *Math. Comput.* 64.212 (1995), pp. 1541–1555.
doi:10.2307/2153370.
- [Jen] Anders N. Jensen. *Gfan, a software system for Gröbner fans and tropical varieties*. Available at
<http://home.imf.au.dk/jensen/software/gfan/gfan.html>.

- [Jen16a] Anders Nedergaard Jensen. ‘An Implementation of Exact Mixed Volume Computation’. In: *Mathematical Software – ICMS 2016*. Ed. by Gert-Martin Greuel, Thorsten Koch, Peter Paule and Andrew Sommese. Cham: Springer International Publishing, 2016, pp. 198–205.
- [Jen16b] Anders Nedergaard Jensen. *Tropical Homotopy Continuation*. 2016. [arXiv:arXiv:1601.02818](https://arxiv.org/abs/1601.02818).
- [Jos21] Michael Joswig. *Essentials of tropical combinatorics*. English. Vol. 219. Grad. Stud. Math. Providence, RI: American Mathematical Society (AMS), 2021. [doi:10.1090/gsm/219](https://doi.org/10.1090/gsm/219).
- [Kel08] Bernhard Keller. ‘Cluster algebras, quiver representations and triangulated categories’. In: *arXiv preprint arXiv:0807.1960* (2008).
- [LP16] T. Lam and P. Pylyavskyy. ‘Laurent phenomenon algebras’. In: *Cambridge Journal of Mathematics* 4.1 (2016), pp. 121–162.
- [Man86] Yu I Manin. *Cubic forms: algebra, geometry, arithmetic*. Elsevier, 1986.
- [Mou33] R. Moufang. ‘Alternativkörper und der Satz vom vollständigen Vierseit (D_9)’. In: *Abh. Math. Semin. Univ. Hambg.* 9 (1933), pp. 207–222.
- [MS15] Diane Maclagan and Bernd Sturmfels. *Introduction to tropical geometry*. English. Vol. 161. Providence, RI: American Mathematical Society (AMS), 2015, pp. xii + 363.
- [Nak11] Tomoki Nakanishi. ‘Dilogarithm identities for conformal field theories and cluster algebras: simply laced case’. In: *Nagoya Mathematical Journal* 202 (2011), pp. 23–43.
- [Oxl06] James G Oxley. *Matroid theory*. Vol. 3. Oxford University Press, USA, 2006.

- [Oxl92] James G. Oxley. *Matroid Theory*. Oxford Science Publications. The Clarendon Press, Oxford University Press, New York, 1992.
- [Sco06] J. Scott. ‘Grassmannians and cluster algebras’. In: *Proc. Lond. Math. Soc. (3)* 92.2 (2006), pp. 345–380.
- [Sno89] D. Snow. ‘Homogeneous vector bundles’. In: *Group actions and invariant theory (Montreal, PQ, 1988)*. Vol. 10. CMS Conf. Proc. Providence: Amer. Math. Soc., 1989, pp. 193–205.
- [Sou24] Jack Oliver Southgate. ‘Volume rigidity of simplicial complexes’. Available at <https://research-repository.st-andrews.ac.uk/handle/10023/30817>. PhD thesis. University of St Andrews, 2024.
- [Spe08] David E. Speyer. ‘Tropical linear spaces’. English. In: *SIAM J. Discrete Math.* 22.4 (2008), pp. 1527–1558.
doi:10.1137/080716219.
- [Sum74] Hideyasu Sumihiro. ‘Equivariant completion’. In: *Journal of Mathematics of Kyoto University* 14.1 (1974), pp. 1–28.
- [SW05] David Speyer and Lauren Williams. ‘The tropical totally positive Grassmannian’. In: *Journal of Algebraic Combinatorics* 22 (2005), pp. 189–210.
- [SW23] P. Spacek and C. Wang. ‘Towards Landau–Ginzburg models for cominuscule spaces via the exceptional cominuscule family’. In: *J. of Algebra* 630 (2023), pp. 334–393.
- [Zie12] Günter M Ziegler. *Lectures on polytopes*. Vol. 152. Springer Science & Business Media, 2012.